Rizza Ardiyanti

Graduated in Environmental Engineering

Design and Characterization of Chitin-Glucan Polymeric Structures for Wound Dressing Materials

Dissertation for obtaining the Master degree in Membrane Engineering

Erasmus Mundus Master in Membrane Engineering

Advisor : Luísa Neves, Post-Doctoral Researcher, FCT-UNL
Co-advisors : Isabel Coelhoso, Professor, FCT-UNL
João Crespo, Professor, FCT-UNL

Jury:

President : João Crespo, Professor, FCT-UNL
Members : Vitor Alves, Associate Professor, ISA-Universidade de Lisboa
Damien Quemener, Associate Professor, Montpellier University II
Vlastimil Fila, Associate Professor, ICT-Prague

FACULDADE DE CIÊNCIAS E TECNOLOGIA
UNIVERSIDADE NOVA DE LISBOA

July 2014

Rizza Ardiyanti

Graduated in Environmental Engineering

Design and Characterization of Chitin-Glucan Polymeric Structures for Wound Dressing Materials

Dissertation presented to Faculdade de Ciências e Tecnologia, Universidade Nova de Lisboa for obtaining the master degree in Membrane Engineering

July 2014

Design and Characterization of Chitin-Glucan Polymeric Structures for Wound Dressing Materials

The EM3E Master is an Education Programme supported by the European Commission, the European Membrane Society (EMS), the European Membrane House (EMH), and a large international network of industrial companies, research centers and universities (http://www.em3e.eu).

Projecto financiado com o apoio da Comissão Europeia. A informação contida nesta publicação vincula exclusivamente o autor, não sendo a Comissão responsável pela utilização que dela possa ser feita.

Acknowledgments

This report is the outcome of my master thesis work, and conducted to finalize my master program of Membrane Engineering. The research work is supported and executed in the lab of Chemical and Biochemical Engineering Department at Faculdade de Ciências e Tecnologia, Universidade Nova de Lisboa.

During this thesis, I have acquired precious experience as a researcher but also I had the opportunity to deepen in the knowledge I got during my studies. These accomplishments could not have been completed without the support of my supervisor: Dr. Luisa Neves for her motivation, encouragement, critical judgement and moral support throughout this project.

I would like to express my sincere thanks to my co - supervisors, Prof. Isabel Coelhoso and Prof. João Crespo for the opportunity they have provided me to be part of this project and this group. Thank you very much for for your keen observations and invaluable advice.

I would like to thank Carla Rodrigues, for teaching me to use the DSC equipment and helping me doing the DSC analysis. Also, Nuno Costa, for all the work in HPLC analyzes.

For Vitor Alves, I sincerely want to thank you for teaching me and for your assistance during the rheology measurement. You even did the last measurement of my two samples during weekend. Thank you very much.

I am thankful to Diana Araujo and Ines Farinha for having supervised me during the laboratory tests, performed the CGC characterization and for all the help and kindliness shown in the clarification of my very common questions. Special thanks also to all people in the BPEG group that welcome me with open arms, always available to help me in whatever way I need. I want to highlight; Usman Syed, Hugo Andrade, Rita Ferreira, Carla Martins, Carla Daniel and Silvia Antunes for helping me with the experiments and giving me useful practical advice and on the whole making my work highly enjoyable.

I would like to sincerely thank Dr. Elena Vallejo, Chargée de Projets, UM2, France for being so kind and helping us above and beyond her capacity on many occasions, and to the coordinator of the EM3E Program, Prof. André Ayral, for his support and guidance throughout the entire master course. I am also very grateful to all the professors in the EM3E program, research and administrative staff of UM2-France, ICT-Prague and UNL-Portugal for the support and guidance throughout the entire master course.

I would like to thank the European Union and the European Commission for organizing the Erasmus Mundus scholarship program.

Lastly, I would like to thank my family for their patience and everlasting support throughout the duration of this course. It would not have been possible without their love, consideration and understanding.

Rizza Ardiyanti
Lisbon, Portugal
July 2014

Abstract

The main objective of this work was the development of polymeric structures, gel and films, generated from the dissolution of the Chitin-Glucan Complex (CGC) in biocompatible ionic liquids for biomedical applications. Similar as chitin, CGC is only soluble in some special solvents which are toxic and corrosive. Due to this fact and the urgent development of biomedical applications, the need to use biocompatible ionic liquids to dissolve the CGC is indispensable. For the dissolution of CGC, the biocompatible ionic liquid used was Choline acetate.

Two different CGC's, KiOnutrime from KitoZyme and biologically produced CGC from Faculdade de Ciencias e Tecnologia (FCT) - Universidade Nova de Lisboa, were characterized in order to develop biocompatible wound dressing materials. The similar result is shown in term of the ratio of chitin:glucan, which is 1:1.72 for CGC-FCT and 1:1.69 for CGC-Commercial. For the analysis of metal element content, water and inorganic salts content and protein content, both polymers showed some discrepancies, where the content in CGC-FCT is always higher compared to the commercial one. The different characterization results between CGC-FCT and CGC-Commercial could be addressed to differences in the purification method, and the difference of its original strain yeast, whereas CGC-FCT is derived from *P.pastoris* and the commercial CGC is from *A.niger*.

This work also investigated the effect of biopolymers, temperature dissolution, non-solvent composition on the characteristics of generated polymeric structure with biocompatible ionic liquid. The films were prepared by casting a polymer mixture, immersion in a non-solvent, followed by drying at ambient temperature. Three different non-solvents were tested in phase inversion method, i.e. water, methanol, and glycerol. The results indicate that the composition of non-solvent in the coagulation bath has great influence in generated polymeric structure. Water was found to be the best coagulant for producing a CGC polymeric film structure.

The characterizations that have been done include the analysis of viscosity and viscoelasticity measurement, as well as sugar composition in the membrane and total sugar that was released during the phase inversion method. The rheology test showed that both polymer mixtures exhibit a non-Newtonian shear thinning behaviour. Where the viscosity and viscoelasticity test reveal that CGC-FCT mixture has a typical behaviour of a viscous solution with entangled polymer chains and CGC-Commercial mixture has true gel behaviour. The experimental results show us that the generated CGC solution from choline acetate could be used to develop both polymeric film structure and gel. The generated structures are thermally stable at 100° C, and are hydrophilic. The produced films have dense structure and mechanical stabilities against puncture up to 60 kPa.

Keywords: biopolymer, chitin-glucan complex, biocompatible ionic liquid, wound dressing

Table of contents

List of Tables

List of Figures

Abbreviations

AIM	Alkali Insoluble Material
BDL	Below Detection Limit
BPEG	Biochemical and Process Engineering Group
BSM	Basal Salts Medium
CA	Choline Acetate
CGC	Chitin Glucan Complex
CMA	Concomitant Metals Analyser
Comm.	Commercial
DA	Degree of Acetylation
DSC	Differential Scanning Colorimetry
DO	Dissolved Oxygen
EFSA	European Food Safety Authority
EPS	Exopolysaccharide
f	Frequency
FCT	Faculdade de Ciências e Tecnologia
G'	Elastic modulus
G''	Viscosity modulus
HPLC	High Performance Liquid Chromatography
Hz	Hertz
ICP-AES	Inductively Coupled Plasma-Atomic Emission Spectroscopy
ICP-MS	Inductively Coupled Plasma-Mass Spectrometry
IL	Ionic Liquid
ILs	Ionic Liquids
MeOH	Methanol
ND	Not Determined
Pa	Pascal
RH	Relative Humidity
rpm	Rotation per minute
SEM	Scanning Electron Microscopy
s	Second
TGA	Thermogravimetry
T_g	Glass transition Temperature
T_c	Crystallisation Temperature
T_m	Melting Temperature
UNL	Universidade Nova de Lisboa
wt.	Weight

1. Introduction

1.1. Chitin

Chitin is a non-toxic, biodegradable and biocompatible polysaccharide. It is the second most abundant polysaccharide in nature after cellulose [1], found mainly as the exoskeleton material of arthropods and crustaceans, and the cell wall of fungi. Chitin is a homopolymer of 1-4 linked 2-acetamido-2-deoxy-β-D-glucopyranose [2]. It presents a wide diversity of structures and properties that allows several possible chemical and mechanical modifications in order to create novel materials with specific functionalities and properties.

Chitin exists in three different polymorphic forms (α, β and γ). The polymorphic forms of chitin differ in the packing and polarities of adjacent chains in successive sheets; in the β-form, all chains are arranged in a parallel way, which is not the case in α-chitin [4]. The molecular structure of α-chitin and β-chitin is presented in Fig. 1.1.

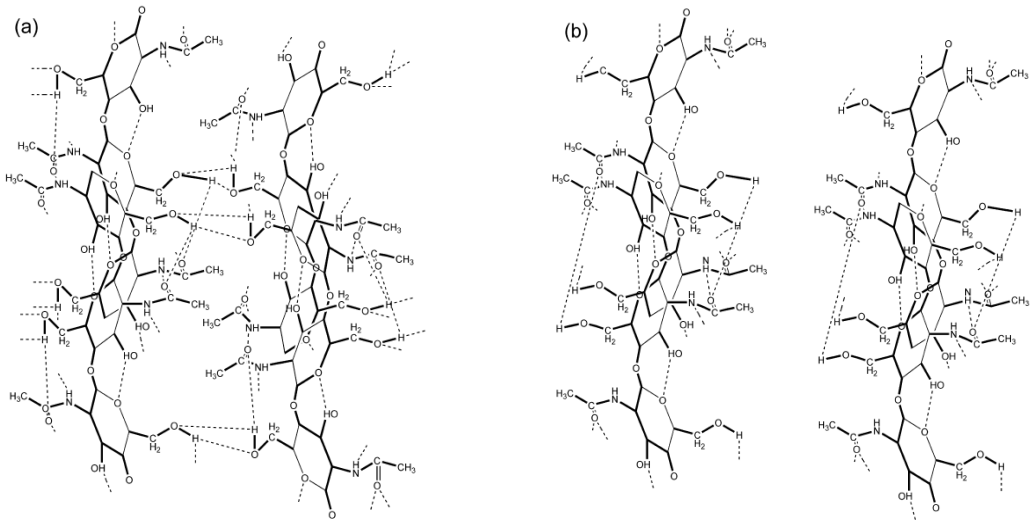

Fig.1.1: Molecular structure and hydrogen bonding in (a) α-chitin and (b) β-chitin [5]

β-chitin is proclaimed to be more reactive than the α-form, an important property in regard to enzymatic and chemical transformations of chitin [4]. Pillai et al reported that a simple treatment with 20% NaOH followed by washing with water is one possible method to convert α-chitin to β-chitin [4]. In both structures, the chitin chains are organized in sheets where they are tightly held by a number of intra-sheet hydrogen bonds with α and β chains packed in antiparallel arrangements. This tight network is dominated by the rather strong C-O-NH hydrogen bonds. The same feature is not found in the structure of β-chitin, which is therefore more susceptible than α-chitin to intra-crystalline swelling [4]. The current model for the crystalline structure of α-chitin indicates that the inter-sheet

hydrogen bonds are distributed in two sets with half occupancy in each set. These aspects make evident the insolubility and intractability of chitin.

1.2. Chitin and Chitosan

Basically, chitin and chitosan are two points on a continuum of materials that share the same basic structure and differ only in their degree of acetylation. Chitin and Chitosan are interesting polysaccharides because of the presence of the amino functionality, which could be suitably modified to convey desired properties and distinctive biological functions including solubility. Apart from the amino groups, they have two hydroxyl functionalities for effecting appropriate chemical modifications to enhance solubility. The structure of chitin and chitosan is shown in Fig.1.2.

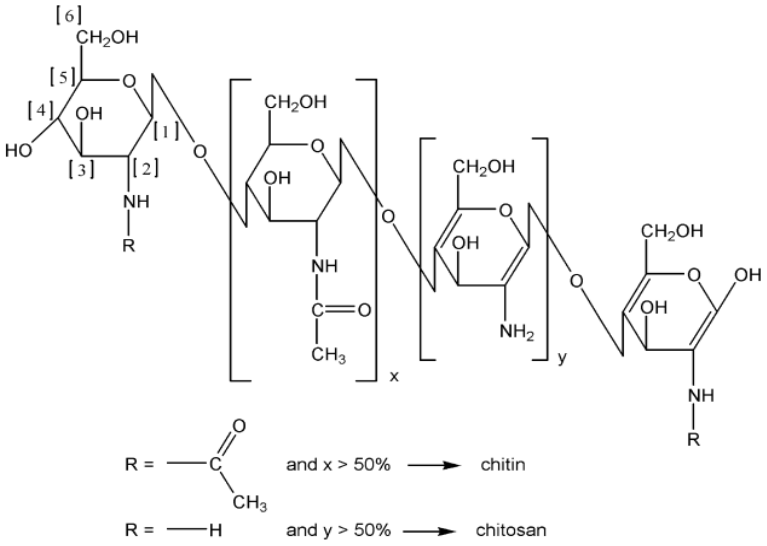

Fig.1.2: Structure of chitin and chitosan [5]

The availability of amino groups on water-soluble chitin allows it to undergo polyelectrolyte complexation with other polyanionic molecules, although the relatively lower charge density (in comparison to chitosan) would affect its complexation properties [6]. It is also reported that the amino functionality gives rise to chemical reactions such as grafting, quaternization, acetylation, chelation of metals, reactions with aldehydes and ketones (to give Schiff's base) alkylation, etc. to grant a variety of products with properties such as such as anti-fungal, antibacterial, anti-acid, anti-viral, non-allergenic, non-toxic, total biodegradability and biocompatibility [4]. The hydroxyl functional groups also give various reactions such as H-bonding with polar atoms, o-acetylation, grafting, etc. Owing to the semi-crystalline structure of chitin with extensive hydrogen bonding, the cohesive energy density and the solubility parameter will be very high and so it will be insoluble in all the usual solvents.

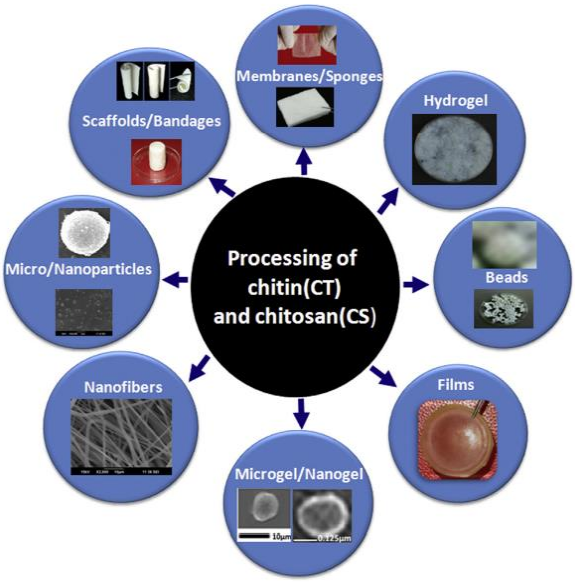

Fig.1.3: Schematic representation on the possibilities of processing chitin and chitosan [5]

Derived from chitin, chitosan is a unique biopolymer that exhibits preeminent properties, beside biocompatibility and biodegradability [32]. These particular properties arise from the presence of primary amines along the chitosan backbone. As a result, this polysaccharide can be a relevant candidate in the field of biomaterials for tissue engineering. The possibilities usage of processing chitin and chitosan is depicted in Fig.1.3.

1.3. Chitin Glucan Complex (CGC)

One material that has shown promise as a component of wound dressings is β-glucan, a polysaccharide comprised of β-linked D-glucose molecules. A variety of β-glucans have been isolated from various sources, such as fungi, baker's yeast, barley, and seaweed. The physicochemical properties of β-glucans differ depending on characteristics of their primary structure, as well as the linkage type, degree of branching, molecular weight, and conformation. β-glucans have been reported to be biocompatible, biodegradable and bio-absorbable, and also expected to promote the therapeutic efficacy of the dressing by increasing the wound healing response [7].

On the other hand, Chitin-glucan is a copolymer composed of metabolites of D-glucosamine, N-acetyl-D-glucosamine and glucose. The polysaccharides related to chitin-glucan, and on which most of the available data, are based on chitin (of crustacean origin), chitosan (derived from chitin, of crustacean origin), β-glucans (of vegetable and fungal origin) and oligomers of chitosan [8]. Molecular structure of yeast β-glucan and chitin is described in Fig.1.4.

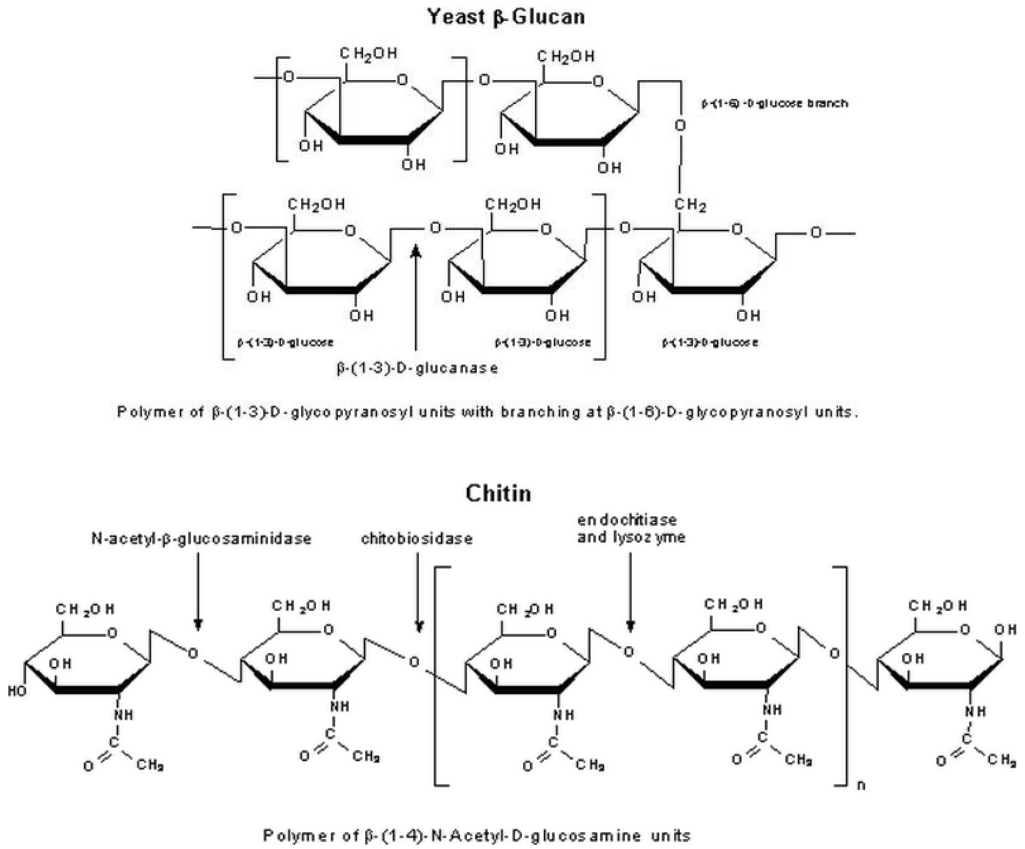

Fig.1.4: Molecular structure of yeast β-glucan and chitin [9]

From the Sigma-Aldrich data, it is reported that in yeast, the cell wall comprises about 30 % of the dry weight of the cell. The yeast cell wall is made of approximately; 25% helical β(1-3) and β(1-6)-D-glucans and 25% oligo-mannans, 20 % protein, 10% lipids, and some chitin. The protein component exists mostly as a mannoprotein complex [9]. Covalent linkages are proclaimed to exist as β(1-4)-linkages between the reducing ends of chitin and the non-reducing end of b(1-3)-glucans1 as well as among glycoproteins, β(1-6)-glucans, and β(1-3)-glucans [9]. The examples of polymeric products that are produced from chitin glucan derivatives are presented in Table 1.1.

Table 1.1: Polymeric product from Chitin-Glucan derivative in the market

Producer	Market name	Usage
KitoZyme, Belgium	KiOnutrime®-CG	Cardiovascular health
	KiOnutrime®-CsG	Weight management
	KiOtransine®	Digestive health
	KiOfine®-B	Wine production (cure contamination)
	KiOfine®-CG	Wine production (clarification)
Clariant Co., USA	Vitipure™	Skin repair and anti-aging
Stratum Nutrition, USA	Artinia®	Arterial/Cardiovascular health

1.4. Biocompatible Ionic Liquid

In recent years, natural renewable resources have been successfully used to produce biomaterials that are biodegradable under certain temperature and humidity conditions. Unfortunately, most biodegradable materials are synthesized by chemical processes using volatile organic solvents, and their emissions and disposal are a large source of pollution worldwide. Alternative solvents such as ionic liquids (ILs) have emerged as a solvents that can be used as templates for porous polymers, components of polymeric matrices and solvents for a wide variety of organic and inorganic compounds [3].

Ionic liquids (ILs) are structurally similar to salts that are a relatively new class of solvents, with potential applications in various fields such as; synthesis, catalysis and electrochemistry, protein stability, polymers conformation and gas separation [13]. Besides, these ILs gained honour as neoteric solvents due to their unique chemical and physical properties such as stability on exposure to air and moisture, extremely low vapour pressure, and high solubility power [11]. The key attraction of ILs is their possibility to be tuned by varying the nature of cations and anions present in their structure.

Recently, ILs have also provided a new processing platform for the dissolution of some natural macromolecules (e.g. cellulose, chitin, starch and lignin) that are otherwise difficult to dissolve due to their inter- and intramolecular hydrogen bonds [1]. In the IL platform, macromolecules can be dissolved, regenerated, derived and functionalized, increasing their potential for exploitation [3].

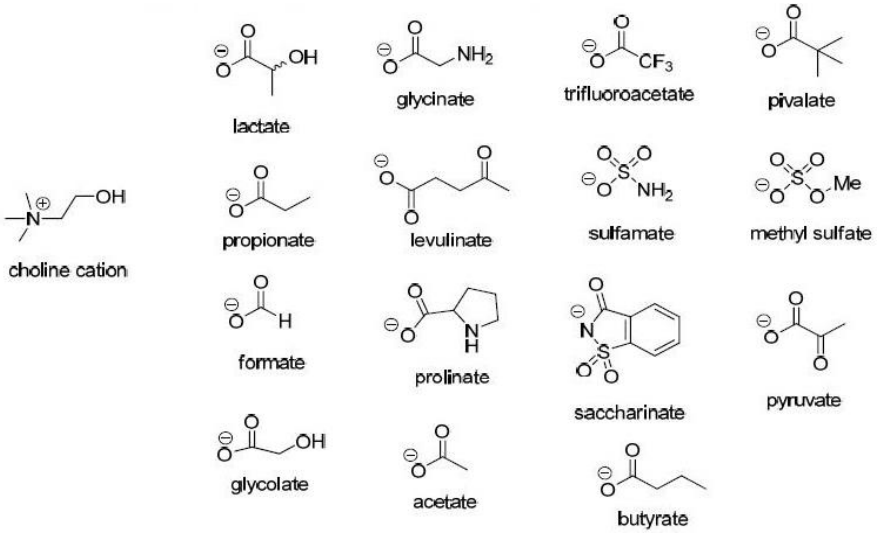

Fig. 1.5: Structure of choline based ionic liquids synthesize [17]

Choline, an essential nutrient, is non-toxic and biodegradable, and choline-based ILs typically exhibit low toxicity, excellent biodegradability, as well as lower-cost synthesis [42]. Amongst the numerous

possibilities of ionic liquids, we selected the choline acetate due to its biocompatibility which allows it to be the best candidate for biomedical application, where acetate anions were known due to its ability in disrupting the inter- and intramolecular hydrogen bonding in the biopolymer [37]. Choline acetate is also recognized to be much more biodegradable than dialkylimidazolium-based ILs [14].

1.5. Dissolution of CGC in Ionic Liquid

Chitin is relatively difficult to process, and due to its insolubility in aqueous solution, has become less accessible to biological laboratories. The use of chitin has been limited due its intractability and insolubility in water and common organic solvents [2] due to its rigid crystalline structure. The structural similarity of chitin to cellulose has induced many authors to try the solvents used for cellulose [12]. As in the case of cellulose, the existence of both intra- and intermolecular hydrogen bonds for chitin in the solid state strongly resists dissolution. But, many of these solvents are corrosive, degradative and toxic. Hence, they cannot be used in medical application and also rise difficulties in scaling up for industrial production.

On the other hand, ILs emerged as a good solvent and can dissolve various substances including biomass i.e. cellulose, lignin and directly wood as well as other renewable polymers such as starch and chitin [12]. Therefore, the dissolution of chitin in ILs has significantly broadened the number of tailored derivatives from this polysaccharide, and consequently enhances its potential use in a number of applications, including in the biomedical field [3]. Using these hydrogels it is possible to develop scaffolds and membranes for the variety of biomedical applications such as tissue engineering and wound dressing. During the last few years vigorous research effort in processing chitin utilizing IL's has been carried out, summarized in Table 1.2.

Table 1.2: Chitin regeneration with Ionic Liquid

Ionic Liquid	Dissolution	Processing	Ref.
1-ethyl-3-methylimidazolium acetate (EAc)	Soluble	100 °C, 12 h	[35]
1-butyl-3-methylimidazolium acetate (BmimAc)	Partly soluble	100 °C, 2 h	[36], [37]
	Soluble	95 °C, 5 h	[41]
1-butyl-3-methylimidazolium chloride (BmimCl)	Partly soluble	110 °C, 2 h	[36]
	Soluble	100 °C, 24 h	[39]
1-allyl-3-methylimidazolium bromide (AmimBr)	Soluble	2h soaked, 100 °C, 48 h	[38]
		100 °C, 24 h	[39],[40]
1-ethyl-3-methylimidazolium acetate (EmimAc)	Soluble	100 °C, 24 h	[40]

From Table 1.2, it can be seen that several works for dissolution chitin in IL have been carried out before. This fact motivates us to develop a research on the dissolution of chitin derivative polymer, CGC, to use more biocompatible IL such as Choline acetate.

Dissolution of CGC with ionic liquids allows the comprehensive utilization of CGC by combining two major green chemistry principles: using environmentally preferable solvents and bio-renewable feed-stocks. Having the same behaviour as chitin, CGC is not easily dissolved in common un-toxic solvent, e.g. water. No research concerning the influence of IL traces in CGC membranes has been reported yet.

1.6. Wound Dressing Materials

Wound management and skin repair are an important area of biomedicine and tissue engineering, wherein intensive research is carried out for the development of advanced wound care systems and promoting satisfying skin regeneration. Chitin and chitosan polymers are amongst the most promising materials for wound dressing materials [5]. They are not antigenic and are perfectly biocompatible. Furthermore, they are biodegradable by enzymatic hydrolysis, for instance in the presence of lysozymes. Due to their anti-thrombogenic and haemostatic character they can be used in all fields of medicine [28]. They might be used to prevent the fibrin bits formation in wounds, to support cell regeneration and to prevent the scar formation.

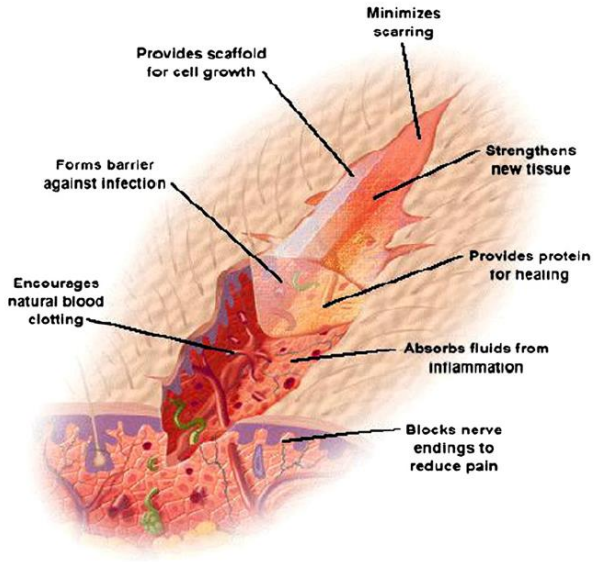

Fig. 1.6: Schematic representation of the required properties of wound dressing material [5]

On the other hand, adhesive nature of chitin and chitosan, together with their antifungal and bactericidal and their permeability to oxygen, is a very essential property associated with the treatment of wounds and burns as expressed in Fig. 1.6.

They can support cellular regeneration while protecting tissues from microbial aggressions. Different derivatives of chitin and chitosan have been prepared for this purpose in the form of fibers, hydrogels, membranes, sponges and scaffolds [5]. One of promising biomaterials based on chitin is Chitin Glucan Complex (CGC).

The high biocompatibility of chitin-based films has been demonstrated for human, chick and mouse fibroblasts by various methods [5, 22].

1.7. Objective of this thesis

This thesis focuses on the development of polymeric structures, namely, hydrogels and films, based on chitin-glucan complex (CGC) for wound dressing materials. Two different CGC, the commercial one from KitoZyme and biologically produced CGC from FCT - Universidade Nova de Lisboa, were characterized in order to develop biocompatible wound dressing materials. The characterization of these biopolymers would include; metal element content, water and inorganic salts content, sugar constituents, protein content and thermal properties analysis.

The CGC dissolution in the biocompatible ionic liquid would be studied in term of viscosity and viscoelasticity in order to understand its influence in the development of the polymeric structure, and also its thermal stability.

The effect of several non-solvents used during phase inversion method would be investigated directly by examining the physical and chemical properties of produced films and gels. The analysis would comprise the thermal stability and sugar composition study of films and gels, and the analysis of total sugar released during the immersion precipitation.

The best film produced by varying non-solvents, i.e. water, methanol and glycerol, in term of physical examination would be subjected to further analysis. The characterization in this phase would involve the mechanical properties in term of puncture resistance and morphological study by SEM (Scanning Electron Microscopy).

2. Material and Methods

In this work, two different CGC polymers were studied. One is produced by BPEG (Biochemical and Process Engineering Group) team of FCT-UNL, Portugal, using *P. pastoris* and the commercial one is KiOnutrime from KitoZyme SA, Belgium.

The solvent tested for the dissolution of CGC polymers is Choline acetate ($C_7H_{17}NO_3$) ionic liquid, supplied by Faculdade de Farmacia, Universidade de Lisboa. Its molecular weight is 163 $g \cdot mol^{-1}$. The synthetic name of Choline acetate is 2-Hydroxy-N,N,N-trimethylethanaminium acetate [7].

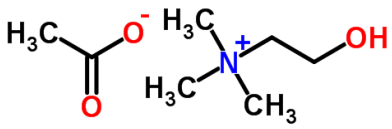

Fig. 2.1: Molecular structure of Choline acetate ionic liquid [15]

The materials and reagents used during the experiment, are described as following:

2.1. CGC-Commercial (KiOnutrime) data

KiOnutrime is chitin-glucan purified ingredient, presented in a powder form, which is composed mainly of two polysaccharides:

- Chitin, composed of repeating units of N-acetyl-D-glucosamine (CAS number 1398-61- 4);
- β(1,3)-glucan, composed of repeating units of D-glucose (CAS number 9041-22-9).

The chitin-glucan component harvested from the cell walls of the mycelium of a fungus from the Ascomycetes family: *Aspergillus niger* (*A. niger*). The two polymers are linked covalently and form a three-dimensional network [20].

This chitin-glucan is obtained from the non-genetically-modified strains of *A. niger* mycelium [20], a microorganism employed in the food and pharmaceutical industries for the production of citric acid. The polymer is a white odourless powder with a yellowish tinge which has a dry matter content >90%. It is insoluble in aqueous and organic media. It is basically intended to be marketed-in for food supplement formats. The appearance of the CGC-Commercial, KiOnutrime, is presented in Fig. 2.2.

Fig. 2.2: KiOnutrime®, KitoZyme SA, Belgium.

The brief specification of KiOnutrime® is presented in Appendix I.

2.2. CGC Extraction from *P. pastoris* biomass

The production of CGC is attained by cultivating *P. pastoris* yeast in a bioreactor containing crude glycerol as carbon source. *P. pastoris* is a methylotrophic yeast commonly used in the pharmaceutical industry as a host for the production of various recombinant heterologous proteins [8]. CGC is developed in *P. pastoris* cell walls to maintain its integrity and, therefore, relatively high amount of CGC can be extracted after biomass production to directly harvest CGC from the cell biomass.

Inoculum for bioreactor experiments were prepared by incubating *P. pastoris* strain DSM 70877 in basal salts medium (BSM) [8], containing crude glycerol. Cultivation was carried out in a 2 L bioreactor with an initial working volume of 1.4 L. The bioreactor was operated with controlled temperature and pH of 30°C and 5, respectively. The DO concentration was controlled by the automatic variation of a stirring rate and supplementation of an air stream with pure oxygen. CGC content in *P. pastoris* cells was evaluated along the cultivation assay. Chitin–glucan content in yeast cells is an indication of its cell age.

For extraction of CGC from the yeast biomass, 1200 mL of culture broth was centrifuged at 8,000 rpm for 15 minutes and the supernatant was discarded. The biomass was washed with water to remove the sodium azide present in culture broth. CGC was recovered from the yeast cell wall by hot alkaline extraction. The wet cell pellet was treated with 1000 mL NaOH (EKA, Portugal) 5 M at 65^{o}C for 2 hours for solubilisation and deproteinization of cell wall components. The alkali-soluble material was separated and discarded from the alkali-insoluble material (AIM) by centrifugation at 8,000 rpm for 15 minutes. The alkaline extraction was followed by repeated washing steps in deionized water. Afterwards, the AIM pellet was re-suspended with minimum amount of water and neutralize with HCl (Sharlau, Spain) 6 M until reach a value of pH 5-6. The AIM was washed several times again with deionized water to remove residual salts until the conductivity is lower than

20µS/cm. pH was adjusted in the range of 6.5 – 7.5 by adding NaOH or HCl. The resulting polymer was freeze dried. The CGC extraction scheme of *P. pastoris* is presented in Fig.2.3.

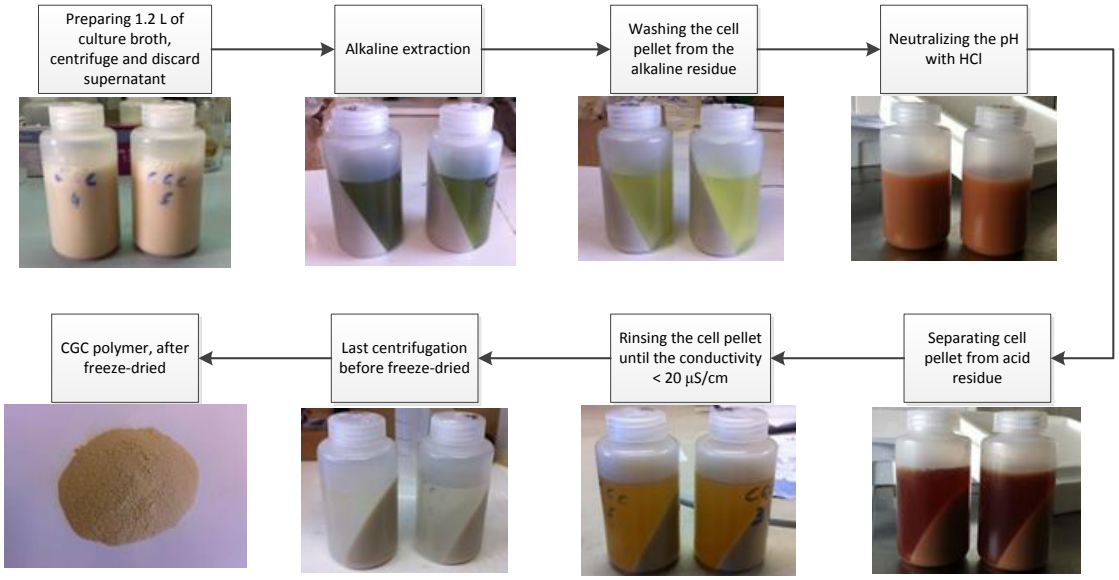

Fig. 2.3: Scheme of CGC extraction from *P. pastoris* cell wall

2.3. CGC chemical analysis

Both biopolymers were characterized in terms of its composition, which include metal element analysis, water and inorganic salts content, quantification of sugar constituents, protein content, and thermal properties analysis.

Duplicates of each measurement were performed in order to obtain reliable data.

2.3.1. Metal element analysis

To analyse chemical elements by ICP-AES (Inductively Coupled Plasma-Atomic Emission Spectroscopy), 5 mg of the CGC samples was treated with 20 mL of H_2SO_4 20% (v/v) from Pancreac, Spain. The tubes were mixed and kept in an oven at 70°C for one hour. The standard was prepared from the same acid solution 20 mL of H_2SO_4 20% (v/v) without polymer.

After the acid treatment, the samples were ready to be subjected for metal analysis. The equipment used is ICP-AES Ultima, from Horiba Jobin-Yvon, France. This model equipped with a 40.68 MHz RF generator, Czerny-Turner monochromator with 1.00 m (sequential), autosampler AS500 and CMA (Concomitant Metals Analyser). The instrument allows analysis of virtually all chemical elements which exhibit emission bands of adequate sensitivity in the range of 180-800 nm, with detection limits of concentration to the ppb of most elements and the simultaneous analysis up to 73

elements in a single sample. The quantity of each metal element was corrected based on the standard. The instrument is presented in Fig.2.4.

Fig. 2.4: ICP-AES, Ultima mode, Horiba Jobin-Yvon, France.

2.3.2. Water and Inorganic salts

To determine the water content in the polymer, 30 mg of CGC polymers on the glass fiber filter (pore size 1.2 µm, VWR Belgium) that was previously weighed were subjected in the oven at 100 °C during overnight. The filter and sample were withdrawn from the oven and weighed for quantification of water content.

The inorganic salts content of the samples was evaluated by subjecting them to pyrolysis at a temperature of 550 °C for 24 h. The set sample and filter were weighed for determination of inorganic salts.

2.3.3. Sugar constituents

For determining the sugar composition of CGC polymers, two acid hydrolysis procedures were performed: Trifluoroacetic acid (TFA), from Sigma Aldrich-Germany, was used to hydrolyse the glucan moiety of the polymer, while a stronger acid (HCl) was necessary for the quantification of the chitin fraction. For the TFA hydrolysis, dried CGC samples (5 mg) were resuspended in deionized water (5 mL) and 0.1 mL TFA 99% were added. The hydrolysis was performed at 120°C, for 2 hours.

For the HCl hydrolysis, the samples (5 mg) were resuspended in HCl 4 N (5 mL). The hydrolysis was performed at 120°C, for 5 hours. Both hydrolysates were used for the quantification of the constituent monosaccharide by HPLC using a CarboPac PA10 column (Dionex), equipped with an amperometric detector. The instrument is presented in Fig.2.5.

The analysis was performed at 30 °C, with sodium hydroxide (NaOH 4 mM) as eluent, at a flow rate of 0.9 mL·min^{-1}. Glucose (Sigma-Aldrich), mannose (Sigma-Aldrich) and glucosamine (Sigma-Aldrich) were used as standards, and being subjected to the same hydrolysis procedures as the polymer samples.

Fig. 2.5: Ion Chromatography – DIONEX, model ICS-3000

For HPLC system employed, identification and quantification of the major sugars present in the samples were achieved by comparing each peak retention time and area with those of the standard. Data of the area is used for the calibration curve. The quantity of each sugar was corrected based on the recovery ratio of the internal standard.

2.3.4. Protein content

To analyse the protein content, dried polymer samples were hydrolysed with 2 M NaOH (7 mg: 1 mL) in sealed vials, at 120 °C for 15 min. The supernatant obtained by centrifugation (10,000×g, 10 min) was used for the protein assay [8], according to the modified Lowry method [25]. A 1-mL aliquot of alkaline copper sulphate reagent was added to 1 mL of the supernatant and allowed to stand for 10 min at room temperature. A 3-mL aliquot of diluted Folin-Ciocalteu reagent was added, and incubated at room temperature for 30 min. Absorbance was read at 750 nm. Bovine serum albumin (BSA, Sigma-Aldrich) was used as standard. The absorbance value of the standards at different concentrations was used to build a calibration curve.

Fig. 2.6: Spectrophotometer - Thermo Spectronic, Hελios α, Germany

The spectrophotometer used is Thermo Spectronic, Hελios α, Germany. Fig.2.6 represents the spectrophotometer utilized for the measurements of absorbance.

2.4. Thermal Properties

To understand the thermal properties and stability of CGC polymers, a differential scanning calorimeter (Setaram, model DSC 131, France) is utilized at a scanning rate for both heating and cooling of 10°C·min^{-1} in the temperature range -130°C to 100°C and 30°C to 400°C. The sample was placed and hermetically sealed in an aluminium crucible while an empty crucible was used as the reference. The sample was heated under a nitrogen stream.

The DSC instrument is presented in Fig. 2.7.

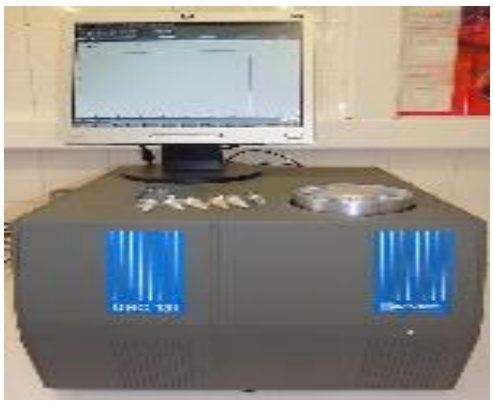

Fig. 2.7: Differential Scanning Calorimeter - Setaram, France, model DCS 131

The DSC measurements were performed on the Ionic Liquid, CGC polymers, mixed polymer and ionic liquid, and the membranes obtained after the phase inversion method.

2.5. Film preparation

To dissolve the polymer for film preparation, CGC powder (5 wt. %) was added in Choline Acetate in a 50 mL beaker glass under continuous agitation (200 rpm) using a magnetic stirrer. During dissolution, the temperature of the solution was well controlled in the oil bath at 80 ^{o}C for FCT-CGC and 110 ^{o}C for the commercial CGC for 24 h.

The beaker glass was placed in the thermostat oil bath. The sample was heated very slowly with continuous stirring. The temperature control of the water bath was governed by using a digital thermo-regulator connected to the heating magnetic stirrer from Velp Scientific, Italy. The dissolution process is depicted in Fig. 2.8.

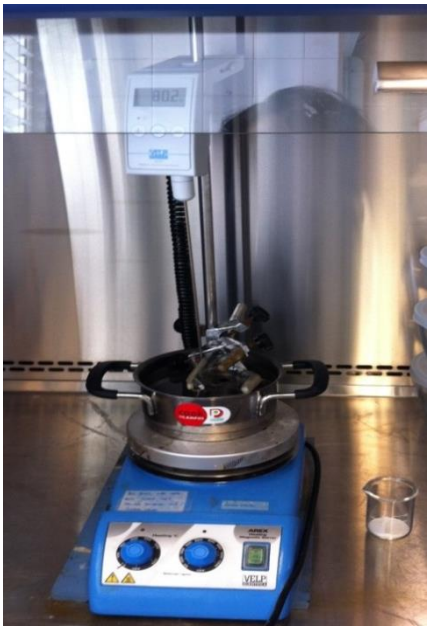

Fig. 2.8: Dissolution of CGC polymers

The CGC solution was later casted onto a metal plate and instantly immersed in a coagulation bath at room temperature for 24 h. The compositions of non-solvent used in coagulation bath were;

1. Demineralized water
2. 50% (v/v) Methanol (MeOH) solution
3. 30% (v/v) Glycerol solution

The membranes were dried in an open space at an ambient room temperature 26±2°C and relative humidity of 35±1% for 72 h, and 5-7 days if desiccator was used.

Controlled evaporation was done by using an empty desiccator. The controlled evaporation and humidity was done by using 200 g of NaBr salt and 80 g of H_2O (demineralised water) at the temperature of 25°C, in order to create 57.7% of relative humidity inside the desiccator.

2.6. Rheology Test

To understand the viscosity and viscoelastic properties of the CGC mixtures, a controlled stress rheometer (Haake RS-75, Thermo Scientific, Germany) is used. The rheometer is equipped with Peltier liquid temperature control unit. A cone and plate geometry of diameter 3.5 cm and 2° angle were used for the measurement. The rheometer is presented in Fig. 2.9.

The rheology measurement of ionic liquid was done at temperature 25 °C, whereas for polymer mixtures were at temperature 80 °C and 110 °C in order to mimic the dissolution temperature of both polymers.

Fig. 2.9: Rheometer Haake RS-75

Flow curves for choline acetate and two CGC mixtures were determined using a steady state flow ramp in the range of shear rate from 0.001 to 1000 s^{-1}.

The viscoelasticity measurement was performed with the same rheometer, operated in an oscillating mode. The strain sweep measurement was carried out to estimate the linear viscoelastic region at a relative low frequency. Referring to this result, the dynamic frequency sweep measurements were carried out in linear response region for both samples. Determination of elastic modulus (G') and viscous modulus (G") as a function of angular frequency (ω) was performed at fixed shear stress of 1 Pa for CGC-FCT mixture, and 0.3 Pa for CGC-commercial mixture.

2.7. Sugar content in coagulation bath

For the analysis of total sugar in the coagulation bath, Dubois method was employed. This method is mainly useful for the determination of small quantities of sugars.

Total sugar content (CHO) was analysed using the phenol-sulphuric method modified to be measured at 490 nm using an absorbance spectrophotometer (Thermo Spectronic, Hελios α, Germany) as presented in Fig. 2.6. Simple sugars, oligosaccharides, polysaccharides, and their derivatives, including the methyl ethers with free or potentially free reducing groups, give an orange-yellow colour when treated with phenol and concentrated sulphuric acid [18]. The reaction is sensitive and the colour is stable.

0.5 mL of sample was mixed with 0.5 mL Phenol (5% wt.) and 2.5 mL of concentrated H_2SO_4. After 10 minutes, each samples were mix in a cortex-mixer for few seconds. The samples were placed in a dark place for 30 minutes prior to measurement at 490 nm using an absorbance spectrophotometer. Glucose (Sigma Aldrich) was used as standard. The absorbance value of the standards at different concentrations was used to build a calibration curve.

2.8. Membrane Characterization

2.8.1. Puncture Test

To know the mechanical resistance of the film against puncture, a TA-Xt plus texture analyser (Stable Micro Systems, Surrey, England) was used for puncture stress measurement. All mechanical tests were performed at ambient conditions, at room temperature of 22±2 °C. Triplicates of each film were analysed. The measuring instrument is presented in Fig. 2.10.

Fig. 2.10: TA-Xt plus texture analyser

Puncture test were carried out by immobilizing the test samples (20×20 mm) on a specially designed base with a hole of about 10 mm diameter. The samples were compressed at a speed of 0.5 $mm \cdot s^{-1}$

and punctured through the hole with a cylindrical probe (2 mm diameter). The puncture stress (τ_P) was expressed as the ratio of the puncture force and the probe contact area as per equation below *(Eq. 2.1)*.

$$\tau_P = \frac{F_P}{A_P} \qquad \textit{(Eq. 2.1)}$$

Where τ_P is a puncture stress in Pa; F_P is the force to the films in N; and A_P is the probe cross sectional area in m^2. This test allows the determination of the strain by the following equation;

$$\varepsilon_P = \frac{L_f - L_i}{L_i} \times 100 \qquad \textit{(Eq. 2.2)}$$

Where ε_P is a puncture elongation; L_f is the final length in meter; and L_i is the initial length in meter.

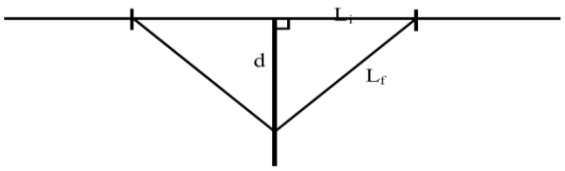

Fig. 2.11: Puncture test scheme

The parameter L_f refers to the film elongation and it is calculated with base in the elongation measured by the probe, *d (Eq. 2.3)*. Fig. 2.11 shows a representation of the test calculation.

$$L_f^2 = d^2 + L_i^2 \leftrightarrow L_f = \sqrt{d^2 + {L_i}^2} \qquad \textit{(Eq. 2.3)}$$

2.8.2. Contact Angle Analysis

To have information regarding the hydrophilicity of the polymeric structure, the contact angle measurement was employed. The contact angle (θ) of the liquid drop on a solid surface is defined by the mechanical equilibrium of the drop under the action of three interfacial tension; solid liquid (γ_{SL}), solid vapour (γ_{SV}) and liquid vapour (γ_{LV}), Fig. 2.12.

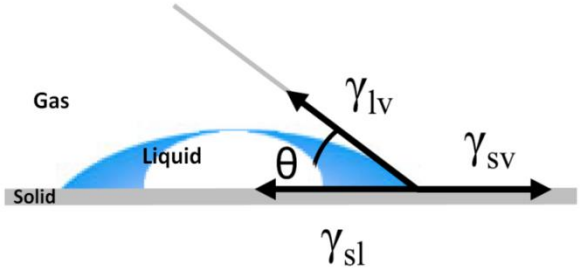

Fig. 2.12: Schematic of a sessile drop, contact angle and the three interfacial tension [29]

The equilibrium spreading coefficient (W_s) is defined by equation and can only be negative or zero *(Eq. 2.4):*

$$W_s = W_a - W_c = \gamma_{SV} - \gamma_{LV} - \gamma_{SL} \qquad \textit{(Eq. 2.4)}$$

W_a and W_c are the work of adhesion and work of cohesion respectively, and can be defined as:

$$W_a = \gamma_{SV} + \gamma_{LV} - \gamma_{SL} \qquad \textit{(Eq. 2.5)}$$

$$W_c = 2 \cdot \gamma_{LV} \qquad \textit{(Eq. 2.6)}$$

$$\gamma_{SV} = \gamma_{LV} \cdot \cos(\theta) + \gamma_{SL} \qquad \textit{(Eq. 2.7)}$$

The contact angle was measured by sessile drop method. A drop of distilled water was deposited manually on the membrane surface by a syringe. 50 images were acquired by the software and the tangent was determined by fitting the drop shape to known mathematical function. The measurements were executed immediately after the drop fell on the surface. Multiple replicates were performed, and the mean contact angle was reported with its standard deviation. The instrument is presented in Fig.2.13.

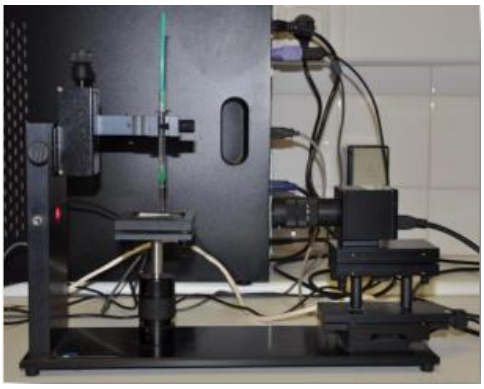

Fig. 2.13: Goniometer for a sessile drop, contact angle and the three interfacial tension [29]

2.8.3. Scanning Electron Microscopy (SEM) Analysis

To understand the mophological structure, the obtained polymeric films were analysed by means of Jeol JSM-7001F-Field emission scanning electron microscope operated with an intensity of electron beam 10 kV, see Fig.2.14. This microscope allows for the observation and characterization of heterogeneous organic and inorganic materials at the scale of micro (10-6) to nano (10-9) meters. Cross section imaging can be done by using the tilt facility which allows the sample to be held at an angle of 45° for analysis.

Fig. 2.14: Scanning Electron Microscopy, Jeol JSM-7001F

The principle of SEM involved the incidence of an electron beam on the sample surface producing secondary electrons, back scattered electrons or retro-diffused x-rays which can be analysed to obtain an image which is magnified over 200,000 times. In our case, the signal consists of secondary electrons from which the surface image is constructed instantly. The primary electron beam is mobile and scans the samples surface obtaining a complete image.

Sample preparation is an important part of this process as the material has to be clean cut surfaces and must be conductor. In order to achieve this, 2 cm^2 pieces of the sample was dipped in a liquid nitrogen environment and then cut by breaking it, to avoid distorting the material surface or cross section. The sample is then impregnated with a thin layer of gold particles to make it a good conductor.

3. Results and Discussion

3.1. CGC Polymer

3.1.1. Metal element analysis

The metal element analysis was measured by ICP-AES. The measurements for the CGC-FCT and CGC-Commercial were executed based on the method described in section 2.3.1. The results are presented in Table 3.1.

Table 3.1: Composition of metal element in CGC polymers

Metal Element	Wavelength (nm)	Concentration of the element (mg/L)	
		CGC-FCT	CGC-Commercial
Boron (B)	249.773	0.013	BDL
Calcium (Ca)	393.366	BDL	0.278
Cadmium (Cd)	226.502	ND	ND
Cobalt (Co)	228.616	ND	ND
Copper (Cu)	224.700	0.046	BDL
Iron (Fe)	259.940	0.201	BDL
Mercury (Hg)	194.164	ND	ND
Potassium (K)	766.490	ND	ND
Magnesium (Mg)	279.553	0.003	0.072
Manganese (Mn)	257.610	ND	ND
Molybdenum (Mo)	202.030	ND	ND
Sodium (Na)	589.592	BDL	0.397
Phosphorus (P)	214.914	0.004	BDL
Zinc (Zn)	213.856	0.118	0.033

***ND = Not Determined**
***BDL = Below Detection Limit**

From the results obtained, it can be observed that CGC-FCT polymer contains more metal elements compared with CGC-Commercial, namely for the elements of Boron, Copper, Iron, Phosphorus and Zinc. However, for Calcium, Magnesium and Sodium are found in higher amount in the commercial CGC.

In general, metal elements in both CGC polymers are detected in very low concentration. The amount of Iron and Zinc seems high but it is still far below the concentration level of Iron and Zinc for chitin-glucan defined by International Oenological Codex [33] for wine stabilizer agent prior to bottling.

The result of our measurement is below the reported value by European Food Safety Authority (EFSA) in literature [20] and in the specification product from Kitozyme (Appendix I). This discrepancy could be addressed to the sensitivity and detection limit of the instruments. It is known that the ICP-MS is more sensitive and accurate compared to ICP-AES [26].

3.1.2. Water and inorganic salts content in CGC

The characterization of water and inorganic salts content in both polymers was carried out based on the method described in section 2.3.2. The result is outlined in Table 3.2.

Table 3.2: Water and inorganic salts content in CGC polymers

Polymer	Water content (wt. %)	Inorganic salts (wt. %)
CGC-FCT	12.51	1.95
CGC-Commercial	7.35	0.98

CGC-FCT contains more water and more inorganic salts, compared to the commercial one.

The inorganic salts content in the CGC-FCT polymer in this experiment is less compared to the previous CGC-FCT result from Henrique Marcal's experiment which was 5.5 % [16]. This could be due to low conductivity set-up value during the polymer extraction, which is 20 $\mu S \cdot cm^{-1}$ in this experiment and 500 $\mu S \cdot cm^{-1}$ in the previous one.

The difference observed from CGC-FCT and CGC-Commercial could be addressed to differences on the purification method of the polymers. The values obtained for water and inorganic salts of CGC-FCT are also less compared with the CGC described in literature [8].

3.1.3. Sugar constituents in CGC

For the determination of sugar composition in two biopolymer samples, CGC were hydrolysed and analysed by HPLC as described in chapter 2.3.3. The composition of glucosamine and glucan in the CGC polymers tested are summarized in Table 3.3.

Table 3.3: Sugar constituents in CGC polymers

Polymer	Glucosamine Conc. (ppm)	Glucan Conc. (ppm)	Mannose Conc. (ppm)	Ratio Glucosamine and Glucan
CGC-FCT	424.93	732.84	37.49	1:1.72
CGC-Commercial	415.16	701.19	63.25	1:1.69

The ratio of chitin and glucan amount in the polymers is represented by the ratio of glucosamine and glucan. The result shows that there is a concurrency between two polymers in term of the ratio of chitin and glucan which is 1:1.72 for CGC-FCT and 1:1.69 for CGC-Commercial. The result of CGC-FCT is different with literature [8]. This difference could be addressed to the dissimilarity in feeding and operating strategy of the bioreactor during the *P. pastoris* production.

The result of sugar constituents in CGC-Commercial also shows a congruity with the result obtained by the literature [20]. The amount of chitin in chitin-glucan copolymers is defined by the organism from which it is extracted. In the case of mycelium of *Aspergillus niger* used in the method according to the invention by Kitozyme, and chitin-glucan copolymers extracted from the mycelium of *A. niger* comprise between 30 and 50% (w/w) of chitin and between 50 to 70% of β-glucan [20].

The calibration curve of the concentration of sugar as a function of absorbance of the standards by HPLC is presented in Appendix II.

3.1.4. Protein content in CGC

Determination of protein content was made between other treatments, hydrolysis and subsequently a measurement of absorbance at 750 nm, as previously described in section 2.3.4. The values of absorbance, protein concentration and percentage of protein in two CGC polymers are presented in Table 3.4.

Table 3.4: Protein content in CGC polymers

Polymer	Mass of sample (mg)	Absorbance	Protein content (mg/mL)	Avg. of protein content (mg/mL)	Protein content (%)	Avg. of protein content (%)
CGC-FCT	7.28	0.681	0.38	0.40	5.22	5.57
	7.26	0.748	0.43		5.92	
CGC-Commercial	7.21	0.120	0.12	0.12	1.66	1.67
	7.17	0.081	0.12		1.67	

From the obtained results, it can be observed that CGC-FCT polymer contains more protein compared with CGC-Commercial. Protein is characterized by amino group as well as glucosamine which known as an amino sugar part in chitin and chitosan structure. Hence, this result could be linked to the sugar constituent analysis in section 3.1.3., where it was observed as well that the CGC-FCT contains more glucosamine than the commercial one.

The discrepancy result between the two polymers could be due to the distinction in extraction and purification method. Because the use of sodium hydroxide for several hours for the extraction of

chitin-glucan from the mycelium is expected to denature or partly hydrolyse any protein component from the source, as it stated in the literature [20].

As additional information, it is reported by European Food Safety Authority (EFSA) that protein content in KiOnutrime is ≤ 6% [20]. The method used for protein determination was based on colorimetry after reaction with ninhydrin and UV-absorption at 564 nm.

The calibration curve depicting the concentration of protein as a function of absorbance of the standards is presented in Appendix III.

3.1.5. Thermal properties of CGC polymer

The analysis using differential scanning calorimetry (DSC) to evaluate CGC polymer helps to explore and understand the intrinsic property, as well as to verify and monitor the thermal properties and phase transitions of the polymer.

However, during the DSC measurement, the glass transition temperature (T_g) of both polymers could not be observed due to the limitation of the instrument. The measurement from low temperature to high temperature could not be conducted continuously. This problem leads to the difficulty in interpreting the DSC results.

The DSC result for CGC measurement in low temperature is presented in Fig. 3.1.

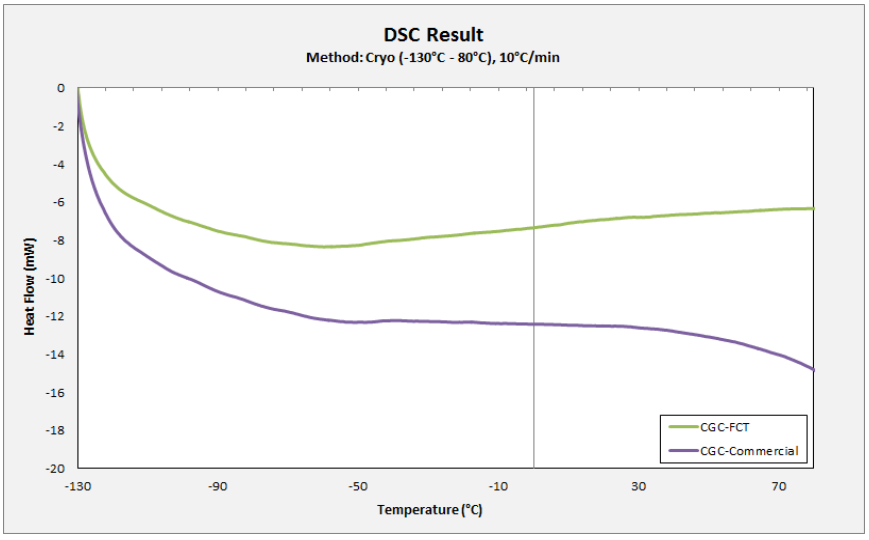

Fig. 3.1: DSC Result for temperature below 100 ^{o}C (Cryo-DSC)

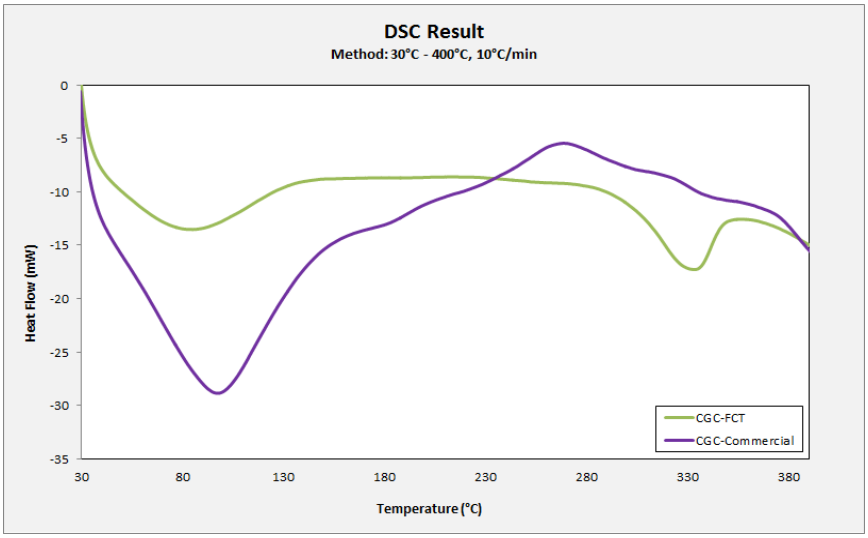

Fig. 3.2: DSC Result for high temperature measurement

By analysing Fig. 3.2, it can be seen that both samples undergo a process of dehydration following by decomposition of biopolymer. The curve between temperature 80°C and 130 °C corresponds to zone of water evaporation.

The first curve of commercial CGC, between temperatures ranges of 80°C–130°C, represents thermal degradation with an endothermic enthalpy change, corresponds to thermal degradation of moisture content present in polymer material. The second curve, between temperatures ranges of 250°C–280°C, has shown an exothermic enthalpy change. This could be addressed to the thermal decomposition of polymer.

As well as the CGC-FCT, it underwent thermal degradation with endothermic enthalpy changes between temperatures ranges of 80°–130°C and 320°C–350°C. The first curve could be addressed to the thermal dehydration and the second one is due to the thermal decomposition. However, these results have to be confirmed by another measurement, TGA analysis, in order to provide us an exact value.

3.2. Polymeric structures produced from CGC

Limited solubility of biopolymers restricts the number and nature of reagents that could be used for their chemical modifications. We found that both biopolymers are soluble in Choline acetate, at 80°C for CGC-FCT and 110°C for CGC-Commercial. The higher temperature is needed to dissolve CGC-commercial because it was observed that the CGC-Commercial is not completely dissolved at temperature of 80°C. However, the viscosity increased so high that it was difficult to stir the solution with a magnetic stirrer.

As mentioned previously, choline acetate was selected for this work due to its CH_3COO^- anion. These anions tend to create more stable bond with the hemiacetal group from CGC. The hydrogen bonds are disrupted by seizing proton from hydroxyl group or amino group from the polymer. The cleavage of the hydrogen bond will demolish the compact crystalline structure of chitin and lead to the dissolution of CGC. Previous studies on dissolving cellulose by ILs have suggested that the solvation mainly involved the interaction of the hydroxyl protons of the CGC polymer with the strong hydrogen bonding and coordinating anions, in particular CH_3COO^- [35].

Biopolymer, such as CGC, is found to be soluble at 80°C in ionic liquids choline acetate, in concentrations up to 12% (w/w). [16]. Higher concentrations of biopolymers in IL resulted in solutions with too high viscosity to cast. In the present work, 5% (w/w) CGC concentration in IL is considered as a good composition. The dissolution of CGC polymer in choline acetate and the casting process are presented in Fig.3.3.

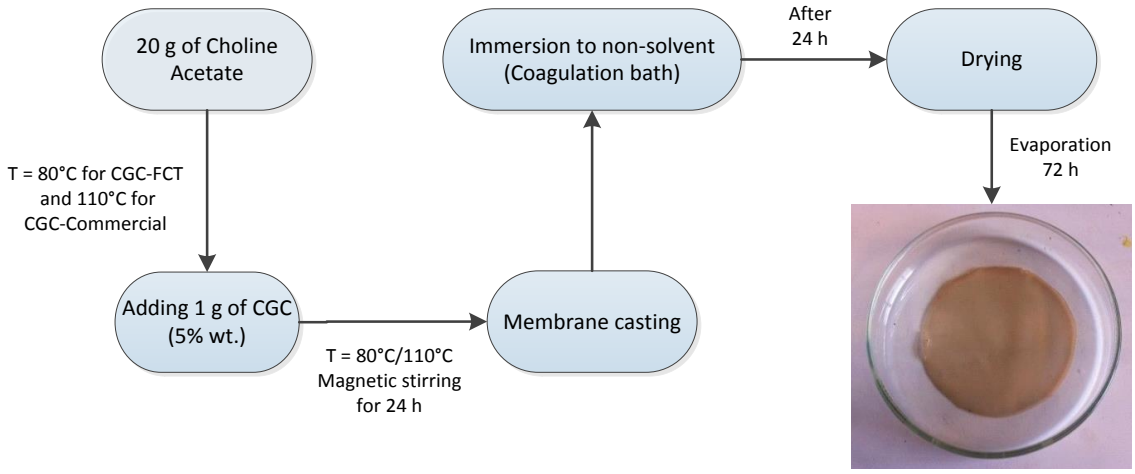

Fig. 3.3: Schematic film casting process

5% (w/w) of polymer dope was generated by dissolving 1 g of CGC polymer in 20 g choline acetate in a 50 mL beaker glass under continuous agitation using a magnetic stirrer (200 rpm). The dissolution was carried out in the oil bath at certain temperature (80°C and 110°C) for 24 hours. After the polymer dissolution, then the polymer dope was casted on to a metal support. The casted polymer was then immersed in non-solvent bath for 24 hours for precipitating the solvent. Afterwards, the casted polymer was dried at ambient room temperature for 72 hours.

Several non-solvents were used to understand its influence in developing polymeric structure by regeneration of CGC polymer in biocompatible ionic liquid, Choline acetate. The different polymeric structures produced from CGC polymers are presented in Fig.3.4.

Non-solvent / Polymer	Water	50% (v/v) Methanol	30% (v/v) Glycerol
CGC-FCT	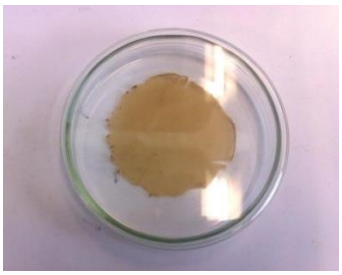	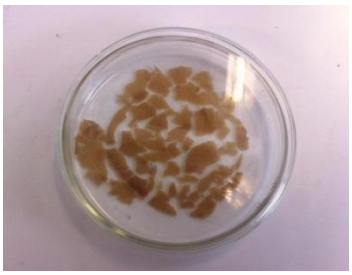	
	Film	Film	Film/Gel
CGC-Commercial		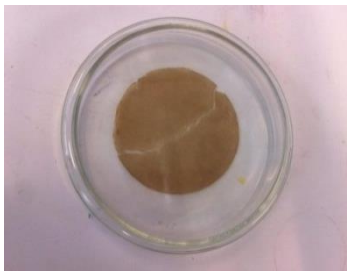	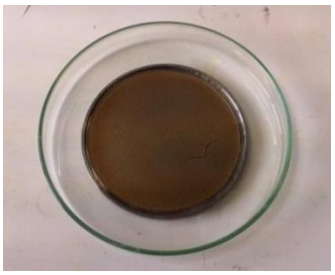
	Film	Film	Gel

Fig. 3.4: Polymeric structures, produced from CGC polymers in different non-solvents

The generated polymer structure from CGC polymers and choline acetate was observed to form film by using water and 50% (v/v) methanol as non-solvent. The gelation occurred when glycerol was used as non-solvent. This could be due to its structure that has three OH groups which could interact with polysaccharide and act as a plasticizer. As the consequence, the casted polymer will maintain the absorbed water in its structure and prevent it from evaporation. Ultimately, water is found to be the best coagulant when CGC film structure is favoured.

Effect of dissolution temperature

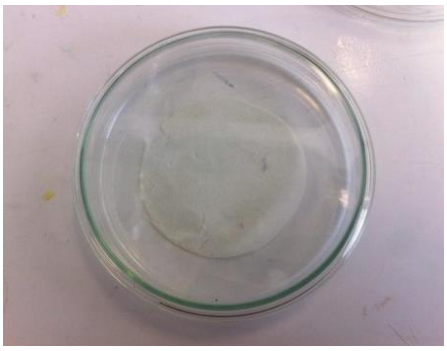

CGC-Commercial, water, 80°C dissolution

CGC-Commercial, water, 110°C dissolution

Fig. 3.5: Produced CGC films with different dissolution temperature

The commercial CGC polymer is difficult to be dissolved in temperature below 100°C. When the polymer is not completely dissolved in the solvent, it leads to faster demixing of solvent and non-solvent. The required higher temperature for dissolving the commercial CGC could be due to the fact that CGC-Commercial contains more glucosamine, if we consider it in term of the ratio of glucosamine and glucan as observed in chapter 3.1.3, whereas hydrogen bond in glucosamine is more difficult to be disrupted by IL. The images of CGC films generated from different dissolution temperature are presented in Fig.3.5.

Effect of evaporation condition

CGC-FCT, 50% MeOH, Normal drying

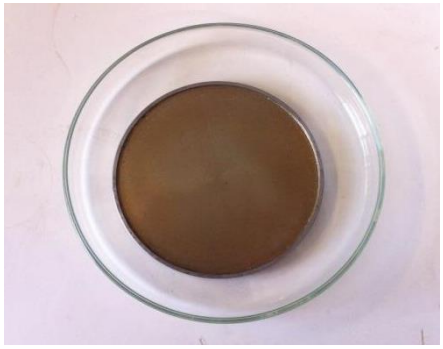

CGC-FCT, 50% MeOH, 57.7% RH at 25°C

Fig. 3.6: Produced CGC films with different evaporation condition

During the experiment, it was confirmed that the evaporation process is one of the most important parameters in developing CGC film structure. It can be observed from Fig. 3.6. that the crack creation upon drying occurred on the CGC-FCT dried in an open space (35±1% RH at 24°C). This problem can be prevented by smooth solidification process. This can be done by controlling the evaporation condition by means of a desiccator.

The characterizations, after the dissolution of CGC polymer and generation of polymeric structure, comprise the viscosity and viscoelasticity test followed by thermal property analysis. Sugar composition study of films and gels, and the analysis of total sugar released during the immersion precipitation were also analysed.

3.2.1. Rheology of CGC Mixtures

From the rheology study, it was observed that Choline acetate exhibits Newtonian liquid behaviour, with apparent viscosity stable at 0.13 Pa·s in room temperature (25°C), see Fig. 3.7.

The rheology study was carried out in temperature 80°C for CGC-FCT mixture and 110°C for CGC-Commercial mixture in order to mimic the processing temperature of both polymers. Interesting result was found in both mixtures, where both solutions exhibit a non-Newtonian shear thinning behaviour. It is discovered that the mixture of CGC-commercial shows stronger shear thinning effect compared to CGC-FCT mixture. It is recognized from the stiffer flow curve of its apparent viscosity when the shear rate was applied, as presented in Fig. 3.7.

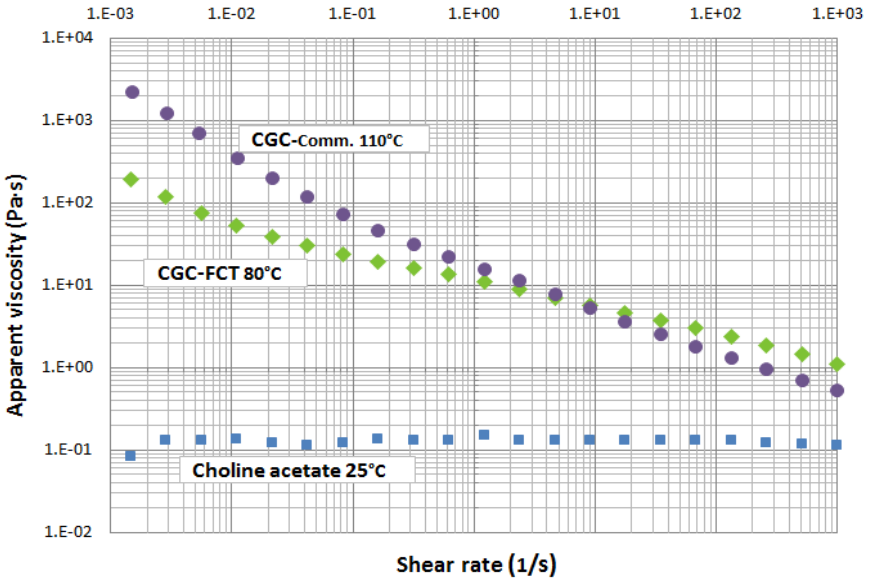

Fig. 3.7: Flow curve of CGC mixtures and choline acetate

The strain sweep measurement was carried out to estimate the linear viscoelastic region at a relative low frequency. Referring to this result, the dynamic frequency sweep measurements were carried out in linear response region for both samples. It was at controlled stress of 1 Pa for CGC-FCT mixture, and 0.3 Pa for CGC-commercial mixture.

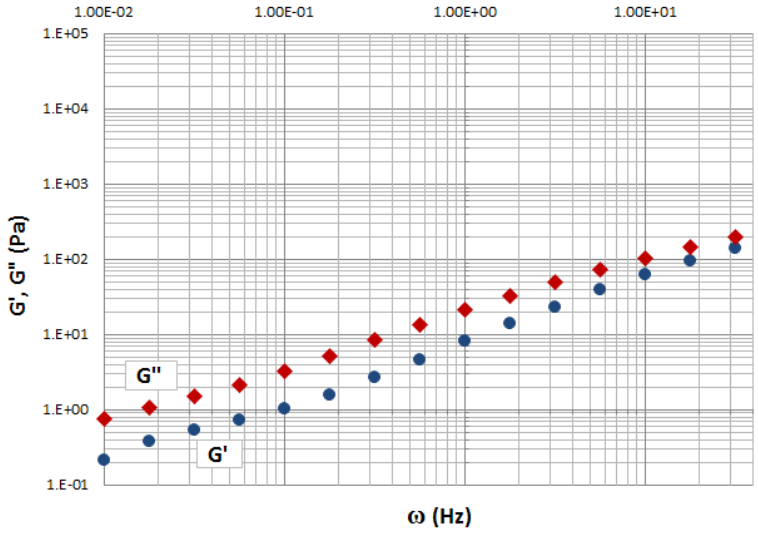

Fig. 3.8: Mechanical Spectrum of CGC-FCT film forming mixtures

Regarding the viscoelastic property, it can be observed from Fig.3.8 that the viscous modulus (G'') higher than the elastic modulus (G'). Both G' and G'' values gradually increase but they do not crossover in the entire frequency range. Such frequency dependence nature in this measurement is the signature of the typical behaviour of a viscous solution with entangled polymer chains.

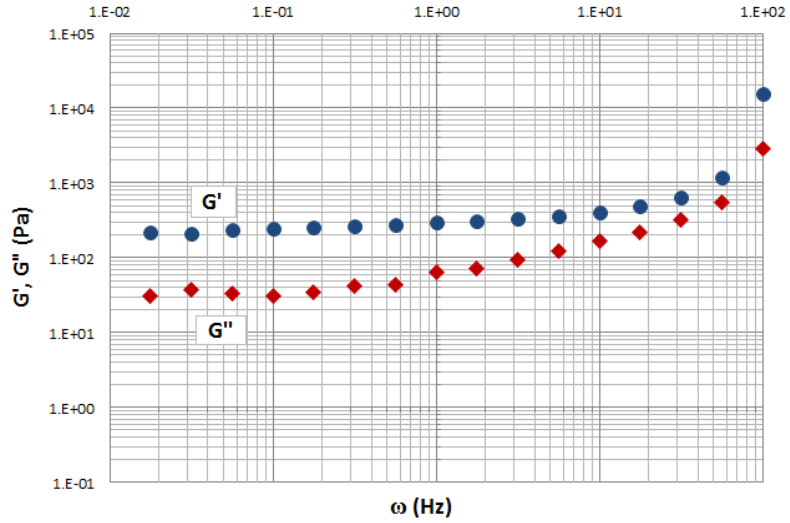

Fig. 3.9: Mechanical Spectrum of CGC-Commercial film forming mixtures

Both the elastic modulus (G') and the viscous modulus (G'') are almost independent of angular frequency. As shown in Fig.3.9, G' exhibits the plateau region at the lower frequency range and G' is always higher than G'' along the entire frequency range. This is the typical behaviour of strong gel.

Additionally, for a strong gel, elastic modulus (G') is typically 10 times larger than the viscous modulus (G'') in plateau region. However, for a soft gel or a physical gel, G' is often almost the same or less than G''. As shown in Fig.3.8, G'' is 3-4 times higher than G' which also reveals that this sample behaves as soft gel.

3.2.2. Thermal properties of polymer mixtures and films

Thermal effects are distinct from the more or less straight line DSC curve. They are caused by the sample undergoing physical transitions or chemical reactions. Glass transition temperature (T_g) was taken at half-height of heat capacity increment. Crystallization (T_c) and melting (T_m) temperatures were taken at the peak maximum of the corresponding exotherm and endotherm. The glass transition temperature of polymer mixtures and generated polymeric structure is presented in Table 3.5.

Table 3.5: Glass transition temperature (T_g) of polymer mixtures and generated polymeric structure

Samples	Glass transition temp. (T_g)
CGC FCT	ND
CGC Commercial	ND
Choline Acetate	-88.34 °C
CGC FCT+Choline acetate 80 °C	-85.27 °C
CGC Comm.+Choline acetate 110 °C	-83.61 °C
CGC FCT film in Water	-97.72 °C
CGC FCT film in MeOH	-106.33 °C
CGC FCT film in Glycerol	-90.99 °C
CGC Comm. film in Water	-97.14 °C
CGC Comm. film in MeOH	-97.37 °C
CGC Comm. film in Glycerol	-92.50 °C

Dried CGC polymers were investigated by differential scanning calorimetry (DSC), see Fig. 3.10. The DSC curve showed an endothermal baseline shift associated with the glass transition (T_g) followed by a cold-crystallization exotherm (T_c) and, finally, by a melting endotherm (T_m).

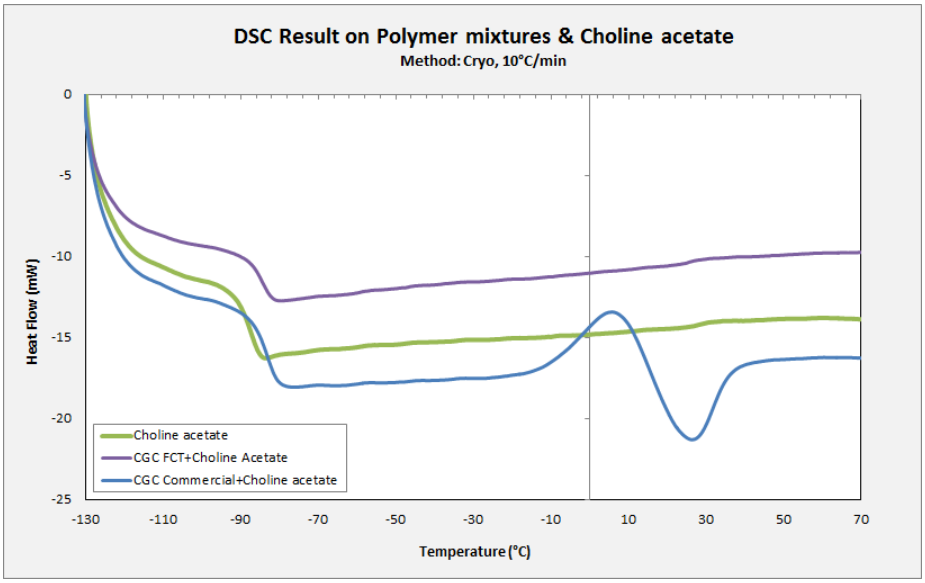

Fig. 3.10: DSC Result on dope solution and choline acetate (Cryo-DSC)

The transition from amorphous solid to crystalline solid is an exothermic process, and results in a peak in the DSC curve. Due to the continuous heating, the sample eventually reaches its melting temperature (T_m). The melting process results in an endothermic peak in the DSC curve. These T_c and T_m can only be seen in the mixture of commercial CGC and choline acetate, which is 5.52 °C and 26.21 °C respectively.

The result shows that the T_g of choline acetate is higher than the previous measurement [16]. This could be the reason why the DSC result of the CGC polymer and Choline acetate mixture for both polymer also gives higher T_g values compared with the result reported by Henrique Marçal [16].

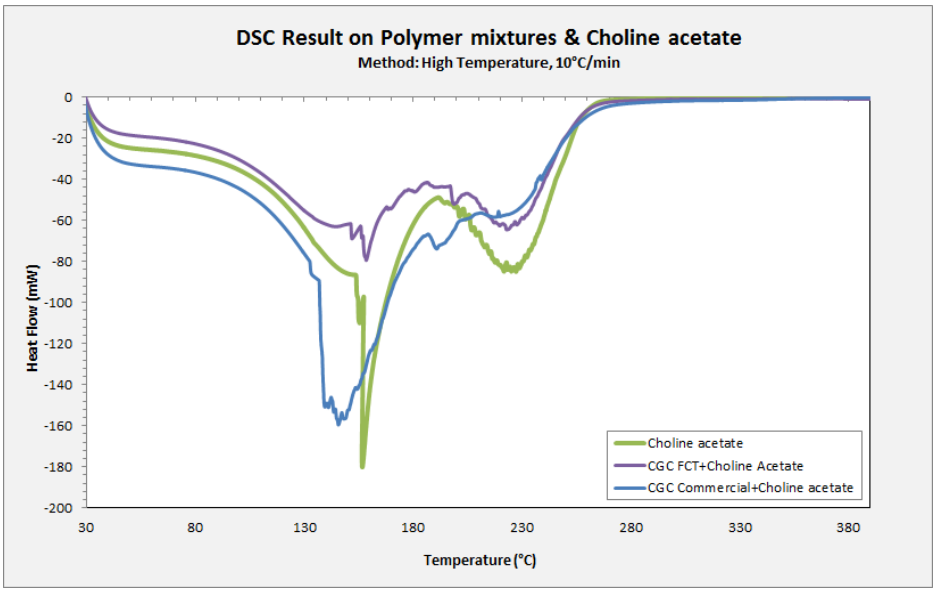

Fig. 3.11: DSC Result on dope solution and choline acetate (T>Ambient temperature)

From Fig. 3.11, it can be noticed as well that both polymer mixtures have similar thermogram behaviours as Choline acetate. This could be addressed to the fact that Choline acetate is the used solvent in both mixtures. Even though the chemical reaction might be happened during the dissolution, however it can be identified that its composition is still dominating the mixture properties.

From Fig. 3.12 and Fig. 3.13, it can be observed that the polymer mixtures and choline acetate underwent dehydration between temperature 80 °C and 150 °C. They were decomposed at temperature close to 230 °C. The precise value of dehydration and decomposition temperature is shown in Table 3.6.

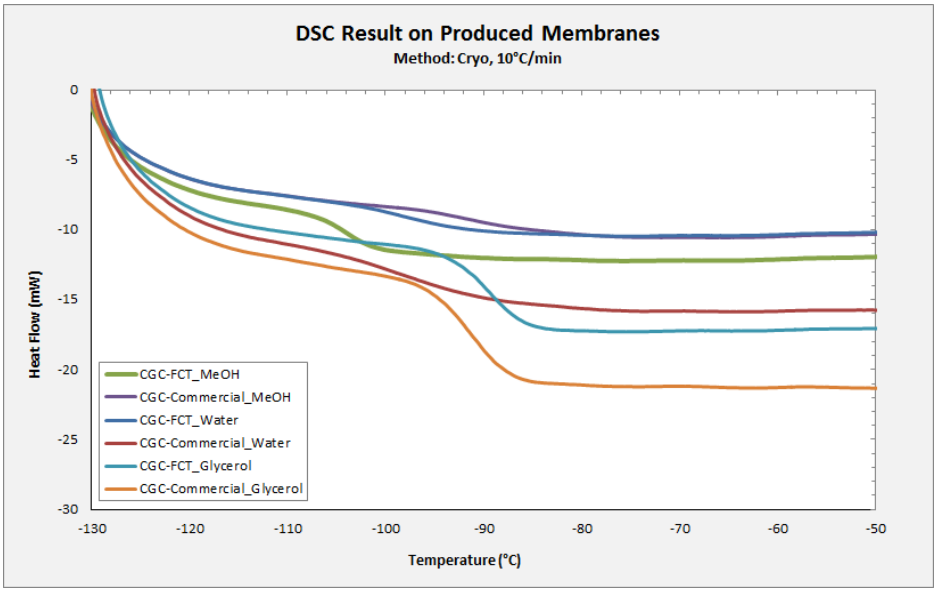

Fig. 3.12: DSC Result on produced membranes (Cryo-DSC)

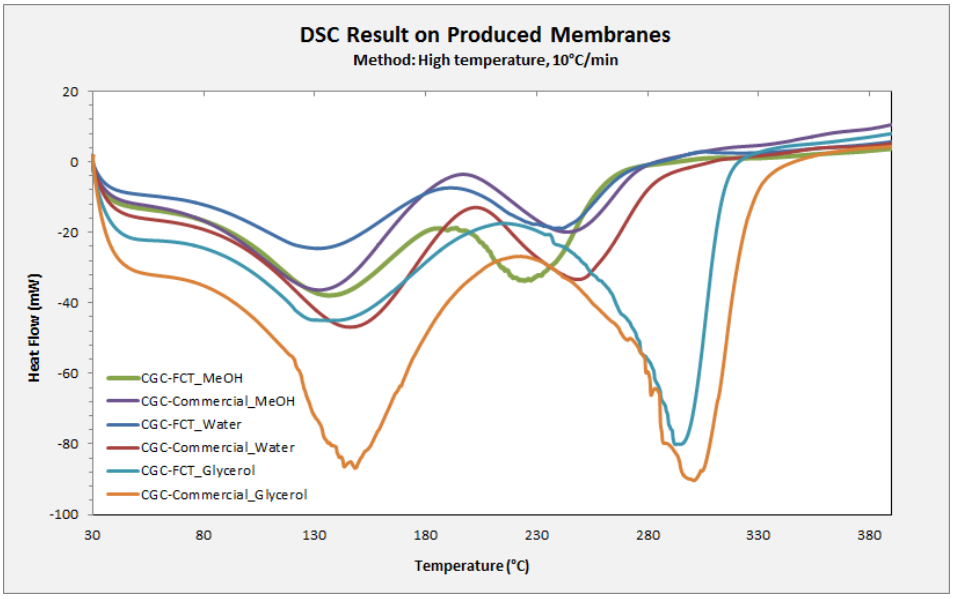

Fig. 3.13: DSC Result on produced membranes (T>Ambient temperature)

Membranes that are produced by immersion in the same non-solvent show the same thermogram behaviour. From Fig. 3.13, it can be observed that all membranes underwent dehydration between temperature 80°C and 150°C. CGC-FCT and CGC-Commercial membranes immersed in glycerol have higher degradation and decomposition temperature compared with the produced membranes immersed in water and methanol. The difference is that the membrane produced with the commercial CGC has higher transition enthalpy compared to CGC-FCT membranes.

Table 3.6: Melting temperature and decomposition temperature of polymer mixtures and membranes

Samples	1st degradation (dehydration) temperature	2nd degradation (decomposition) temperature
Choline Acetate	156.68 °C	227.24 °C
CGC FCT+Choline acetate 80 °C	158.46 °C	222.99 °C
CGC Comm.+Choline acetate 110 °C	145.68 °C	190.81 °C
CGC FCT film in Water	131.49 °C	241.28 °C
CGC FCT film in MeOH	136.35 °C	224.45 °C
CGC FCT film in Glycerol	136.16 °C	292.60 °C
CGC Comm. film in Water	145.85 °C	248.25 °C
CGC Comm. film in MeOH	132.07 °C	243.44 °C
CGC Comm. film in Glycerol	148.16 °C	300.66 °C

All membranes encountered melting with decomposition behaviour. It can be recognized by the appearance of the second endothermic curve. These phenomena occurred due to the presence of impurities [29].

3.2.3. Sugar constituents in CGC films

During the phase inversion, the non-solvent was not only precipitated choline acetate but also sugar components from the casted polymer. Hence, it is necessary to study the sugar composition in our produced films and gels. For the determination of sugar composition, the gnerated films and gel were hydrolysed and analysed by HPLC as described in section 2.3.3. The composition of glucosamine, glucan and mannose in CGC produced films and gel is summarized in Table 3.7.

Table 3.7: Sugar composition in produced films and gel

Polymer	Glucosamine Conc. (ppm)	Glucan Conc. (ppm)	Mannose Conc. (ppm)	Ratio Glucosamine and Glucan
CGC-FCT Water	19.09	223.48	16.05	1:11.68
CGC-FCT MeOH	12.07	126.79	10.50	1:10.50
CGC-FCT Glycerol	5.34	73.08	9.70	1:13.68
CGC-Comm. Water	36.64	202.77	19.81	1: 5.53
CGC-Comm. MeOH	12.98	205.50	20.26	1:15.83
CGC-Comm. Glycerol	7.12	59.74	7.72	1:8.39

In general, the sugar composition is found higher in the membrane immersed in water as non-solvent, followed by methanol and glycerol. This phenomenon could be explained from the fact that the membrane is organic and water is an aqueous solvent where methanol and glycerol are an organic solvent. Hence, during the phase inversion, water will dissolve less sugar, followed by methanol because methanol only has one OH group. The non-solvent that could attract and interrupt most with our polysaccharide is glycerol because glycerol has three OH group, known as tri-hydroxyl alcohol. Hence, the sugar composition was found in small amount in the produced polymeric structures. The molecular structure of water, methanol and glycerol is presented in Fig. 3.14.

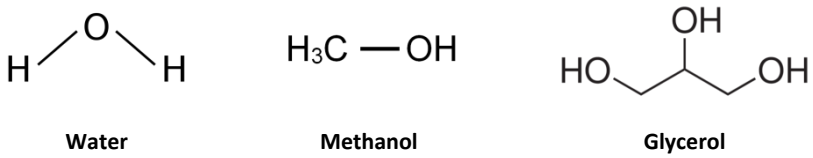

Fig. 3.14: Molecular structure of non-solvents

The ratio of glucosamine and glucan is reduced a lot compared with its ratio when is still in the polymer form. This could be due to the different solubility between glucan and glucosamine in ionic liquid. Glucosamine is known to be more difficult to dissolve than Glucan. As the consequence, glucosamine is easier to be washed out during the immersion precipitation process where glucan is able to maintain its composition in the casted polymer. Hence, in the end the composition of glucan in the membrane is much higher compared with glucosamine.

3.2.4. Total sugar analysis in coagulation bath

Total sugar analysis in the coagulation baths was measured using Dubois method. Phenol in the presence of sulphuric acid can be used for the quantitative colorimetric micro determination of sugars and their methyl derivatives, oligosaccharides, and polysaccharides [18]. The colour produced is

permanent and stable, thus it is used for quantification. The result of the measurement is presented in Table. 3.8

Table 3.8: Total sugar content in coagulation bath

Polymer	Total Sugar (mg/L)
CGC-FCT Water	45.28
CGC-FCT MeOH	193.08
CGC-FCT Glycerol	52.05
CGC-Commercial Water	81.99
CGC-Commercial MeOH	74.88
CGC-Commercial Glycerol	149.29

The measurement was done two times. It was observed that CGC-FCT mixture precipitated more sugar when it was immersed in methanol compared to other non-solvent, namely water and glycerol.In the case of CGC-Commercial, it was observed that this mixture released most sugar when it was immersed in glycerol followed by other non-solvent, which are water and methanol respectively.

3.2.5. Contact Angle Analysis

Water contact angle measurement is the most common method for determining a material wettability. If the solid surface is hydrophilic, the contact angle will be less than 90°. The contact angle for produced films is presented in Fig. 3.15.

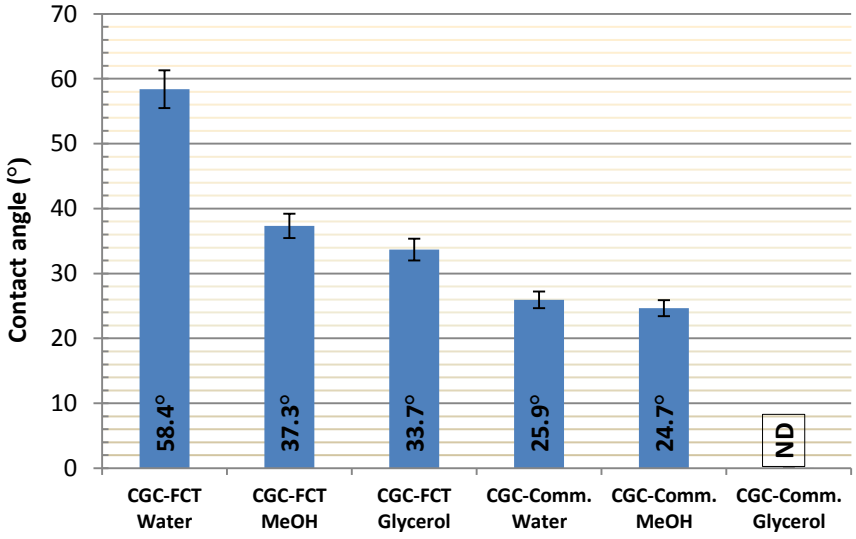

Fig. 3.15: Contact angle of CGC films produced in different non-solvents

The result reveals the hydrophilic nature of CGC films. The hydrophilicity is one of the most important factors that affect the cytocompatibility of biomaterials. The cell adhesion and growth are directly influenced by the wettability of the surfaces, once a major part of the cells prefers to anchor in hydrophilic surfaces [31]. However, for CGC-Commercial polymer immersed in glycerol is not possible to measure the contact angle because its polymeric structure is gel.

It is important to understand that in this experiment the associated gross error is significant. In each trial, several samples replicates were used to have a stable measurement. The concluding result recorded was for the trial considered by the operator to be the best. For best results the contact angle recorded in the first 100 ms was considered.

The characterization in the next phase would only involve the mechanical properties in term of puncture resistance and morphological study by SEM (Scanning Electron Microscopy) of the chosen films which are CGC-FCT and CGC-Commercial films generated with water as the non-solvent.

3.2.6. Puncture Test

Puncture helps to determine the stress at which the membrane will break. The puncture force (N) and the deformation (mm) of the probe at break were determined from the force deformation curves with the help of the TA-xT texture analyser software. Thickness of the membrane is measured using a micrometre. All experiments were performed in triplicate and the average values were calculated and given in Table 3.9.

For this measurement, only two types of films that were measured; CGC-FCT water and CGC-Commercial water. The stress strain data for the produced films in the present work is presented.

Table 3.9: Result of puncture test strain on CGC films

Sample	Thickness (µm)	Force at break (N)	$\tau_{puncture}$ (kPa)	Normalisation, $\tau_{puncture}$ (kPa) per thickness (µm)
CGC-FCT film	230±15	0.162	51.66	0.225
CGC-Commercial film	124±3	0.189	60.08	0.484

The force needed to puncture the CGC-FCT membranes and CGC-Commercial membranes is nearly the same. In average, 51 kPa is needed to puncture CGC-FCT membranes until it breaks and 60 kPa for CGC-Commercial ones. From the result in Table 3.9, it can be seen that CGC-Commercial can sustain more puncture stress ($\tau_{puncture}$) compared to CGC-FCT. However, from the behaviour of force deformation curve in Appendix IV, it can be observed that CGC-Commercial film is less ductile than CGC-FCT film.

The puncture stress and elongation at break are dependent on the membrane thickness. Hence, the membrane thickness can be used to normalise the puncture measurement in order to provide better correlation. Refer to the normalisation data, it can be concluded that with the same thickness, the film produced from CGC-Commercial is able to sustain forces two times higher compared to CGC-FCT film.

Table 3.10: Comparison of puncture stress with other polymers from the literature

Polymer	Thickness (µm)	$\tau_{puncture}$ (kPa)	Normalisation, $\tau_{puncture}$ (kPa) per thickness (µm)	Ref.
CGC-FCT	230	51.7	0.225	Present study
CGC (KiOnutrime®)	124	60.1	0.484	Present study
Chitosan	35	3.7	0.106	[45]
Chitosan	39.9	520.7	13.01	[49]
85% (v/v) Chitosan+ 15% (v/v) Guar Gum	35	11.0	0.314	[45]
Kefiran	74	678.5	9.17	[46]
Kefiran+Glycerol	64	636.6	9.95	[47]
Guar Gum+Glycerol	16.6	732.1	44.1	[48]
Whey Protein Isolate	50	3,676	73.59	[50]

Table 3.10 compares the puncture stress obtained in this work with selected examples from the literature. It shows that the obtained CGC films from this work have similar puncture resistance as chitosan film obtained from the literature [45]. Yet, it is relatively fragile compared with other films.

The elongation at break could not be measured due to a problem with the instrument. The device only began to register a value when it felt a minimum force of 0.05 N, at the time when the films already underwent elongation. Hence, the elongation data at break is not presented due to inaccuracy. The measurement curve depicting the applied force as a function of elongation is presented in the Appendix VI.

3.2.7. SEM Analysis

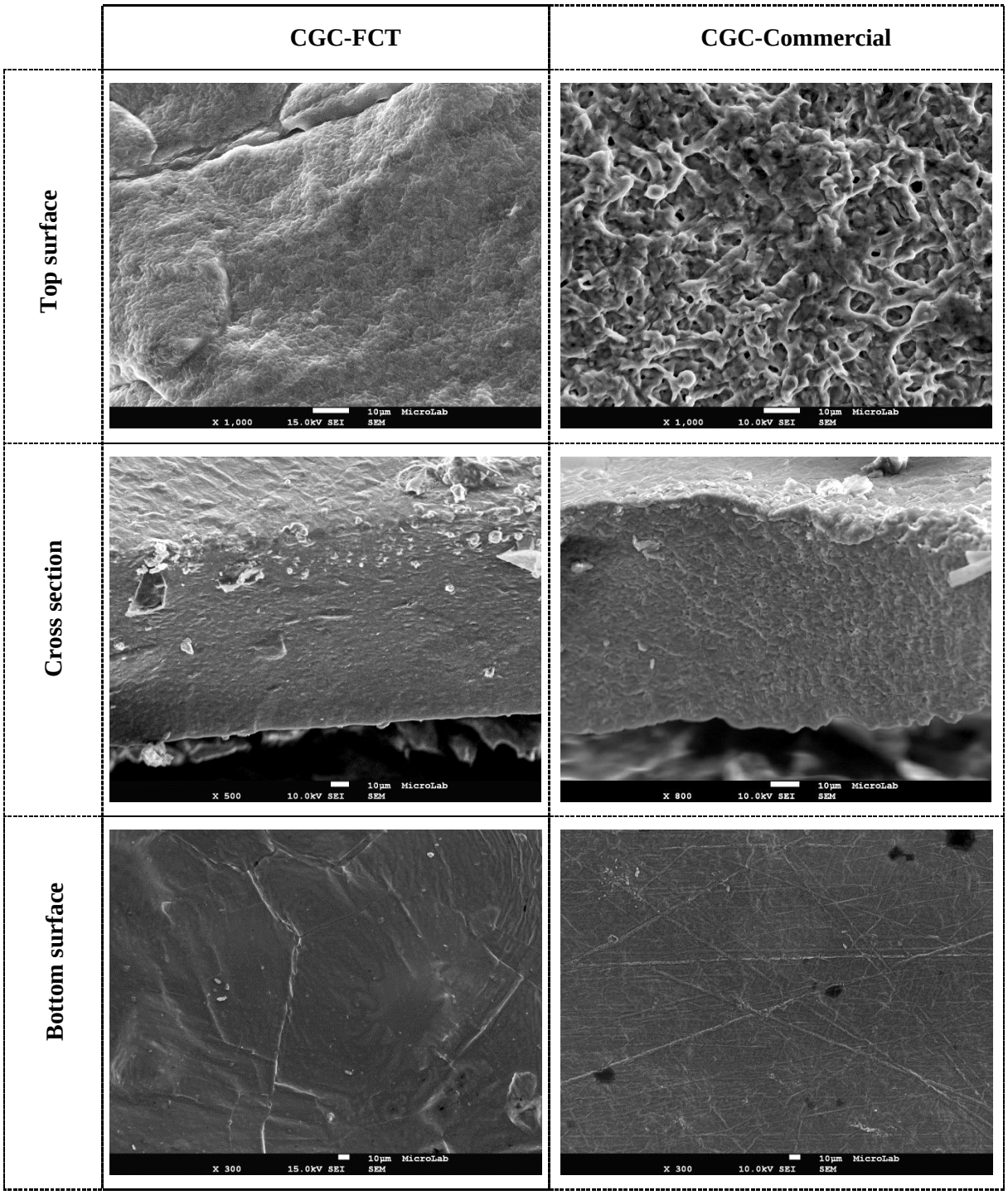

Fig. 3.16: SEM images of CGC films

The SEM analysis, in Fig.3.16, provides an adequate examination of film surface. It is clear from the images that distinctive film structures were formed on the surface. CGC-commercial has random pattern where CGC-FCT has smoother surface. From its cross section images, it is shown that both

membranes have dense polymeric structures. The bottom surface of both films seems more flat and has fingerprint of the mould.

Having some roughness on the surface could be a positive influence to promote dermal fibroblast adhesion as a strong basis for future healing on skin regeneration, whereas the dense structure could prevent the wound from secondary infection [51]. However, small free volumes in polymeric structure will be needed to enable gaseous exchange of O_2 and CO_2.

Refer to the result of viscoelasticity test in chapter 3.2.1, CGC-FCT mixture exhibits a typical behaviour of a viscous solution with entangled polymer chains, where it is reported by Prasad et al. that the entanglement of polymer chains in the case of casting solutions will result in dense resulting membranes [38]. Hence, this rheology data shows a good agreement with the dense CGC-FCT film structure observed by SEM.

During the phase inversion process, precipitation kinetics provides important fundamental information regarding the membrane formation process. *Delayed demixing* is the term commonly used in membrane preparation to refer to a low precipitation rate, whereas *instantaneous demixing* refers to a high precipitation rate lead to film formation immediately after immersion.

In this experiment, when the cast polymer mixture was contacted with the non-solvent, liquid‑liquid demixing occurs in low precipitation rate. It was observed that the film structure was not formed within finite period of time after immersion. Based on the literature [39], delayed demixing will result in a relatively dense film as it is confirmed by the SEM analysis.

The discrepancy result between CGC-FCT water and CGC-Commercial water for the contact angle measurement in chapter 3.2.5 could be explained from the SEM result. CGC-FCT water exhibits higher contact angle (58.4°) compared to CGC-Commercial (25.9°) water because its top surface is less rough. As it is known that hydrophilicity is highly influenced by surface roughness.

4. Conclusions

In this work, two different CGC, KiOnutrime from KitoZyme and biologically produced CGC from Biochemical Engineering group in FCT-UNL, were characterized in order to develop biocompatible wound dressing materials. The similarity of CGC-FCT and CGC-Commercial is shown in term of the ratio of chitin:glucan, which are 1:1.72 and 1:1.69 respectively. However, the other measurement showed different result. In general CGC-FCT contains more metal traces, water, inorganic salts and protein compared with the commercial one. The different characterization results between CGC-FCT and CGC-Commercial could be addressed to differences in the purification method, and its distinctive original strain yeast.

During the membranes preparation, different non-solvents were used in phase inversion method. The result indicates that composition of non-solvent in the coagulation bath has great influence in generated polymeric structure. Water was found to be the best coagulant for producing a CGC polymeric film structure. Intrinsic component of polymer mixtures and generated polymeric structures were characterized and compared.

The characterizations that have been done include the analysis of viscosity and viscoelasticity measurement, as well as sugar composition in the membrane and total sugar that was released during precipitation. The rheology test shows that both polymer mixtures exhibit a non-Newtonian shear thinning behaviour. Where the viscosity and viscoelasticity test reveal that CGC-FCT mixture has a typical behaviour of a viscous solution with entangled polymer chains and CGC-Commercial mixture exhibits true gel behaviour.

To the best of our knowledge, this is the first time that choline acetate was used to regenerate CGC polymeric solution. This experiment result shows us that the generated CGC solution from choline acetate could be used to develop film structure and gel. The generated polymeric structures are thermally stable at 100°C, and are hydrophilic. The produced films have dense structure and mechanical stabilities against puncture up to 62 kPa.

5. Future Work

To guarantee the potential use of generated CGC films as a wound dressing material, further investigation are essential. One of the most important tests is a biocompatibility study. It can be done in-vitro by using fibroblast cell in order to assure that the material is safe for medical usage and able to promote the cell proliferation for new skin regeneration.

An ideal dressing should maintain evaporative water loss from the skin at an optimal rate to provide an adequate level of moisture [22]. The vapour permeability through the film for wound dressing is important to keep the wound comfortable and help in the healing process, where excessive dehydration can result in scar formation. Thus, water vapour permeation is important to be studied.

Besides all other properties, a transfer efficacy of CO_2 and O_2 will be an important aspect for cell growth. A dressing material has to possess adequate permeance for those gases. It is one of important factor for cell seeding which affects distribution of cell suspension throughout the material.

It was observed during the experiment that the generated films from CGC dissolution in ionic liquid are fragile. For that reason, the improvement of the mechanical properties of the produced film could be considered in the future. This could be done by using cross-linker or combining CGC with another biopolymer that could raise its mechanical properties.

Because this work related with introducing a new solvent for biopolymer dissolution, it will be interesting to have FTIR and NMR analysis to confirm the dissolution of CGC in choline acetate.

6. References

[1] Kyoko Kofuji, Yuzhou Huang, Kazufumi Tsubaki, Fumihiko Kokido, Kazunori Nishikawa, Takashi Isobe, Yoshifumi Murata. *Preparation and evaluation of a novel wound dressing sheet comprised of β-glucan–chitosan complex*. Reactive & Functional Polymers 70 (2010) 784–789.

[2] Andrew C.A. Wan, Benjamin C.U. Tai. *CHITIN - A promising biomaterial for tissue engineering and stem cell technologies*. Biotechnology Advances 31 (2013) 1776–1785.

[3] Simone S. Silva, Ana Rita C. Duarte, Ana Paula Carvalho, João F. Mano, Rui L. Reis. *Green processing of porous chitin structures for biomedical applications combining ionic liquids and supercritical fluid technology*. Acta Biomaterialia 7 (2011) 1166–1172.

[4] C.K.S. Pillai, Willi Paul, Chandra P. Sharma. *Chitin and chitosan polymers: Chemistry, solubility and fiber formation*. Progress in Polymer Science 34 (2009) 641-678.

[5] R. Jayakumar, M. Prabaharan, P.T. Sudheesh Kumar, S.V. Nair, H. Tamura. *Biomaterials based on chitin and chitosan in wound dressing applications*. Biotechnology Advances 29 (2011) 322–337.

[6] Andrew C.A. Wan, Benjamin C.U. Tai. *CHITIN - promising biomaterial for tissue engineering and stem cell technologies*. Biotechnology Advances 31 (2013) 1776-1785.

[7] Samuel M. Hudson, David W. Jenkins. *Chitin and chitosan, Encyclopedia of Polymer Science and Technology*, John Wiley, 569–580.

[8] Christophe Roca, Bárbara Chagas, Inês Farinha, Filomena Freitas, Luís Mafra, Filipe Aguiar, Rui Oliveira, Maria A.M. Reis. *Production of yeast chitin-glucan complex from biodiesel industry by product*. Process Biochemistry 47 (2012) 1670-1675.

[9] Lysing Enzymes. Available: http://www.sigmaaldrich.com/life-science/metabolomics/enzyme-explorer/learning-center/lysing-enzymes.html#sthash.uvGHl7JY.dpuf . Accessed 04.06.2014.

[10] Stoscheck C. M. *Quantitation of protein*. Methods Enzymol 182 (1990) 50–69.

[11] Thi Phuong Thuy Pham, Chul-Woong Cho, Yeoung-Sang Yun. *Environmental fate and toxicity of ionic liquids: A review*. Water research 44 (2010) 352–372.

[12] Fangchao Cheng, Hui Wang, Gregory Chatel, Gabriela Gurau, Robin D. Rogers. *Facile pulping of lignocellulosic biomass using choline acetate*. Bioresource Technology 164 (2014) 394‑401.

[13] Varadhi Govinda, P. Madhusudhana Reddy, Pankaj Attri, P. Venkatesu, P. Venkateswarlu. *Influence of anion on thermophysical properties of ionic liquids with polar solvent*. The Journal of Chemical Thermodynamics 58 (2013) 269–278.

[14] Joana M. Lopes, Ana B. Paninho, Marta F. Môlho, Ana V.M. Nunes, Angelo Rocha, Nuno M.T. Lourenço, Vesna Najdanovic-Visak. *Biocompatible choline based ionic salts: Solubility in short-chain alcohols*. The Journal of Chemical Thermodynamics 67 (2013) 99-105.

[15] Molecular structure of Choline acetate ionic liquid. Available: http://www.chemspider.com/Chemical-Structure.9818719.html . Accessed 09.06.2014.

[16] Henrique Marçal. *Master thesis: Producao de Filmes de Quitina com Liquidos Ionicos Biocompativeis para Aplicacoes Biomedicas*. FCT-UNL, Portugal. 2013.

[17] Matthew C. Davis. Final report: New ionic liquids from natural products for environmental benign aircraft deicing and anti-icing. SERDP Project 2010.

[18] Michel Dubois, K.A.Gilles, J.K. Hamilton, P.A. Rebers, and Fred Smith. *Colorimetric Method for Determination of Sugars and Related Substances*. Analytical Chemistry 28 (1956) 350–356.

[19] A Biswas, RL Shogren, DG Stevenson, JL Willett. *Ionic liquids as solvents for biopolymers: Acylation of starch and zein protein*. Carbohydrate (2006) 546-550.

[20] EFSA (European Food Safety Authority) Panel on Dietetic Products, Nutrition and Allergies (NDA); *Scientific Opinion on the safety of "Chitin-Glucan" as a Novel Food ingredient*. EFSA Journal 8 (2010) 1687.

[21] Mulder, M. (2003). Basic Principles of Membrane Technology, 2nd edition. Kulwer Academic Publishers, The Netherlands.

[22] R.A.A. Muzzarelli, P. Morganti, G. Morganti, P. Palombo, M. Palombo, G. Biagini, M.M. Belmonte, F. Giantomassi, F. Orlandi, C. Muzzarelli. *Chitin nanofibrils/chitosan glycolate composites as wound medicaments*. Carbohydrate Polymers 70 (2007) 274–284.

[23] Riccardo A.A. Muzzarelli. *Chitins and chitosans for the repair of wounded skin, nerve, cartilage and bone*. Carbohydrate Polymers 76 (2009) 167–182.

[24] A. Anithaa, S. Sowmyaa, P.T. Sudheesh Kumara, S. Deepthia, K.P. Chennazhia, H. Ehrlichb, M. Tsurkanc, R. Jayakumara. *Chitin and chitosan in selected biomedical applications*. Progress in Polymer Science 83 (2014) 288-311.

[25] Lowry, O., Rosebrough, N., Fan, A., Randall, R. *Protein measurement with the folin phenol reagent*. J Biol Chem 193 (1951) 265–75.

[26] Henk J van de Wiel. *Determination of elements by ICP-AES and ICP-MS*. National Institute of Public Health and the Environment (RIVM) 2003. Bilthoven, The Netherlands.

[27] Geoffrey Tyler. Product Specification: *ICP-MS, or ICP-AES and AAS? - A comparison*. Varian Australia Pty Ltd 1994. Australia.

[28] KitoZyme Patent: *Cell wall derivatives from biomass and preparation thereof*. Available: http://www.lens.org/images/patent/WO/2003068824/A1/WO_2003_068824_A1.pdf . Accessed 22.06.2014.

[29] Differential Scanning Colorimetry. University of Bradford, 2006. Available: http://www.mmsconferencing.com/pdf/eyp/c.rawlinson.pdf . Accessed 26.06.2014.

[30] Yuan, Y., and T. R. Lee. *Surface Science Techniques*. (Eds.2) G. Bracco, B. Holst.2013. ISBN: 978-3-642-34242-4

[31] D. Archana, Joydeep Dutta, P.K. Dutta. *Evaluation of chitosan nano dressing for wound healing: Characterization, in vitro and in vivo studies*. International Journal of Biological Macromolecules 57 (2013) 193–203.

[32] Florence Croisier, Christine Jérôme. *Chitosan-based biomaterials for tissue engineering*. European Polymer Journal 49 (2013) 780–792.

[33] International Oenological Codex - COEI-1-CHITGL: 2009. *Chitin-Glucan*. Available: http://www.oiv.int/oiv/info/enplubicationoiv#codex . Accessed 04.07.2014.

[34] Sigma Aldrich. *ChemFiles: Ionic Liquids. Voume 6, Nomer 9, 2006.* Available: http://www.sigmaaldrich.com/content/dam/sigma-aldrich/docs/Aldrich/Brochure/al_chemfile_v6_n9.pdf . Accessed 05.07.2014.

[35] Hongyang Ma, Benjamin S. Hsiao, Benjamin Chu. *Thin-film nanofibrous composite membranes containing cellulose or chitin barrier layers fabricated by ionic liquids*. Polymer 52 (2011) 2594–2599.

[36] Jianmei Lua, Feng Yana, John Texter. *Advanced applications of ionic liquids in polymer science*. Progress in Polymer Science 34 (2009) 431–448

[37] Yusong Wu, Takashi Sasaki, Satoshi Irie, Kensuke Sakurai. *A novel biomass-ionic liquid platform for the utilization of native chitin*. Polymer 49 (2008) 2321–2327.

[38] Kamalesh Prasad, Masa-aki Murakami, Yoshiro Kaneko, Akihiko Takada, Yoshifumi Nakamura, Jun-ichi Kadokawa. *Weak gel of chitin with ionic liquid, 1-allyl-3-methylimidazolium bromide.* International Journal of Biological Macromolecules 45 (2009) 221–225.

[39] Akihiko Takegawa, Masa-aki Murakami, Yoshiro Kaneko, Jun-ichi Kadokawa. *Preparation of chitin/cellulose composite gels and films with ionic liquids*. Carbohydrate Polymers 79 (2010) 85–90.

[40] S.S. Silva, T.C. Santos, M.T. Cerqueira, A.P. Marques, L.L. Reys, T.H. Silva, S.G. Caridade, J.F. Manoa, and R.L. Reisa. *The use of ionic liquids in the processing of chitosan/silk hydrogels for biomedical applications.* Green Chemistry 14 (2012) 1463-1470.

[41] Simone S. Silva, Ana Rita C. Duarte, Ana Paula Carvalho, João F. Mano, Rui L. Reis. *Green processing of porous chitin structures for biomedical applications combining ionic liquids and supercritical fluid technology*. Acta Biomaterialia **7 (**2011) 1166–1172.

[42] Duan-Jian Tao, Zheng Cheng, Feng-Feng Chen, Zhang-Min Li, Na Hu, and Xiang-Shu Chen. *Synthesis and Thermophysical Properties of Biocompatible Cholinium-Based Amino Acid Ionic Liquids*. J. Chem. Eng. Data 58 (2013) 1542−1548.

[43] R. M. Vrikkis, K.J. Fraser, K. Fujita, D.R. MacFarlane and G.D. Elliott. *Biocompatible Ionic Liquids: A New Approach for Stabilizing Proteins in Liquid Formulation*. Journal of Biomechanical Engineering 131 (2009) 074514-1: 074514-4.

[44] Marija Petkovic, Jamie L. Ferguson, H. Q. Nimal Gunaratne, Rui Ferreira, Maria C. Leitao, Kenneth R. Seddon, Luis Paulo N. Rebeloa. *Novel biocompatible cholinium-based ionic liquids-toxicity and biodegradability*. Green Chem. 12 (2010) 643-649.

[45] M.S. Rao, S.R. Kanatt, S.P. Chawla, A. Sharma. *Chitosan and guar gum composite films: Preparation, physical, mechanical and antimicrobial properties*. Carbohydrate Polymers 82 (2010) 1243–1247.

[46] Mohsen Zolfi, Faramarz Khodaiyan, Mohammad Mousavi, Maryam Hashemi. *The improvement of characteristics of biodegradable films made from kefiran–whey protein by nanoparticle incorporation.* Carbohydrate Polymers 109 (2014) 118–125.

[47] Mehran Ghasemlou, Faramarz Khodaiyan, Abdulrasoul Oromiehie. *Physical, mechanical, barrier, and thermal properties of polyol-plasticized biodegradable edible film made from kefiran*. Carbohydrate Polymers 84 (2011) 477–483.

[48] Chaturbhuj K. Saurabh, Sumit Gupta, Jitendra Bahadur, S. Mazumder, Prasad S. Variyar, Arun Sharma. *Radiation dose dependent change in physiochemical, mechanical and barrier properties of guar gum based films*. Carbohydrate Polymers 98 (2013) 1610–1617.

[49] J. Li, S. Zivanovic, P.M. Davidson, K. Kit. *Characterization and comparison of chitosan/PVP and chitosan/PEO blend films*. Carbohydrate Polymers 79 (2010) 786–791.

[50] Lizhe Wang, Mark A.E. Auty, Joe P. Kerry. *Physical assessment of composite biodegradable films manufactured using whey protein isolate, gelatine and sodium alginate.* Journal of Food Engineering 96 (2010) 199–207.

[51] H.V. Pawar, J. Tetteh, J.S. Boateng. *Preparation, optimisation and characterisation of novel wound healing film dressings loaded with streptomycin and diclofenac*. Colloids and Surfaces B: Biointerfaces 102 (2013) 102–110.

7. Appendices

Appendix I: Specification of CGC-Commercial

KitoZyme

V123264

Specifications
KIOnutrime-CG®

Composition

	Specifications	Methods
Chitin-glucan content (% w/wet weight)	≥ 85	KZ PT-CQ-111
Loss on drying (% w/wet weight)	≤ 10	KZ PT-CQ-124

Heavy metals

	Specifications	Methods
Total heavy metals (mg/kg)	≤ 20	Total ICP-MS
Mercury (mg/kg)	≤ 0.1	ICP-MS
Lead (mg/kg)	≤ 1	ICP-MS
Arsenic (mg/kg)	≤ 1	ICP-MS
Cadmium (mg/kg)	≤ 0.5	ICP-MS

Microbial

	Specifications	Methods
Total viable aerobic microbial count (cfu/g)	≤ 1000	ISO4833
Total yeasts and molds count (cfu/g)	≤ 1000	ISO7954
Escherichia coli/1g	≤ 10	EP 2.6.12
Bile-tolerant gram-negative/1g	≤ 10	EP 2.6.12
Salmonella	Absence/25g	ISO 6579
Listeria monocytogenes	Absence/25g	ISO 11290-1

Physico-chemical and organoleptic characteristics

	Specifications	Methods
Granulometry (% w/wet weight)	≥ 90% trough 180 µm	KZ PT-CQ-117
Tapped density (g/cm³)	0.7 - 1	EP2.9.34
Appearance	Fine free-flowing powder	Visual observation
Aspect	Light yellowish to brown	KZ PT-CQ-120
Odor	Odorless	KZ PT-CQ-127

Labelling – Ingredient list: chitin-glucan
Chemical Name: chitin, beta-glucan.
CAS: [1398-61-4]; [9041-22-9]

Store at room temperature
Shelf life: 36 months

KitoZyme sa
Rue Haute Claire 4 • Parc Industriel des Hauts Sarts, Zone 2 • 4040 Herstal - Belgium
tel +32 4 259 85 00 • fax +32 4 259 85 09 • info@kitozyme.com • www.kitozyme.com
VAT BE 0473 676 932 Liège • Dexia 068 2332141 94

Appendix II: Sugar Constituents by HPLC

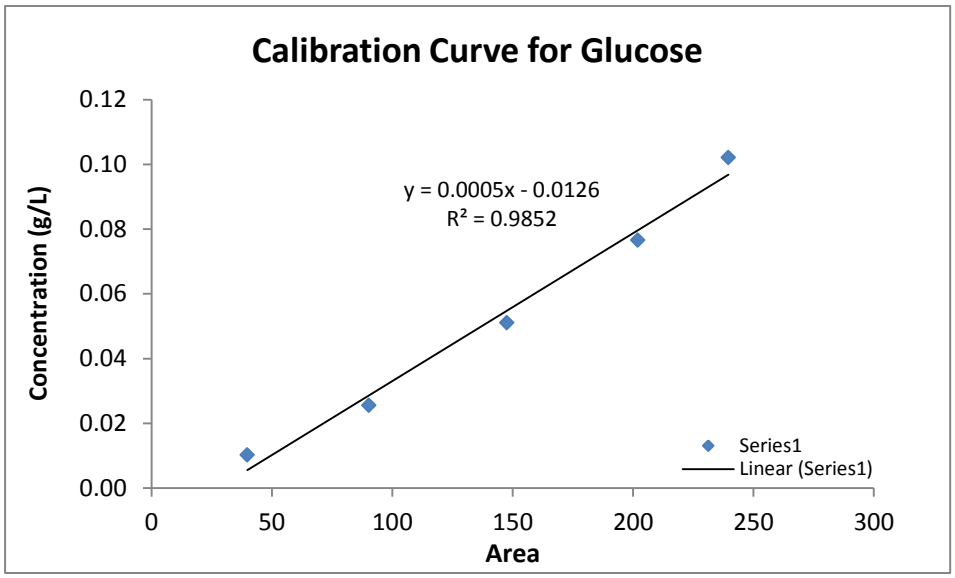

Fig. 7.1: Calibration curve represents Glucose concentration as a function of area

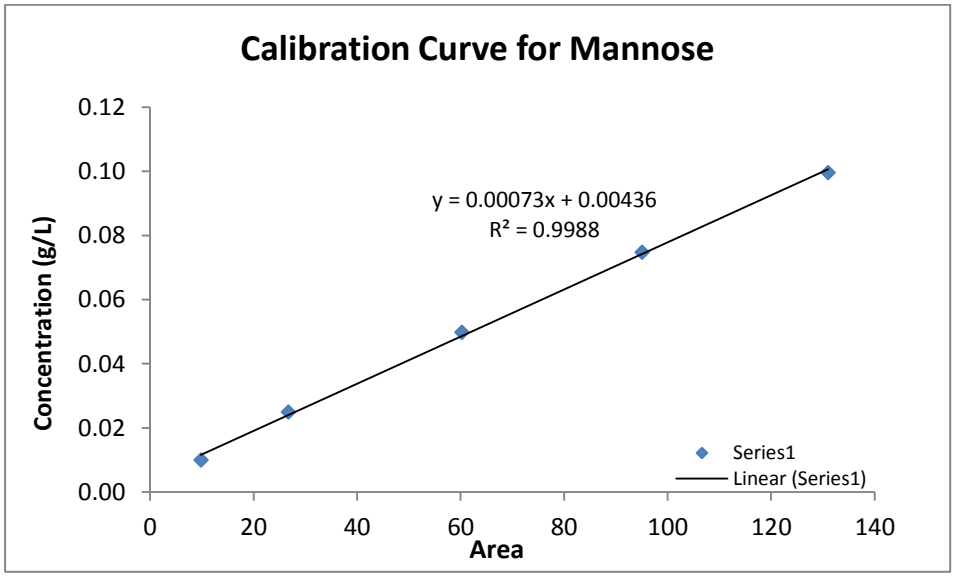

Fig. 7.2: Calibration curve represents Mannose concentration as a function of area

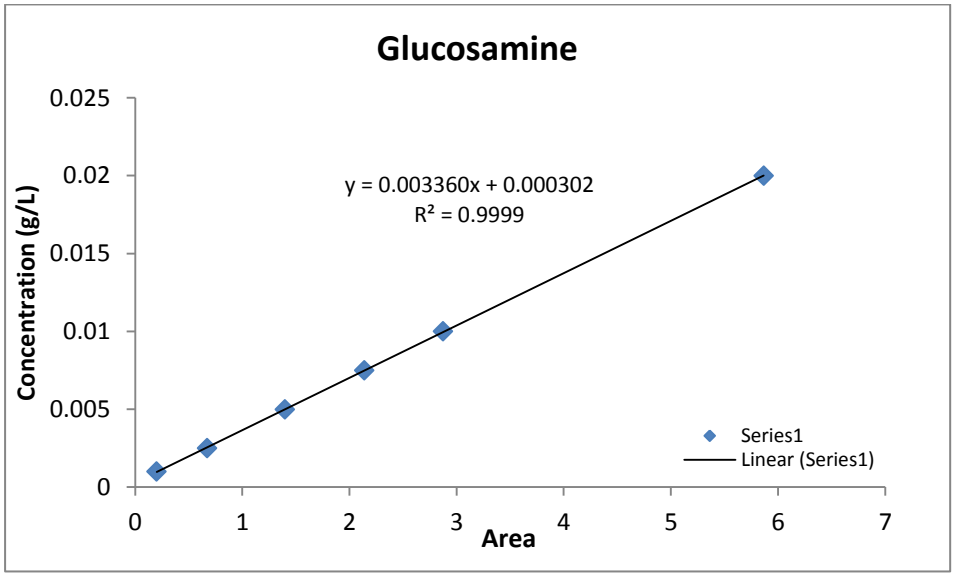

Fig. 7.3: Calibration curve represents glucosamine concentration as a function of area

Appendix III: Protein Analysis

Data of Albumin concentration and its absorbance, as the standard:

Table 7.1: Albumin data for standards

Mass of Albumin (mg)	Absorbance
0.00	0.044
0.55	0.640
1.54	1.549
2.99	2.357
4.57	2.638
6.11	>3.5

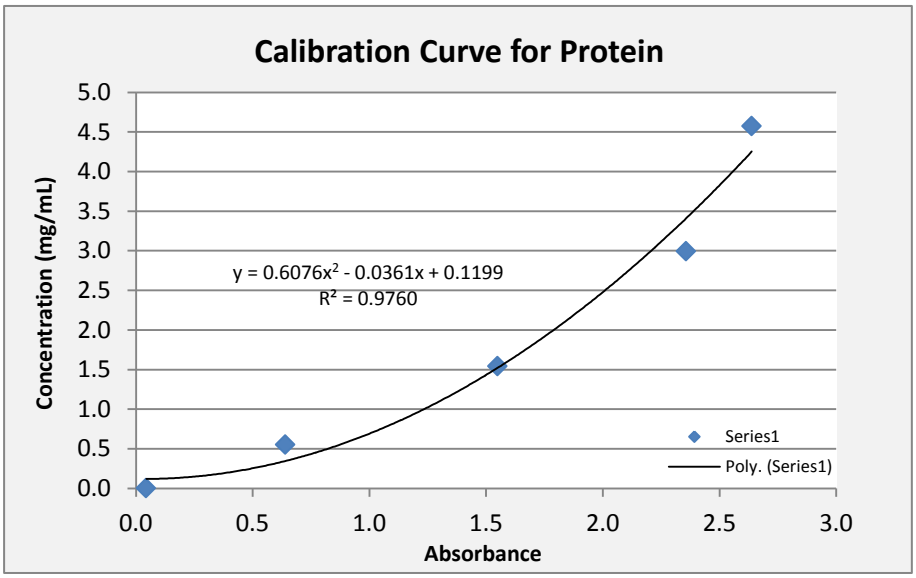

Fig. 7.4: Calibration curve represents the protein concentration as a function of absorbance

Appendix IV: DSC Analysis

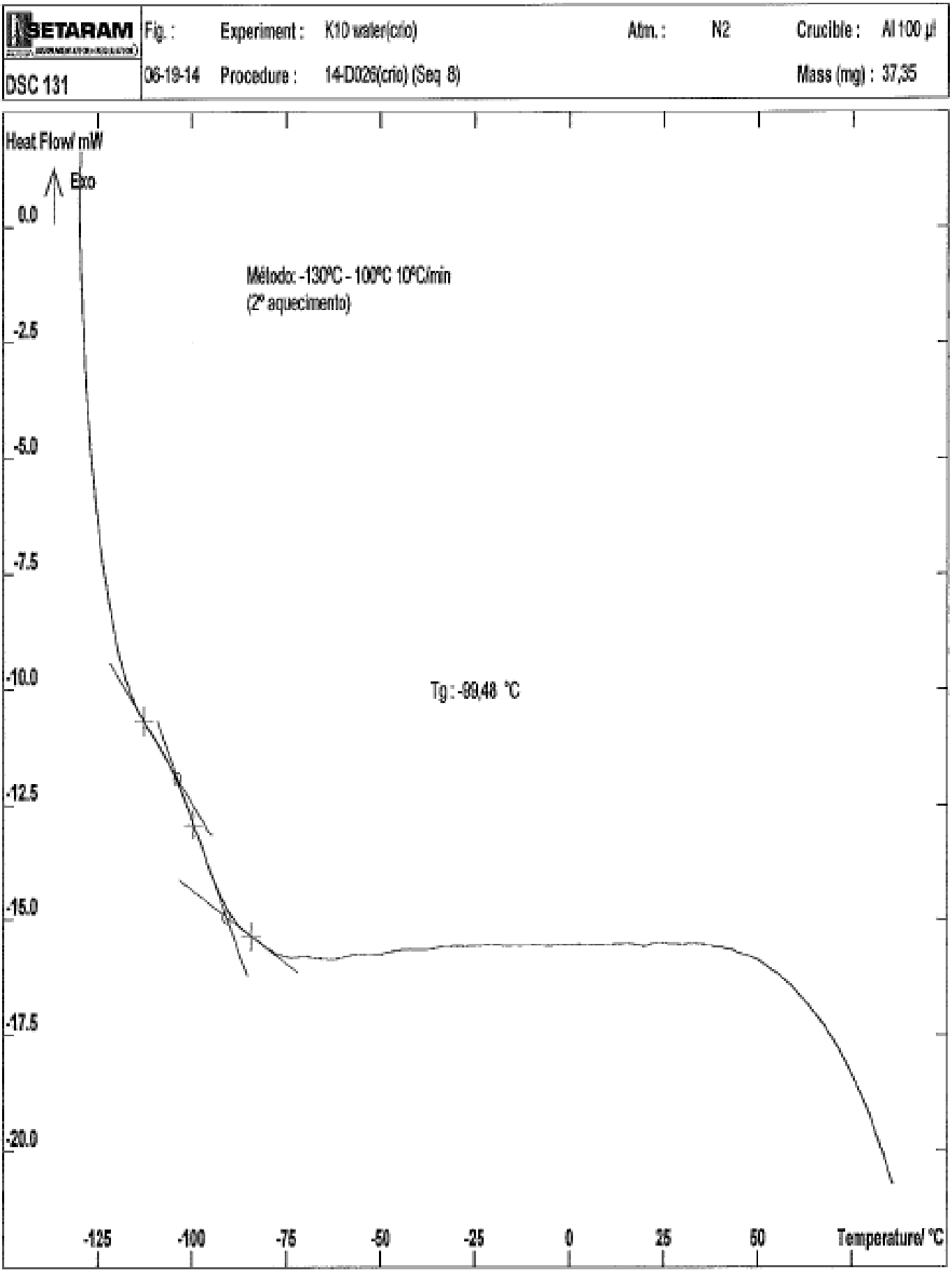

SETARAM INSTRUMENTATION - REGULATION	Fig. :	Experiment :	1(CSC)	Atm. :	N2	Crucible :	Al 100 µl
DSC 131	04-22-14	Procedure :	14-D017 (Seq 2)			Mass (mg) :	14,107

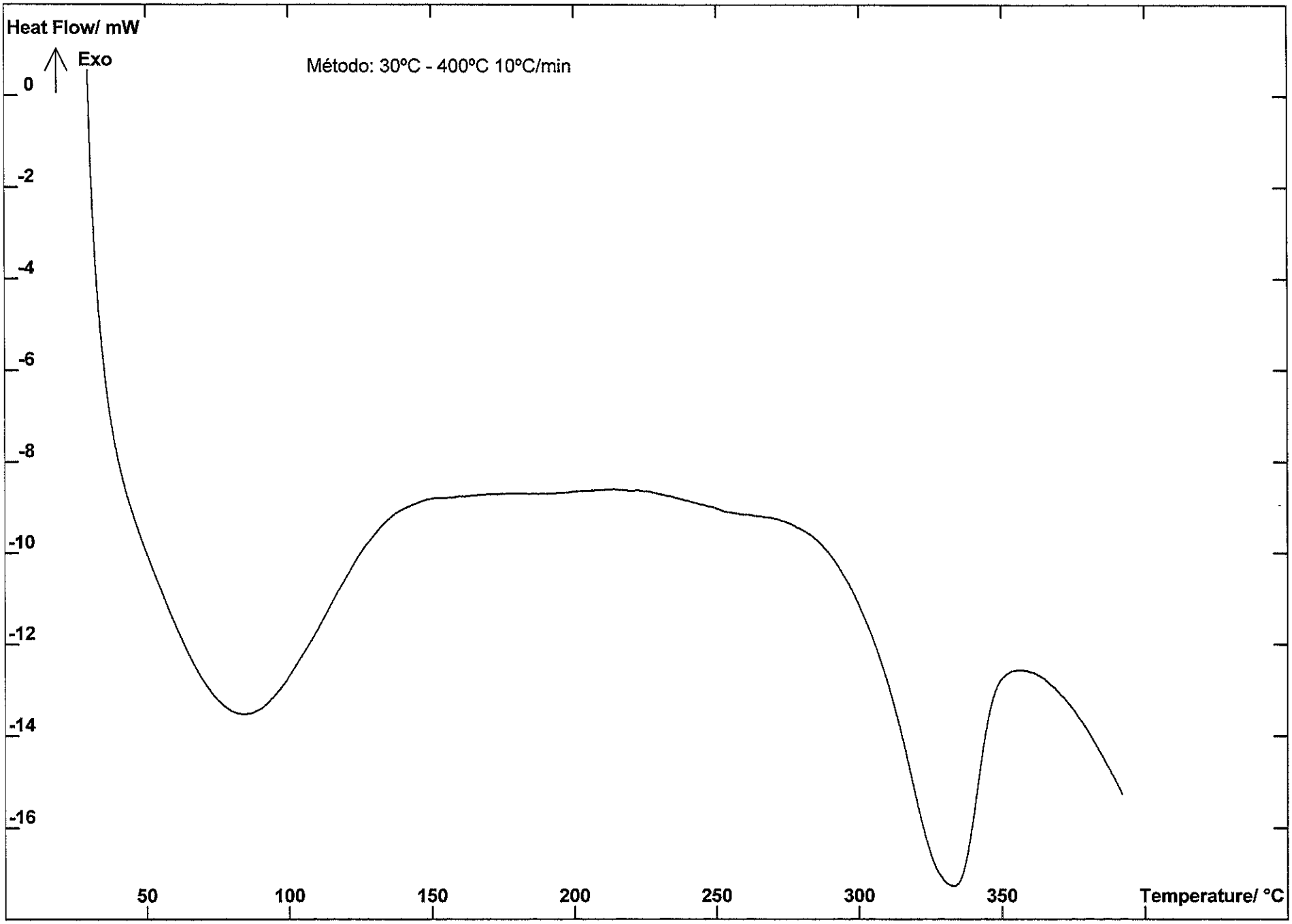

SETARAM INSTRUMENTATION - REGULATION

DSC 131

Fig. :		Experiment :	1(CGC)(crio)	Atm. :	N2	Crucible :	Al 100 µl
04-29-14		Procedure :	14-D012/013/014 (Seq 4)			Mass (mg) :	10,735

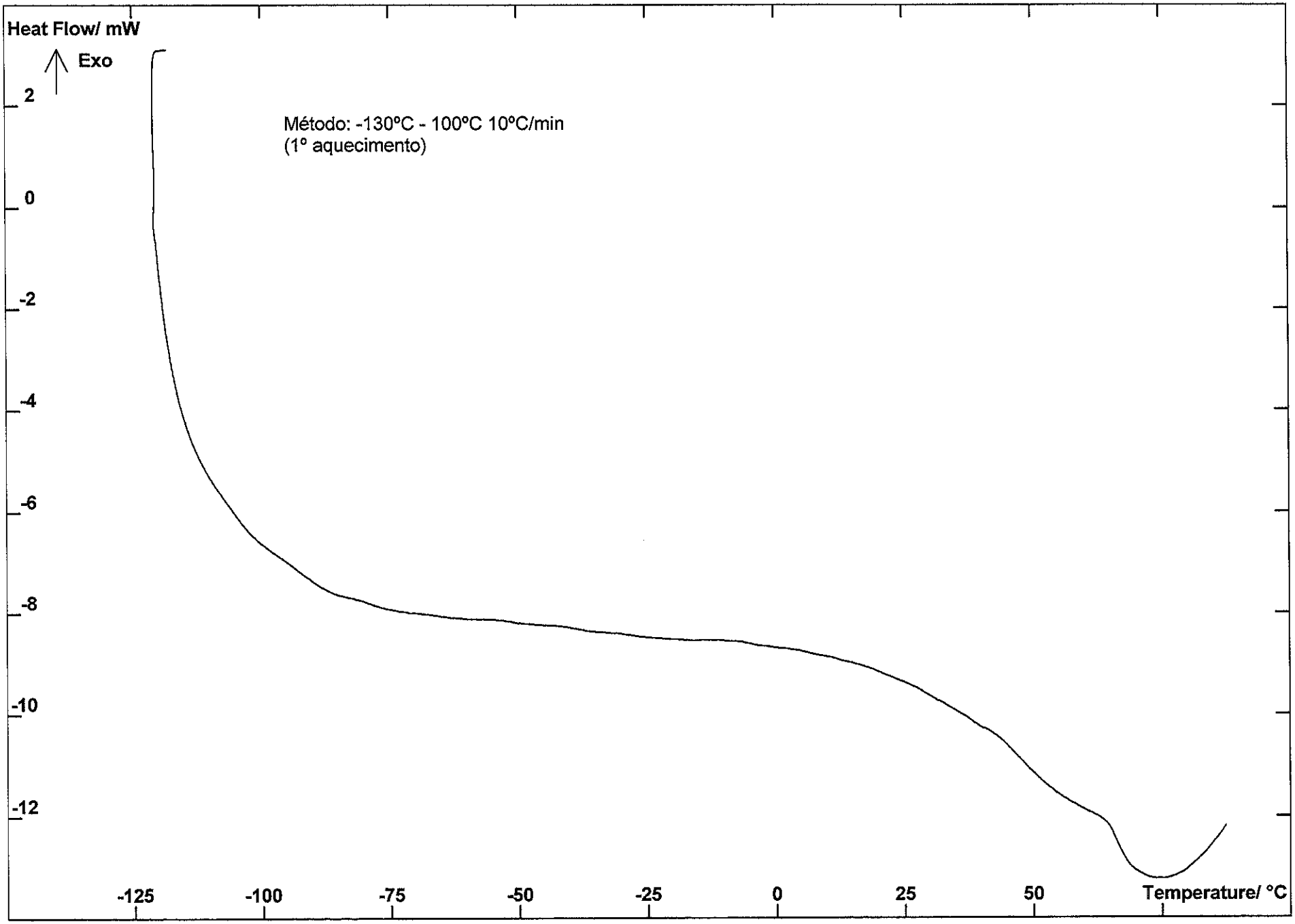

SETARAM INSTRUMENTATION - REGULATION	Fig. :	Experiment :	1(CGC)(crio)	Atm. :	N2	Crucible :	Al 100 µl
DSC 131	04-29-14	Procedure :	14-D012/013/014 (Seq 8)			Mass (mg) :	10,735

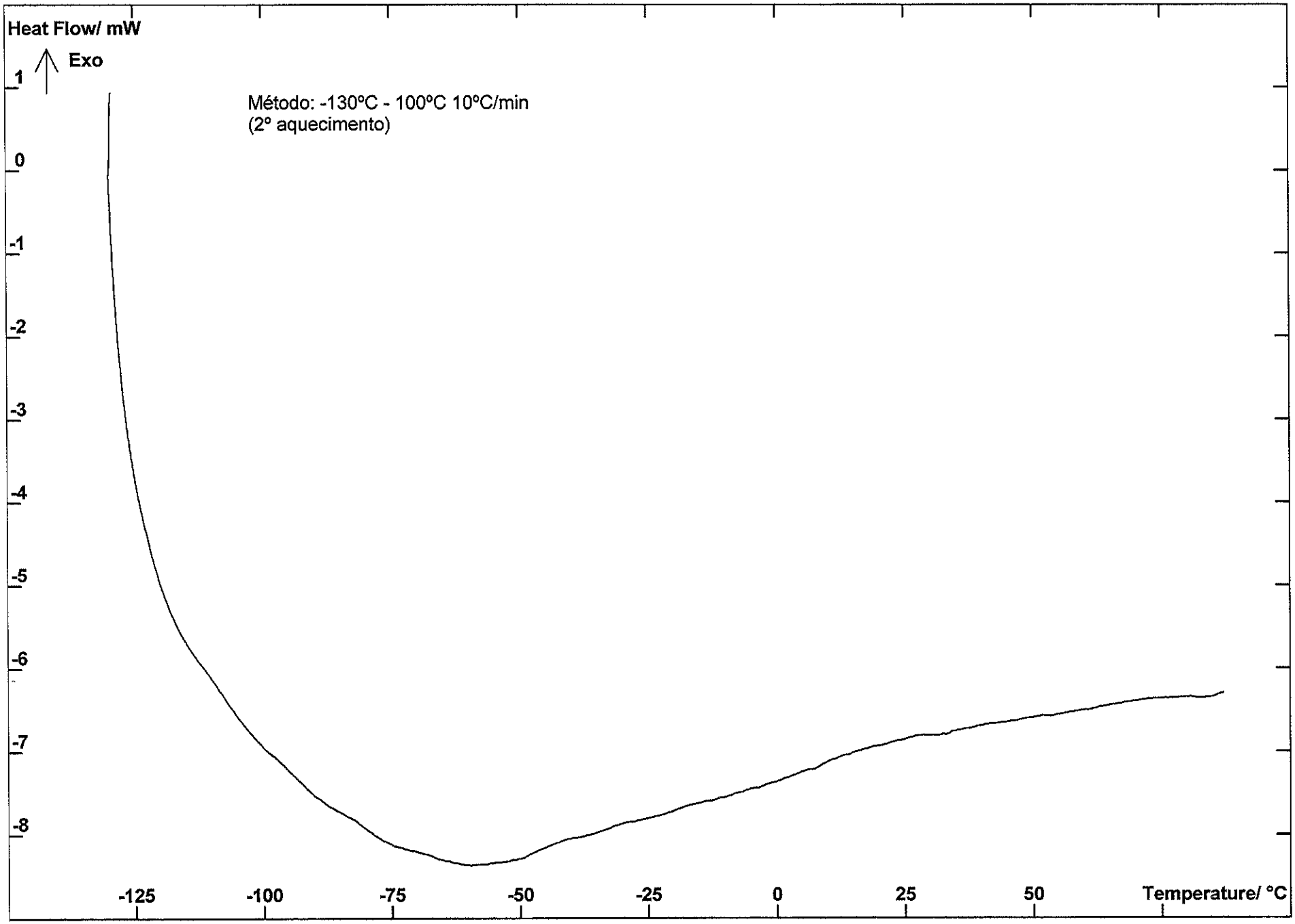

SETARAM INSTRUMENTATION - REGULATION	Fig. :	Experiment :	2(kio)	Atm. :	N2	Crucible :	Al 100 µl
DSC 131	04-22-14	Procedure :	14-D017 (Seq 2)			Mass (mg) :	26,658

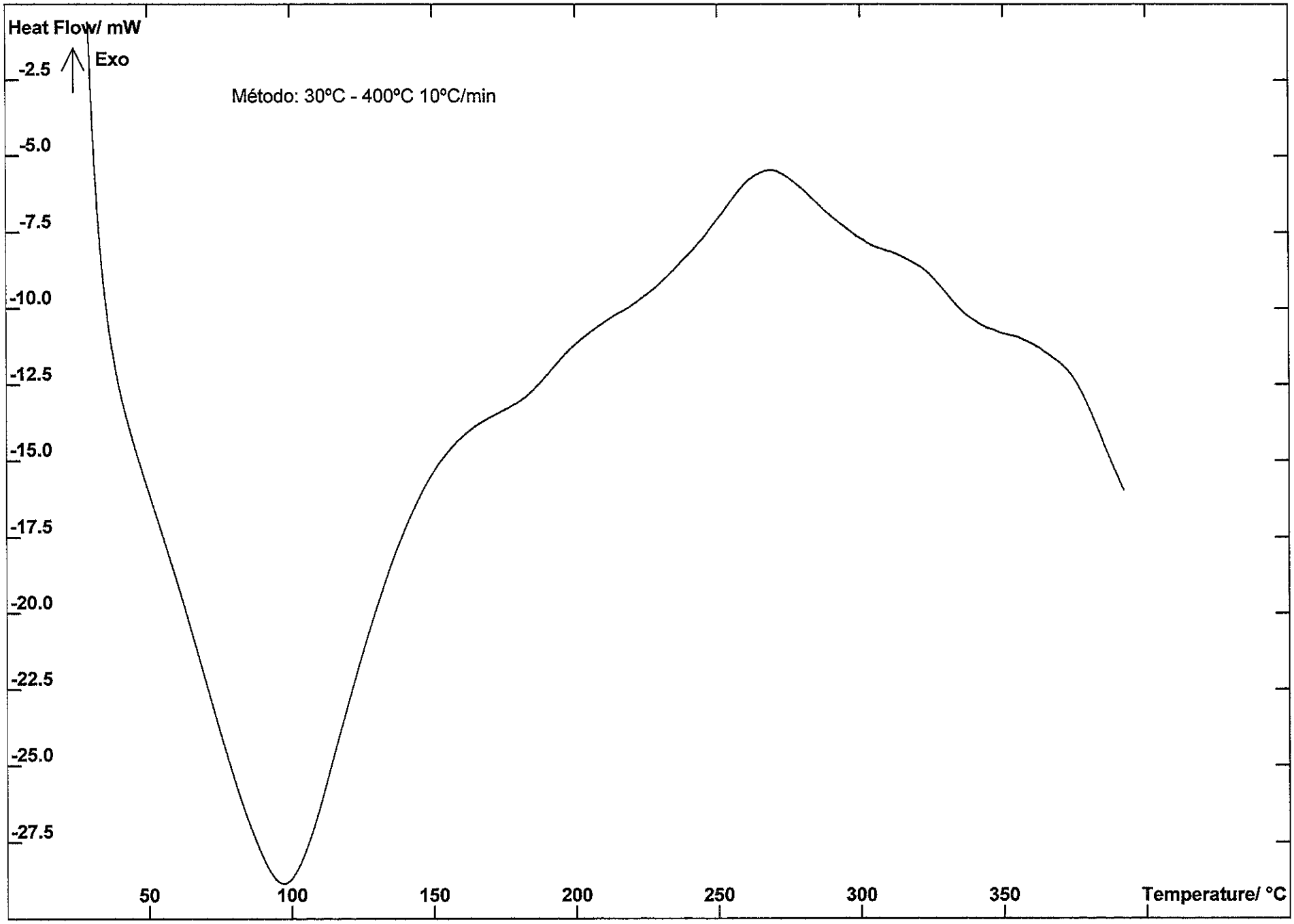

SETARAM INSTRUMENTATION - REGULATION

DSC 131

Fig. :		Experiment :	2(kio)(crio)	Atm. :	N2	Crucible :	Al 100 µl
04-29-14		Procedure :	14-D012/013/014 (Seq 4)			Mass (mg) :	38,831

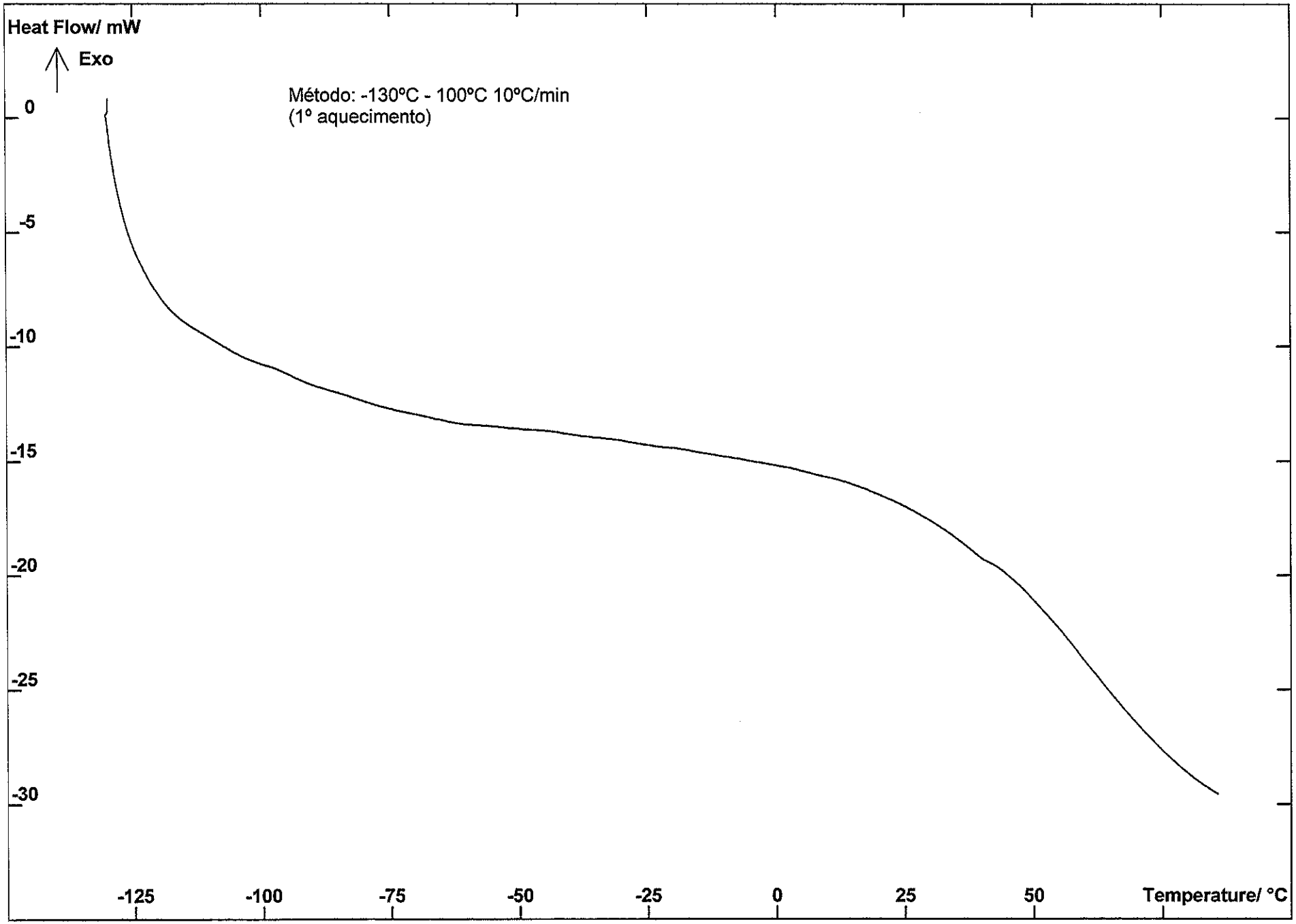

SETARAM INSTRUMENTATION - REGULATION

DSC 131

Fig. :		Experiment :	2(kio)(crio)	Atm. :	N2	Crucible :	Al 100 µl
04-29-14		Procedure :	14-D012/013/014 (Seq 8)			Mass (mg) :	38,831

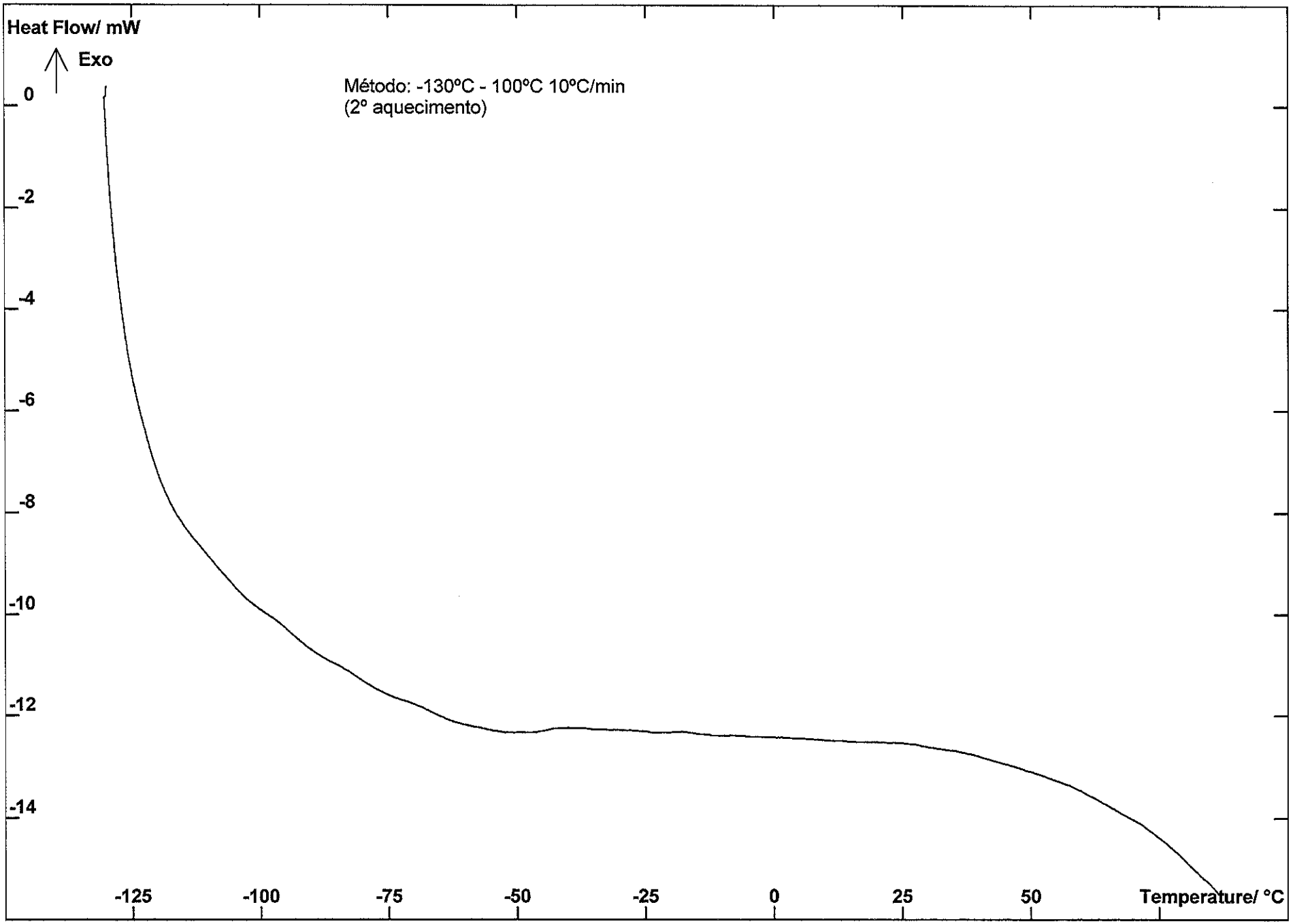

SETARAM INSTRUMENTATION - REGULATION

DSC 131

Fig. : 06-18-14

Experiment : CGC MeOH(crio)

Procedure : 14-D026(crio) (Seq 4)

Atm. : N2

Crucible : Al 100 µl

Mass (mg) : 24,952

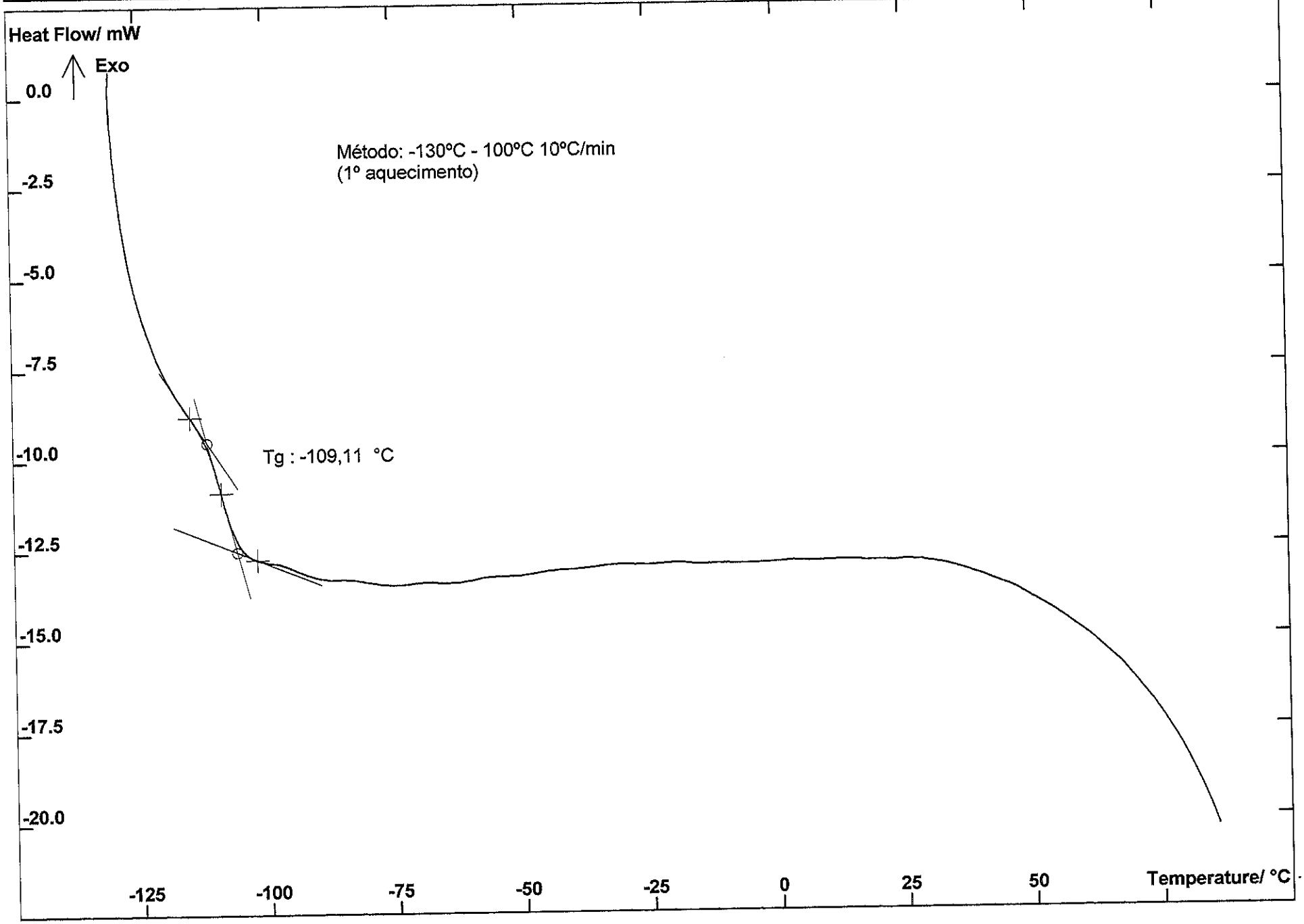

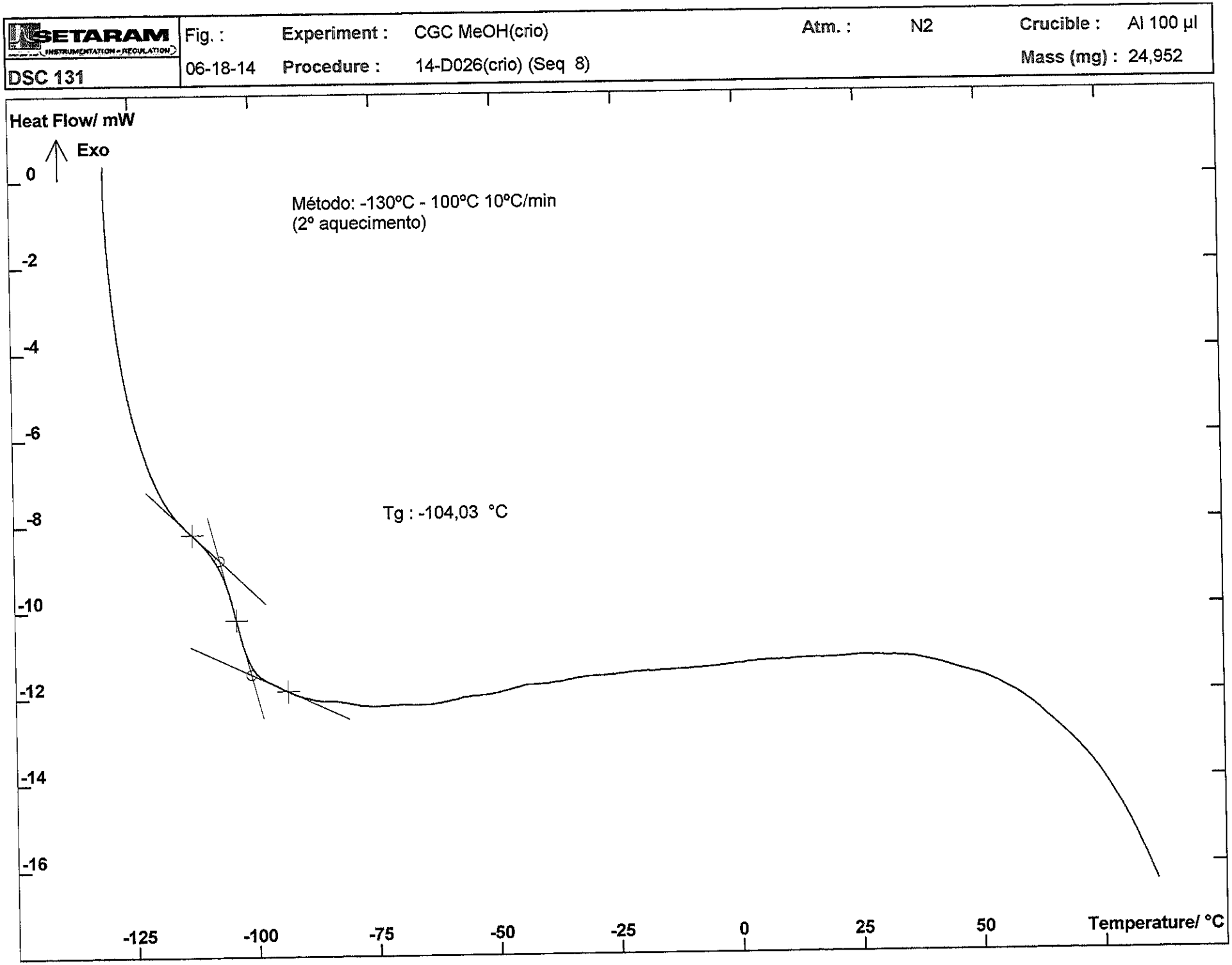
SETARAM
INSTRUMENTATION - REGULATION
DSC 131
Fig. : 06-18-14
Experiment : CGC MeOH(crio)
Procedure : 14-D026(crio) (Seq 8)
Atm. : N2
Crucible : Al 100 µl
Mass (mg) : 24,952
Heat Flow/ mW
Exo
0
-2
-4
-6
-8
-10
-12
-14
-16
Método: -130°C - 100°C 10°C/min
(2° aquecimento)
Tg : -104,03 °C
-125
-100
-75
-50
-25
0
25
50
Temperature/ °C

DSC 131	Fig. :	Experiment :	K10 MeOH(crio)	Atm. :	N2	Crucible :	Al 100 µl
	06-16-14	Procedure :	14-D026(crio) (Seq 4)			Mass (mg) :	22,701

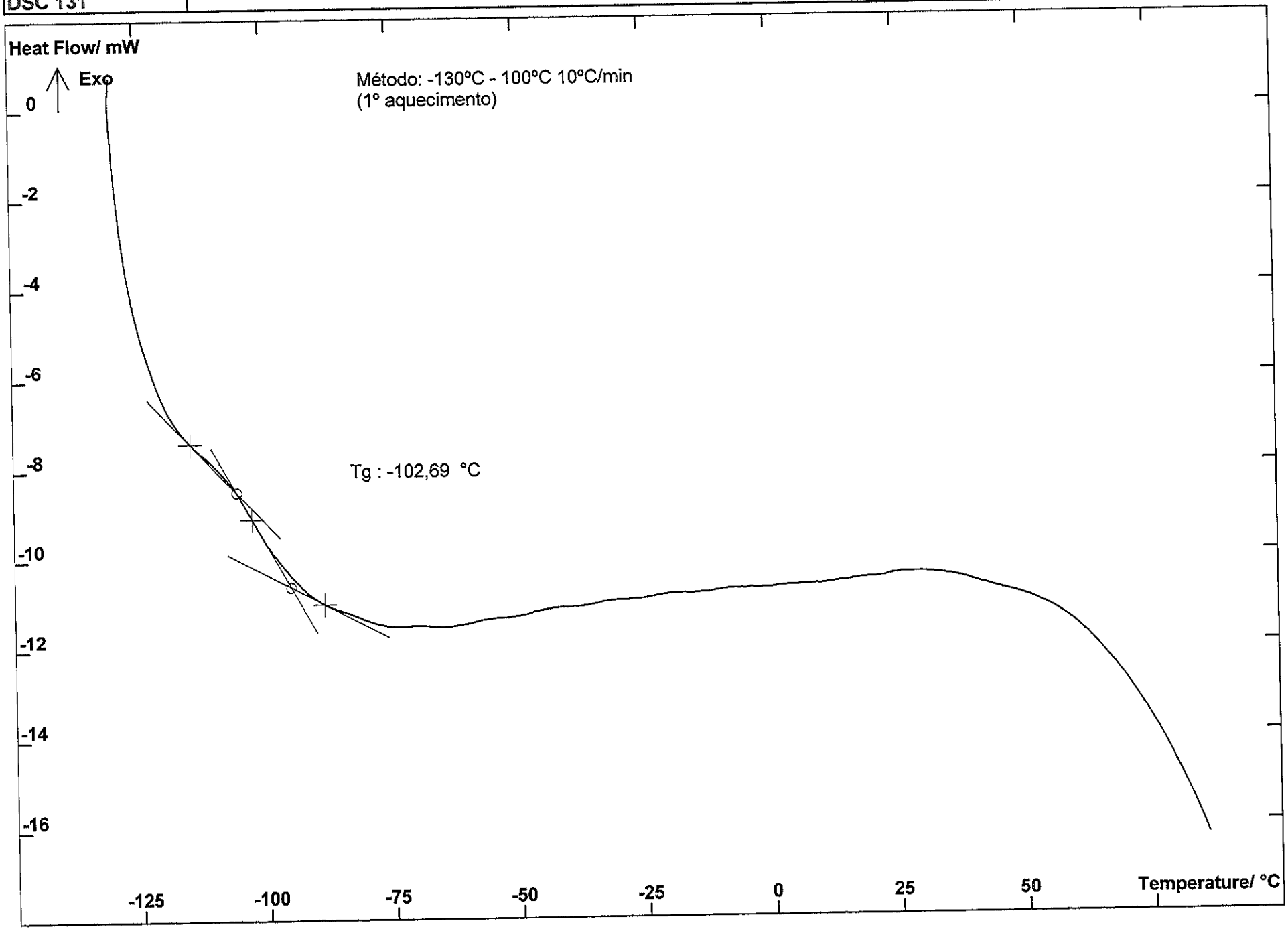

SETARAM INSTRUMENTATION - REGULATION

DSC 131

Fig. : 06-16-14

Experiment : K10 MeOH(crio)

Procedure : 14-D026(crio) (Seq 8)

Atm. : N2

Crucible : Al 100 µl

Mass (mg) : 22,701

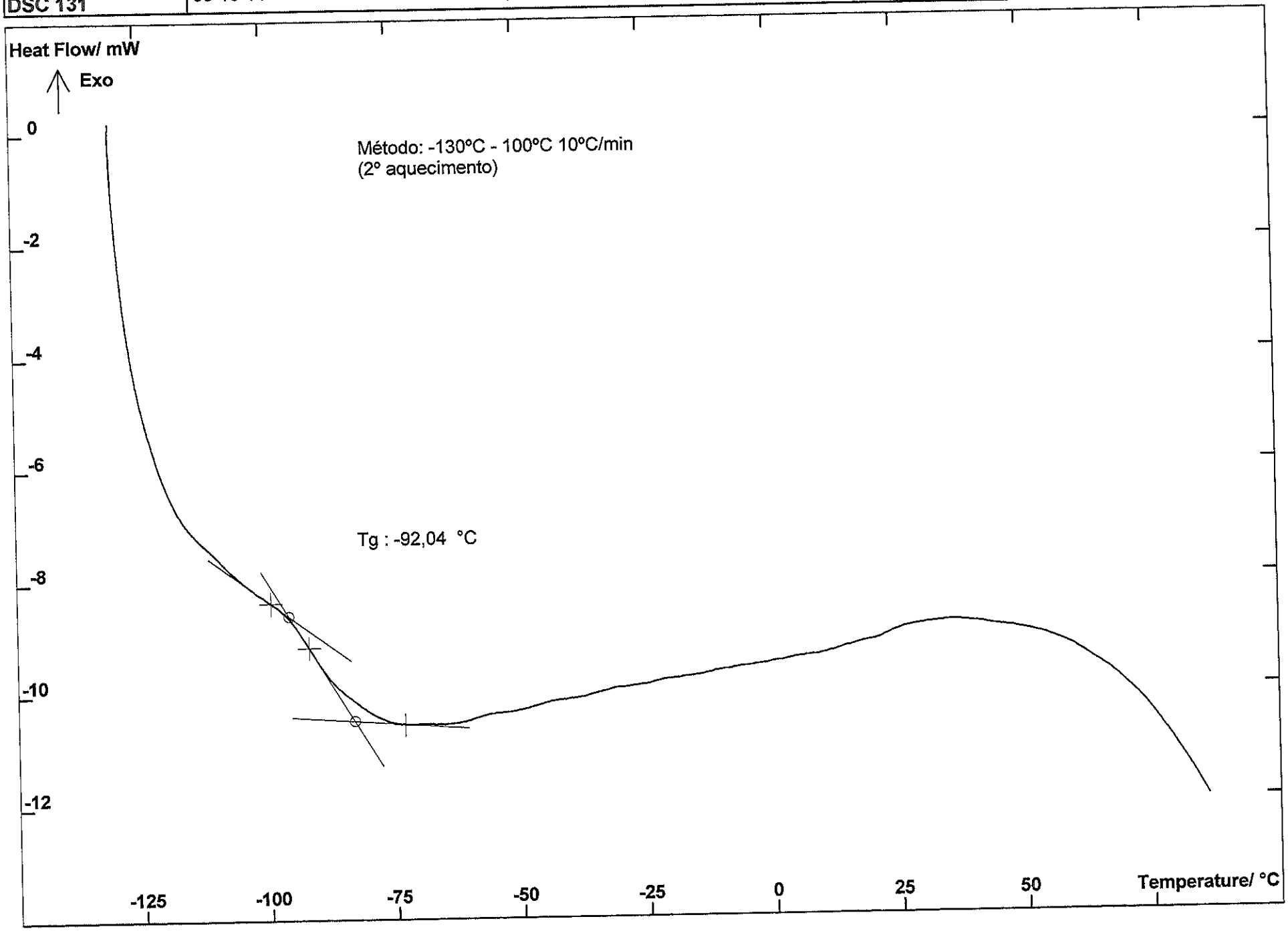

SETARAM INSTRUMENTATION - REGULATION

DSC 131

Fig. : 06-16-14

Experiment : K10 glycerol(crio)

Procedure : 14-D026(crio) (Seq 4)

Atm. : N2

Crucible : Al 100 µl

Mass (mg) : 50,307

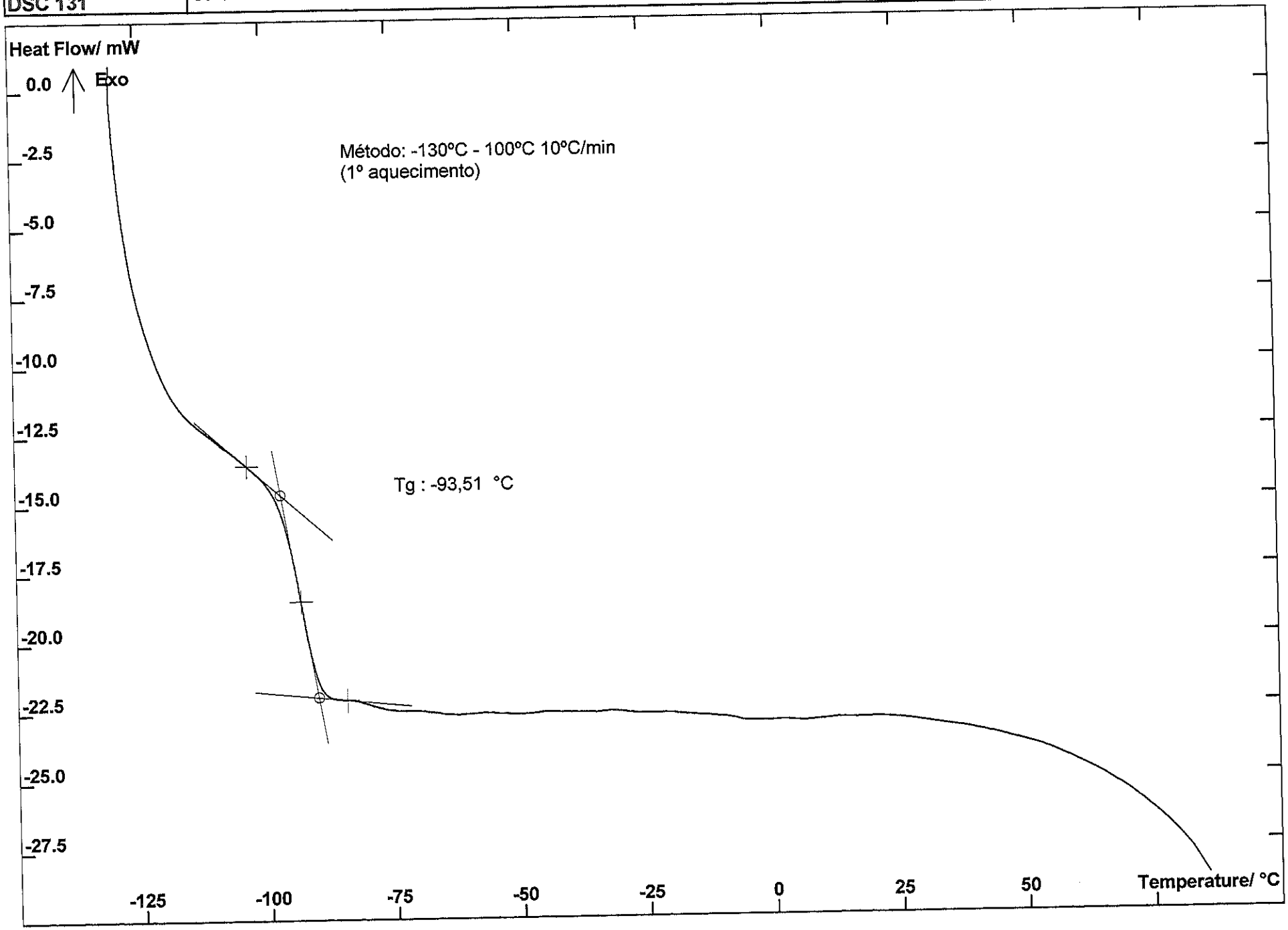

SETARAM INSTRUMENTATION - REGULATION

DSC 131

Fig. : 06-16-14

Experiment : K10 glycerol(crio)

Procedure : 14-D026(crio) (Seq 8)

Atm. : N2

Crucible : Al 100 µl

Mass (mg) : 50,307

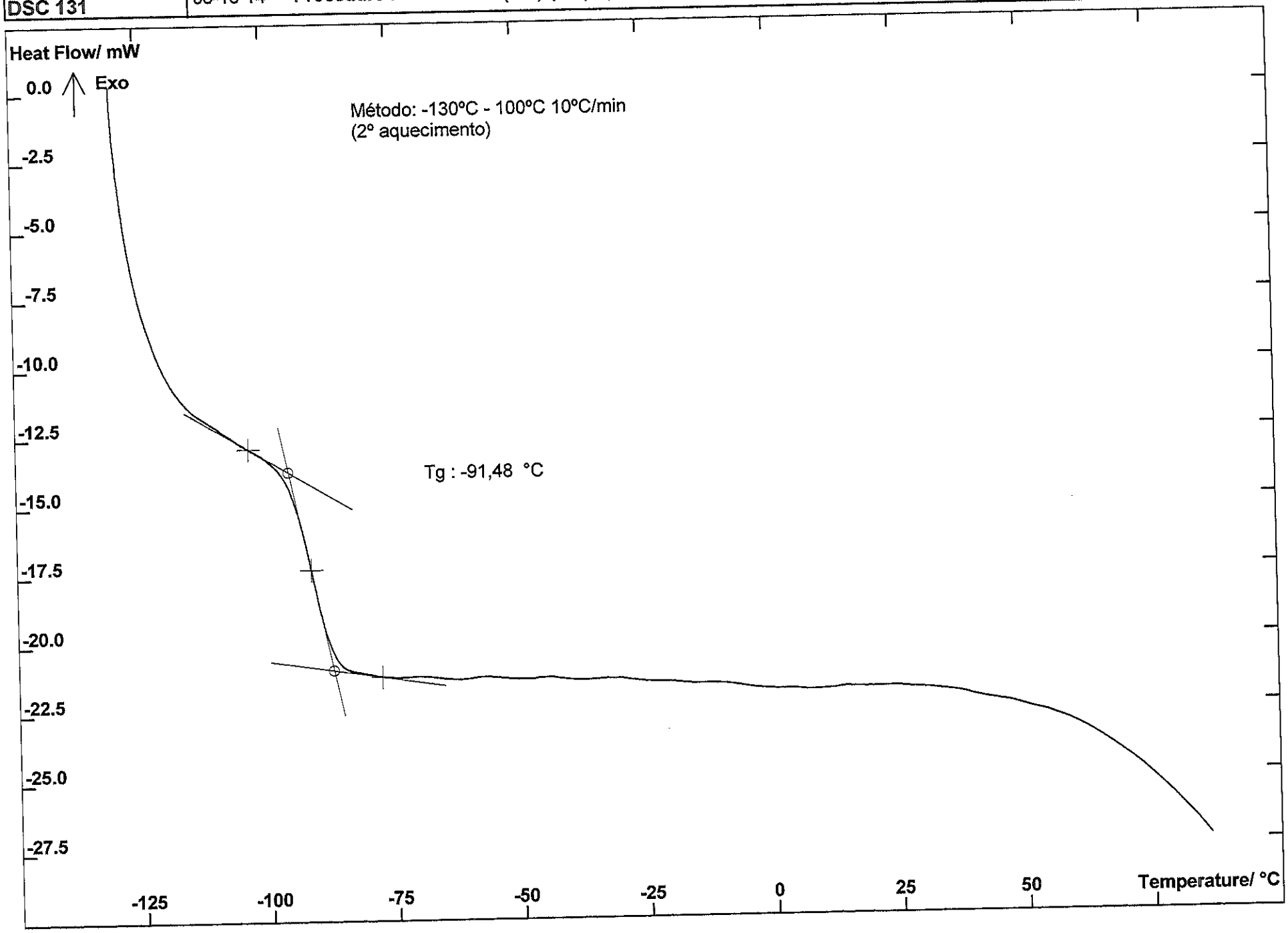

SETARAM INSTRUMENTATION - REGULATION

DSC 131

Fig. : 06-18-14

Experiment : CGC water(crio)

Procedure : 14-D026(crio) (Seq 4)

Atm. : N2

Crucible : Al 100 µl

Mass (mg) : 19,144

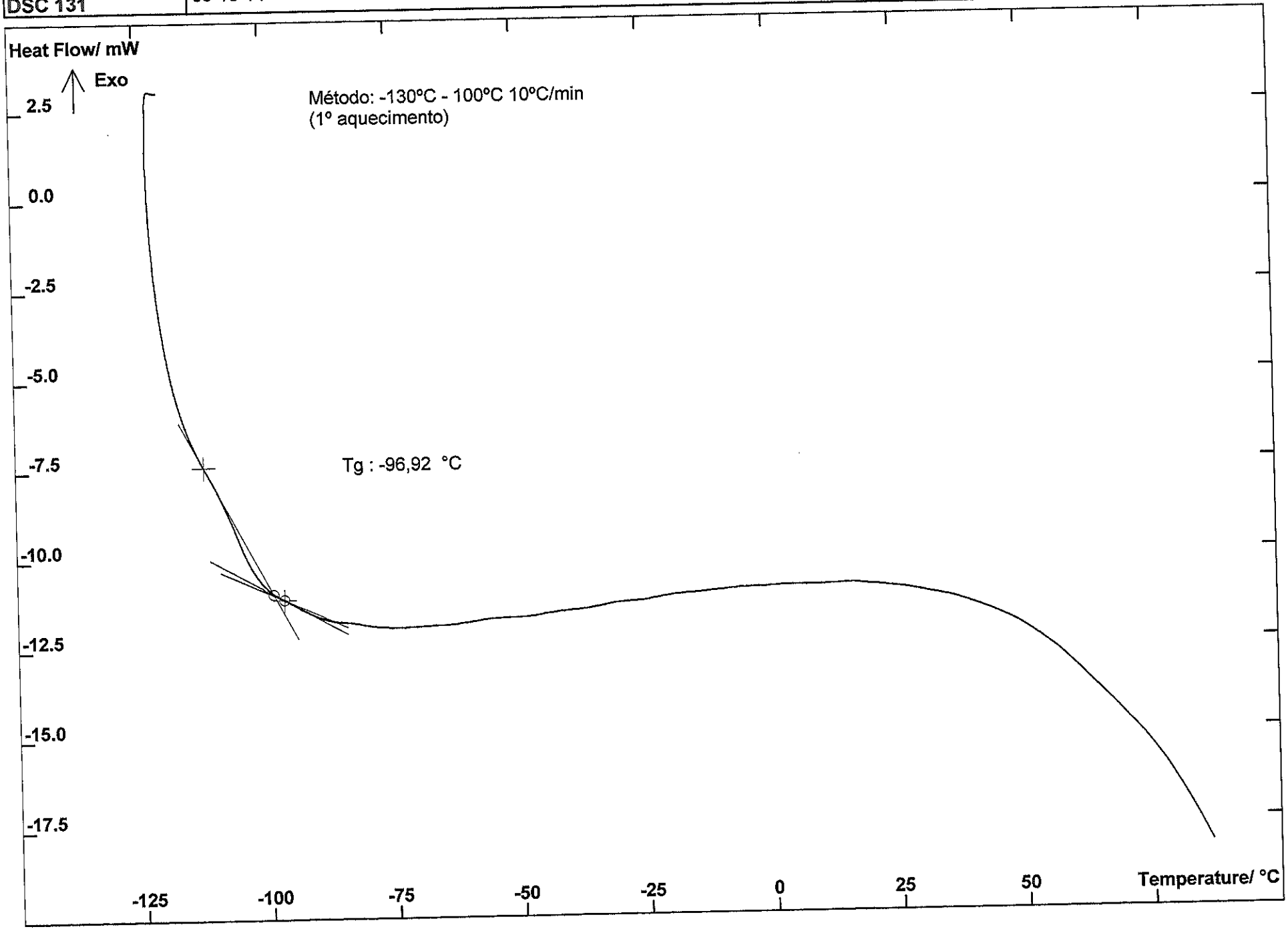

SETARAM INSTRUMENTATION - REGULATION

DSC 131

Fig. : 06-18-14

Experiment : CGC water(crio)

Procedure : 14-D026(crio) (Seq 8)

Atm. : N2

Crucible : Al 100 µl

Mass (mg) : 19,144

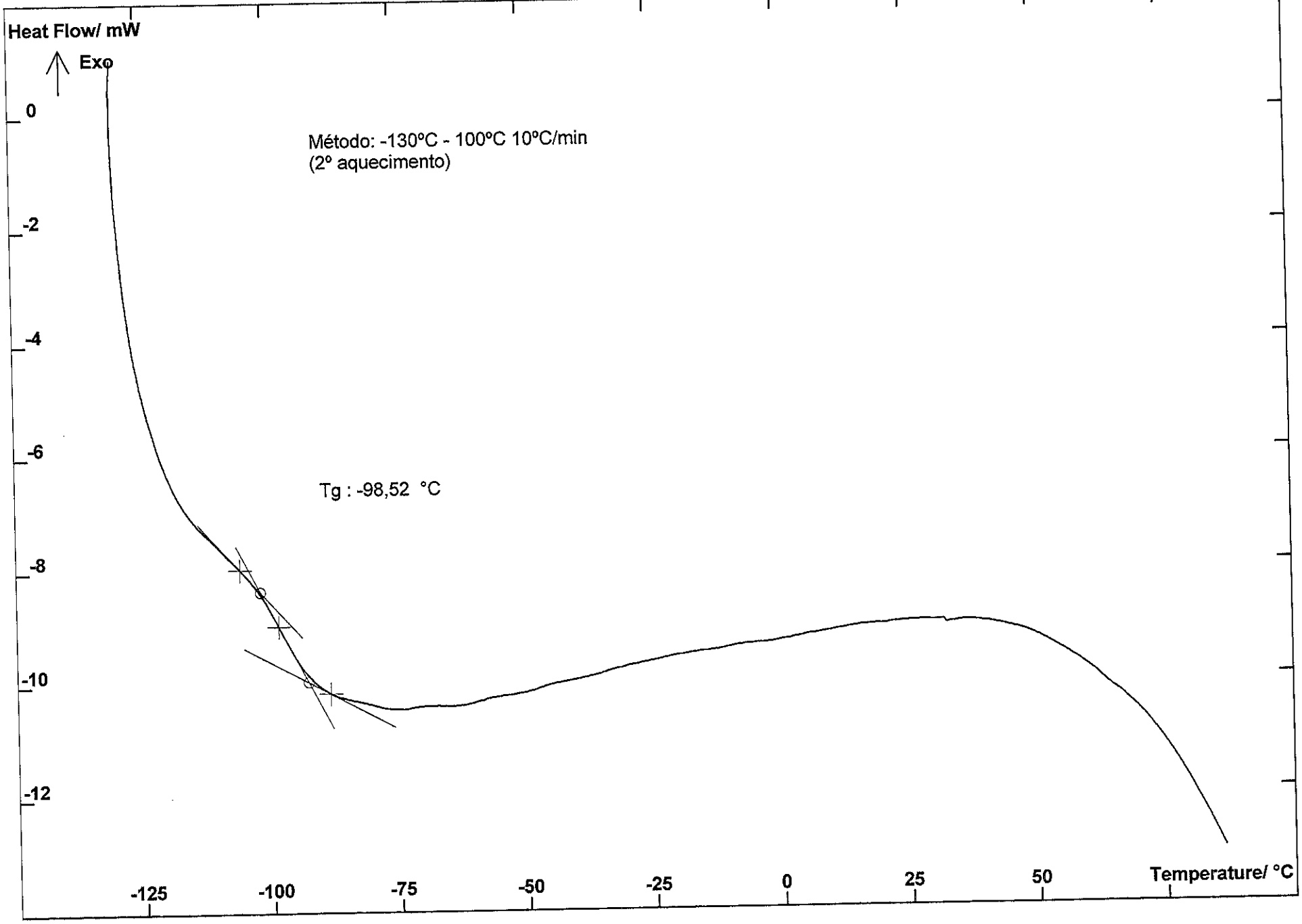

SETARAM INSTRUMENTATION - REGULATION

DSC 131

Fig. : 06-16-14

Experiment : PEG glycerol(crio)

Procedure : 14-D026(crio) (Seq 4)

Atm. : N2

Crucible : Al 100 µl

Mass (mg) : 40,276

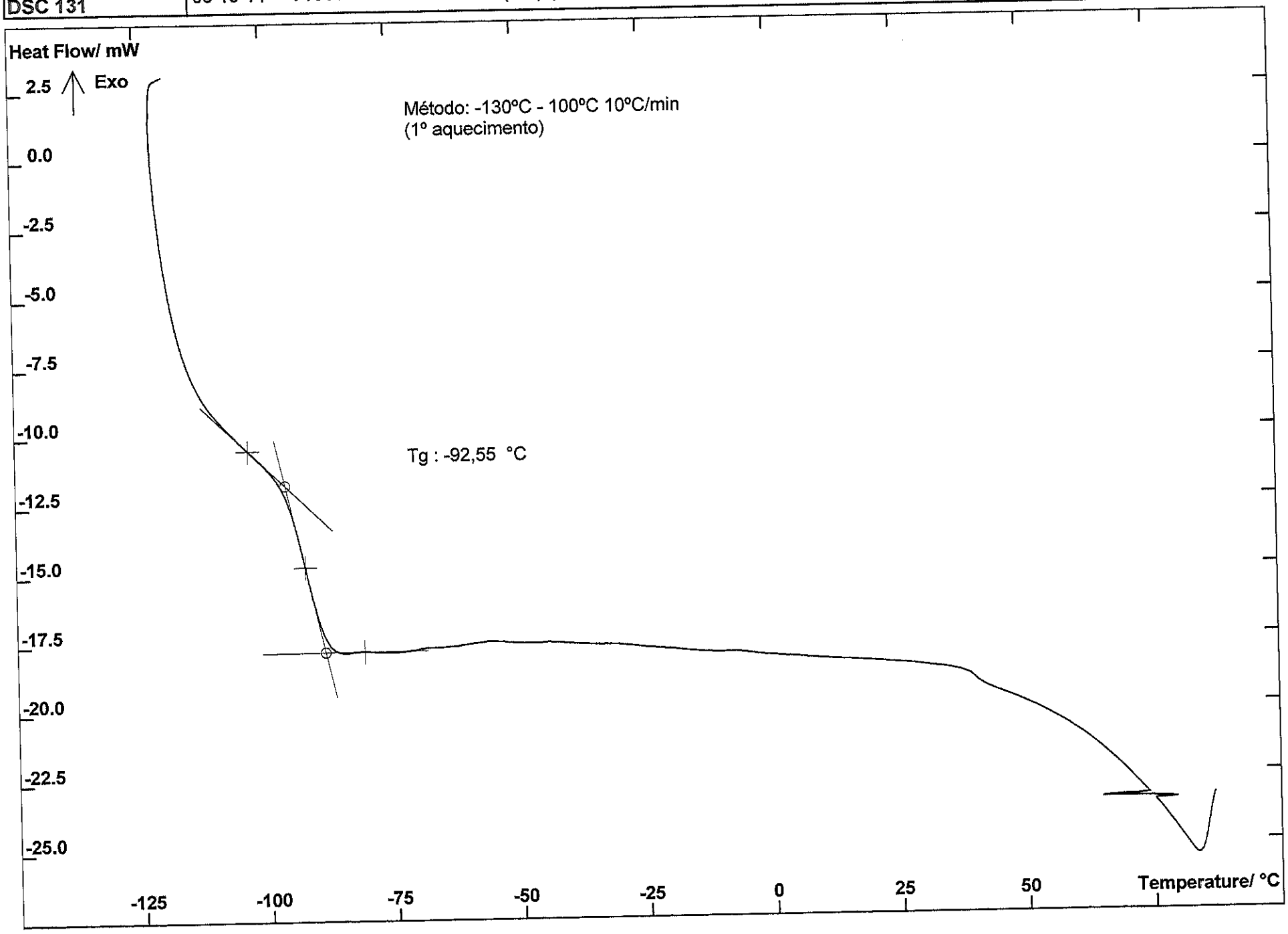

SETARAM INSTRUMENTATION – REGULATION

DSC 131

Fig. : 06-16-14

Experiment : PEG glycerol(crio)

Procedure : 14-D026(crio) (Seq 8)

Atm. : N2

Crucible : Al 100 µl

Mass (mg) : 40,276

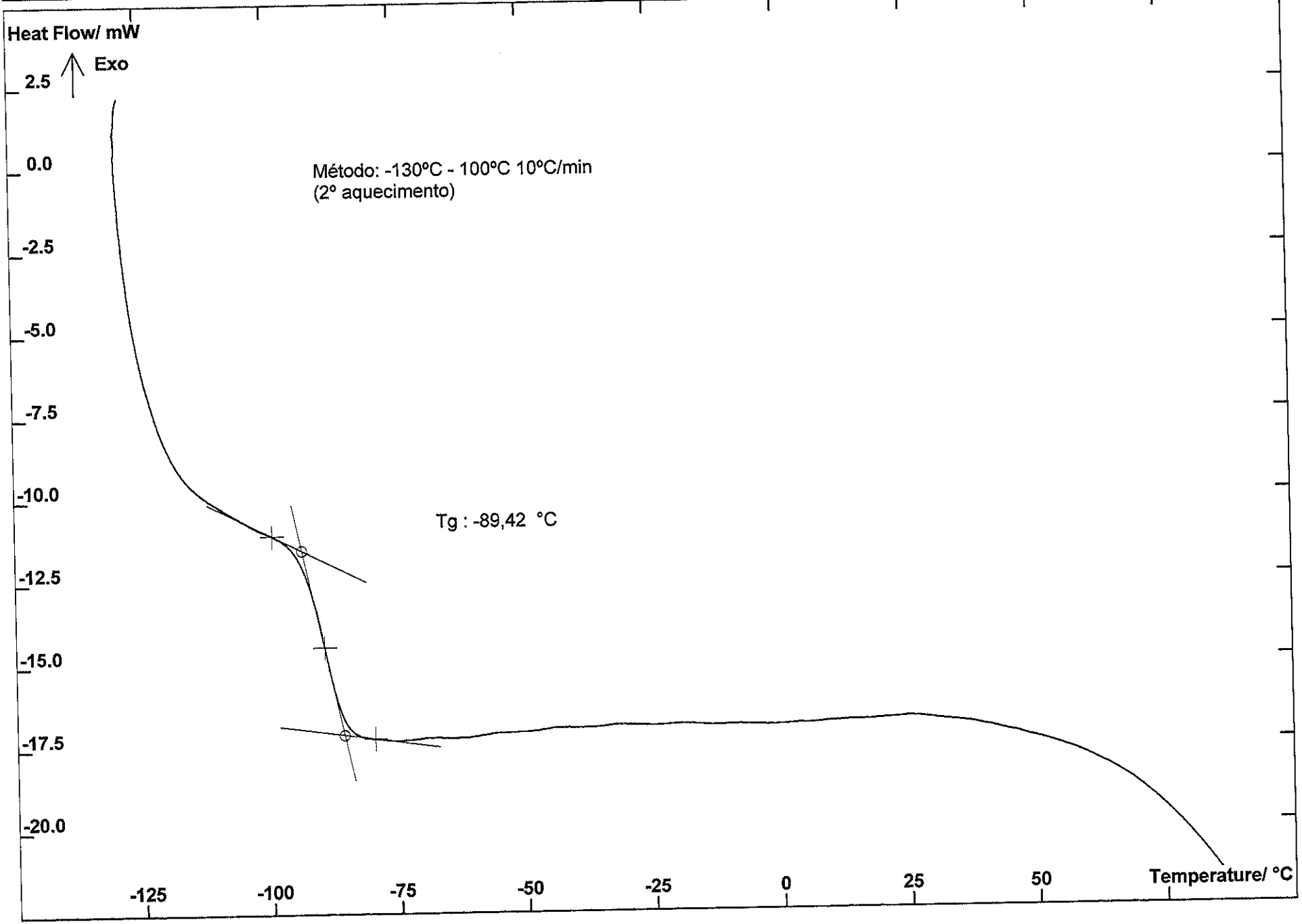

SETARAM INSTRUMENTATION - REGULATION

DSC 131

Fig. : 06-13-14

Experiment : CGC(crio)

Procedure : 14-D026(crio) (Seq 4)

Atm. : N2

Crucible : Al 100 µl

Mass (mg) : 25,523

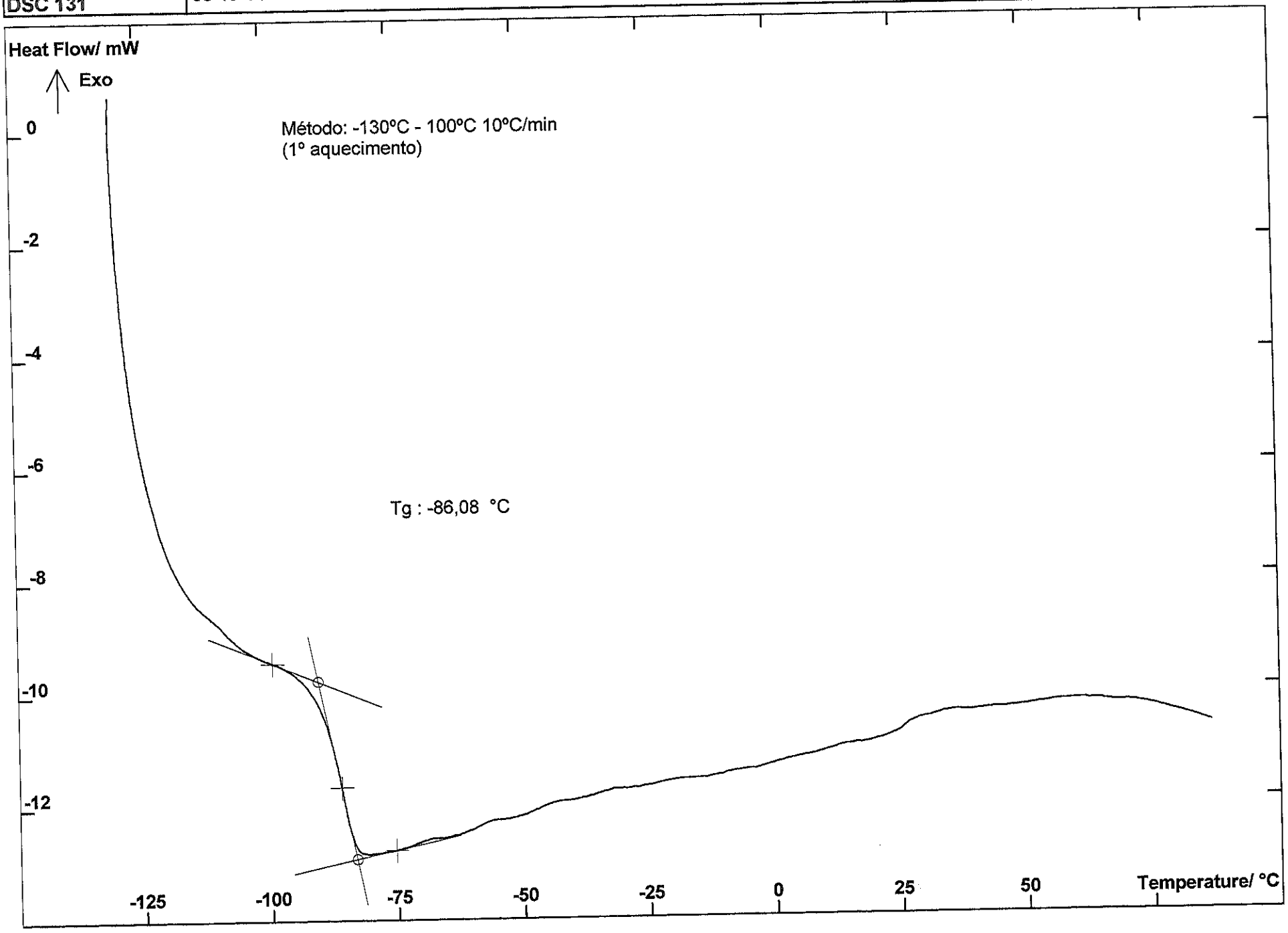

SETARAM INSTRUMENTATION - REGULATION

DSC 131

Fig. : 06-13-14

Experiment : CGC(crio)

Procedure : 14-D026(crio) (Seq 8)

Atm. : N2

Crucible : Al 100 µl

Mass (mg) : 25,523

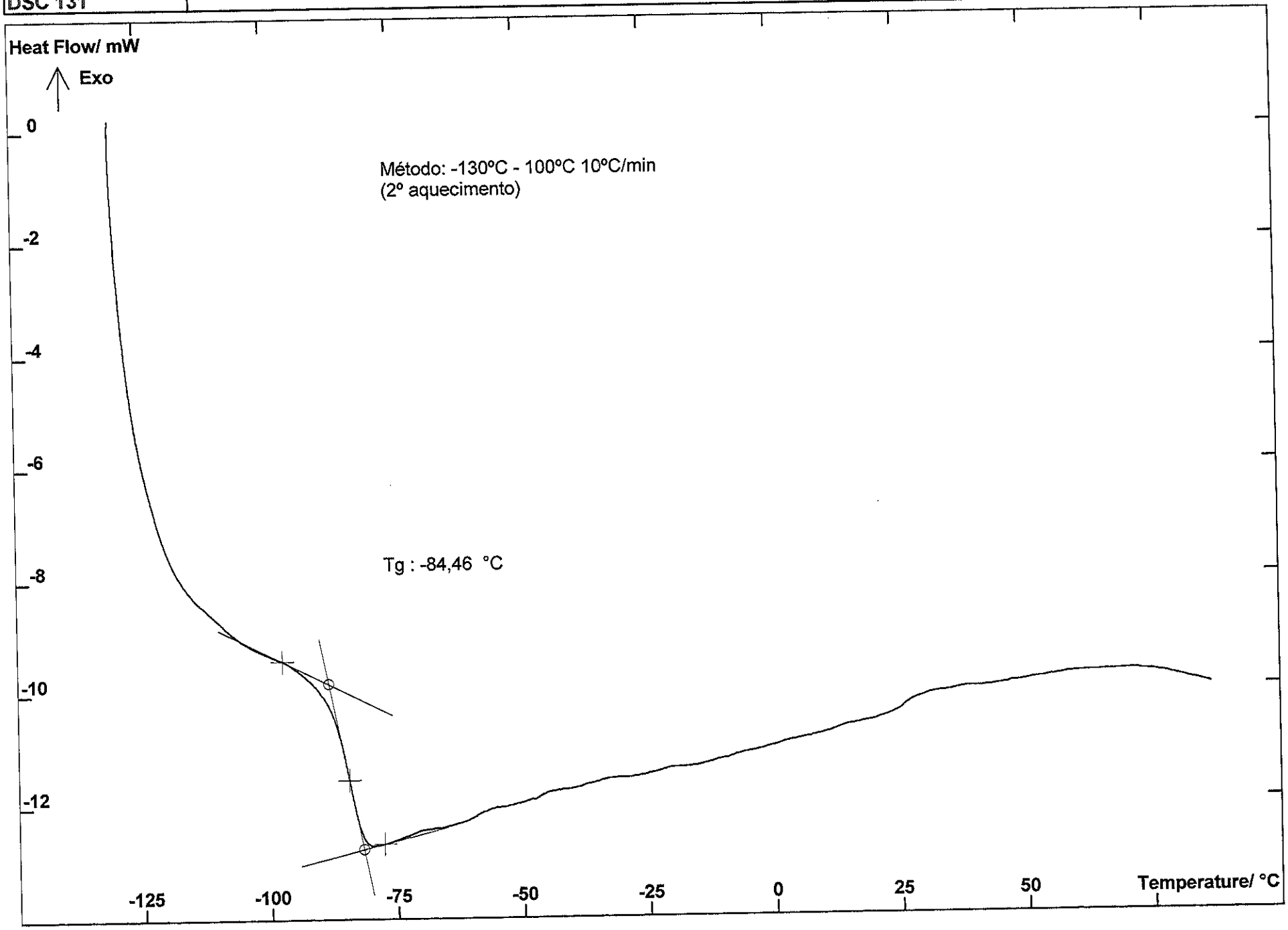

SETARAM INSTRUMENTATION - REGULATION

DSC 131

Fig. : 06-13-14

Experiment : K10(crio)

Procedure : 14-D026(crio) (Seq 4)

Atm. : N2

Crucible : Al 100 µl

Mass (mg) : 43,696

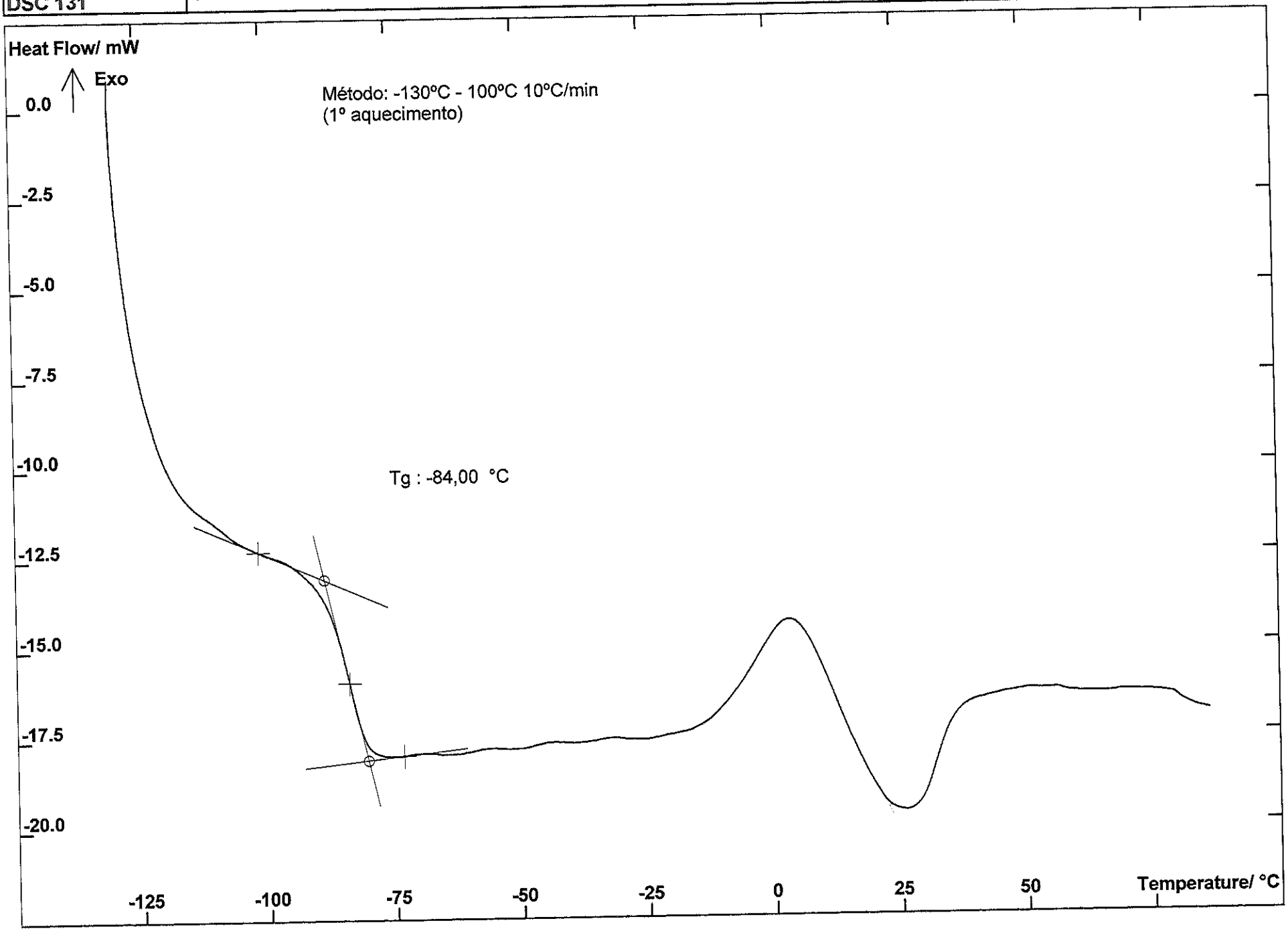

SETARAM INSTRUMENTATION - REGULATION

DSC 131

Fig. : 06-13-14

Experiment : K10(crio)

Procedure : 14-D026(crio) (Seq 8)

Atm. : N2

Crucible : Al 100 µl

Mass (mg) : 43,696

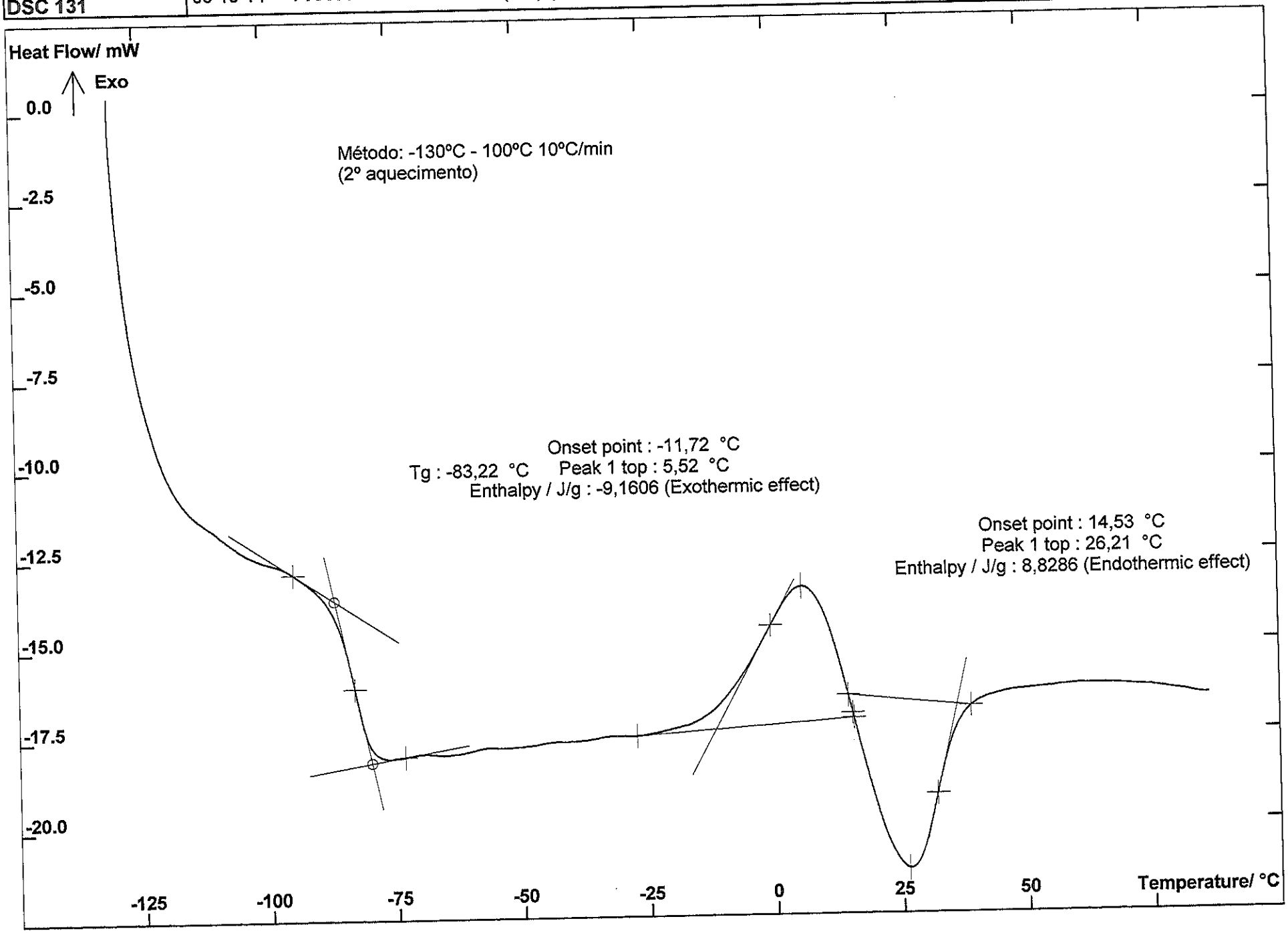

SETARAM INSTRUMENTATION - REGULATION

DSC 131

Fig. : 06-13-14

Experiment : CA10(crio)

Procedure : 14-D026(crio) (Seq 4)

Atm. : N2

Crucible : Al 100 µl

Mass (mg) : 34,636

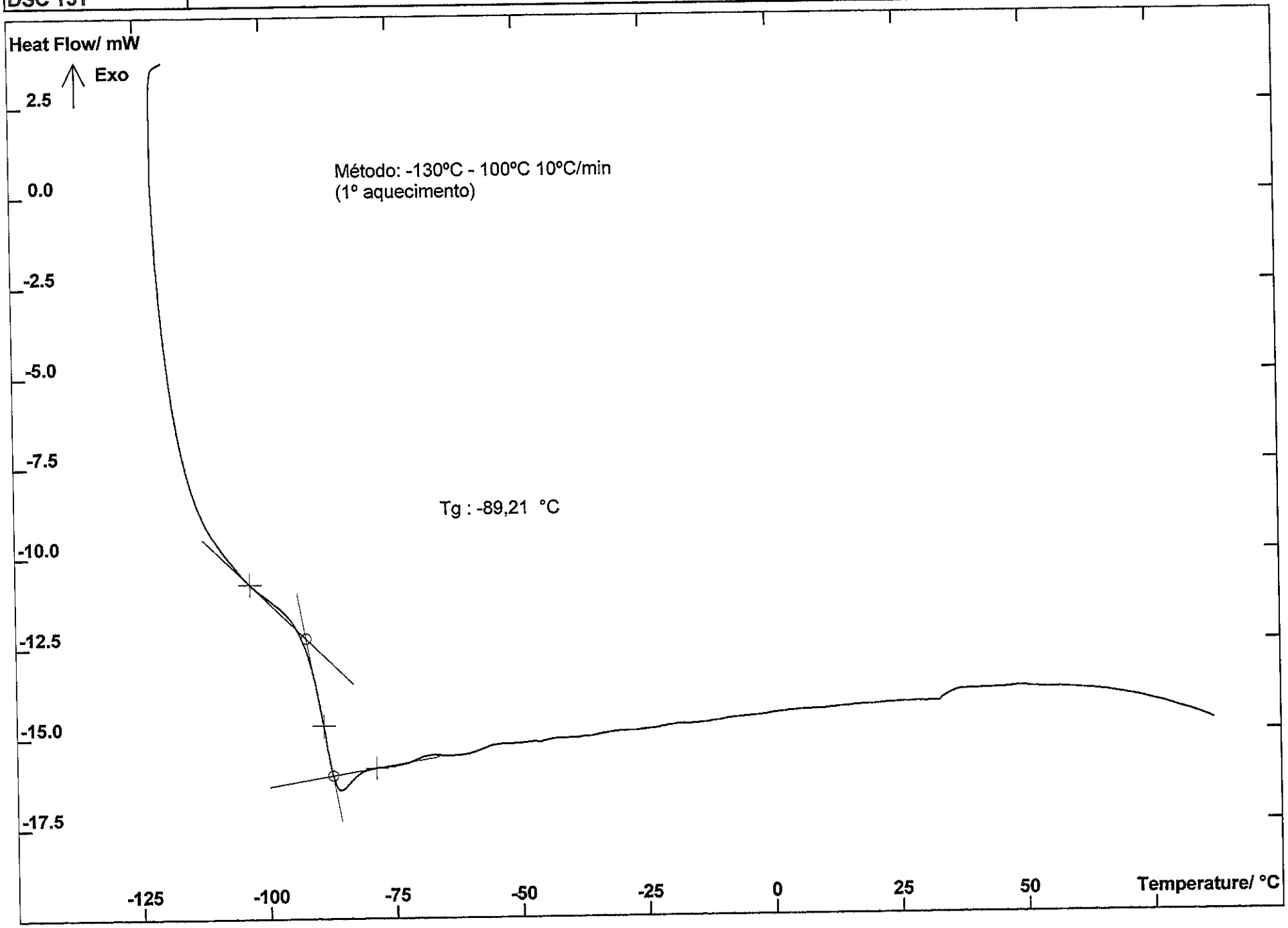

SETARAM INSTRUMENTATION - REGULATION

DSC 131

Fig. : 06-13-14

Experiment : CA10(crio)

Procedure : 14-D026(crio) (Seq 8)

Atm. : N2

Crucible : Al 100 µl

Mass (mg) : 34,636

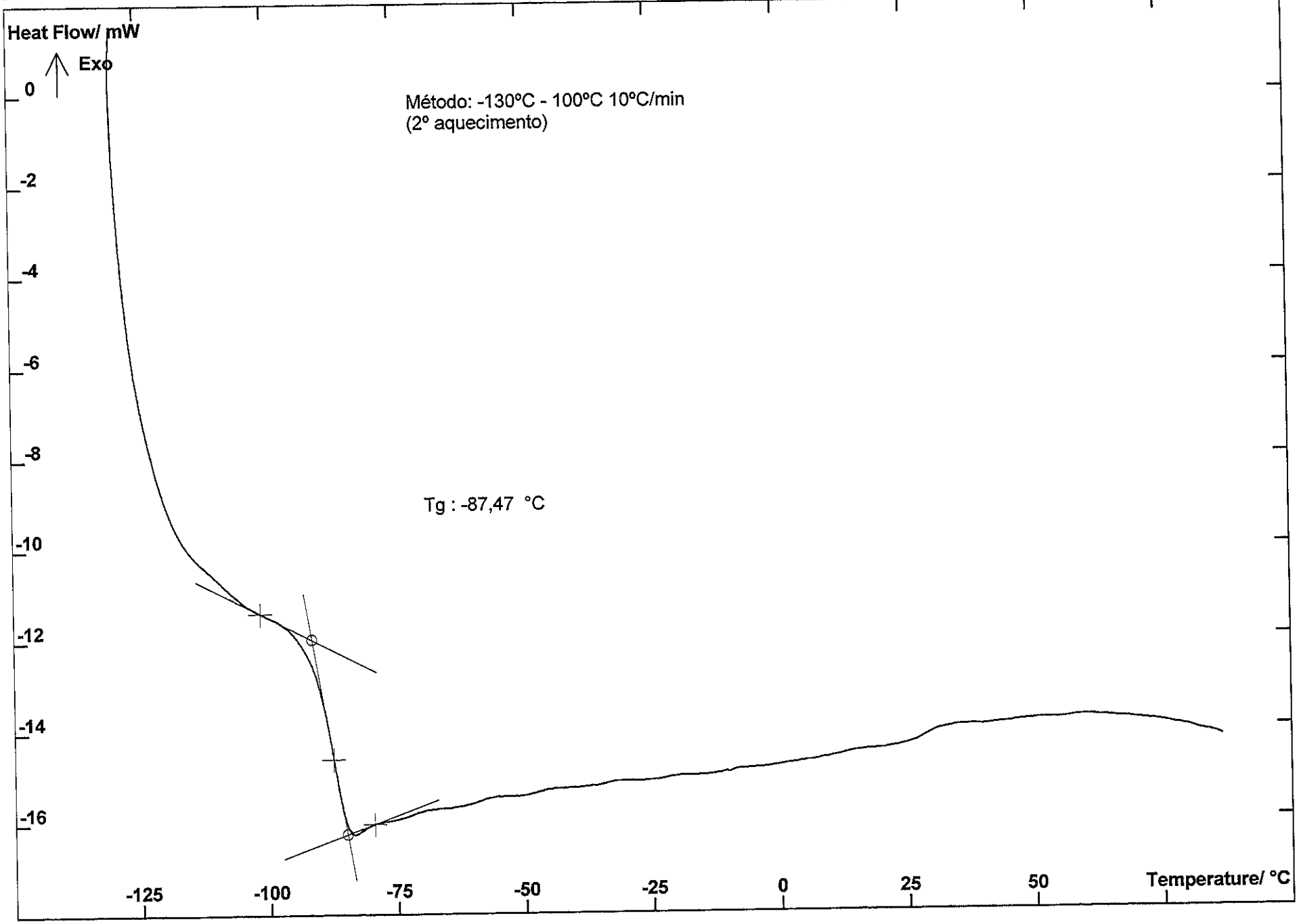

SETARAM INSTRUMENTATION - REGULATION	Fig. :	Experiment :	K10(T>Amb)	Atm. :	N2	Crucible :	Al 100 µl
DSC 131	06-20-14	Procedure :	14-D017 (Seq 2)			Mass (mg) :	43,696

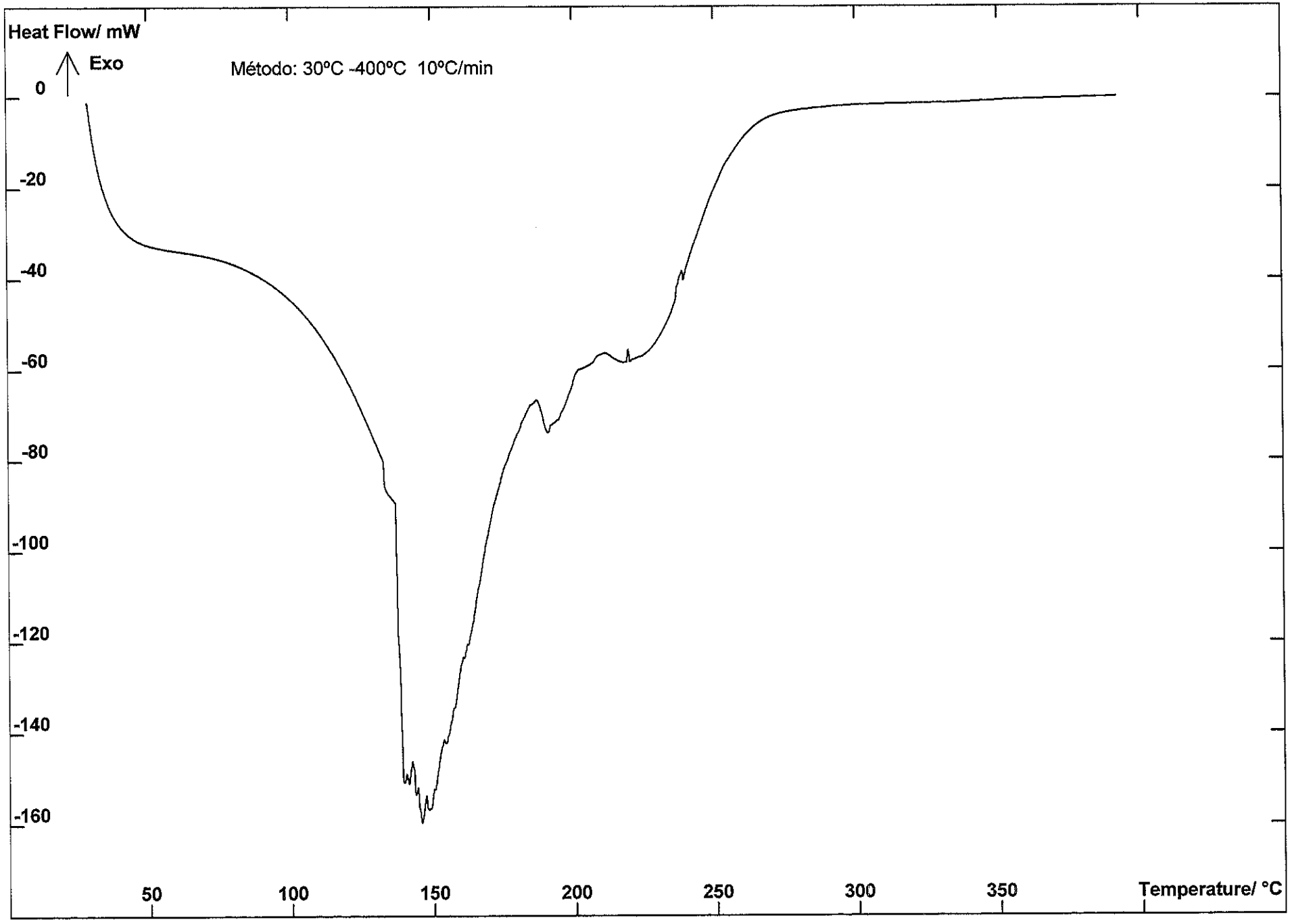

SETARAM INSTRUMENTATION – REGULATION	Fig. :	Experiment : CGC(T>Amb)	Atm. : N2	Crucible : Al 100 µl
DSC 131	06-20-14	Procedure : 14-D017 (Seq 2)		Mass (mg) : 25,523

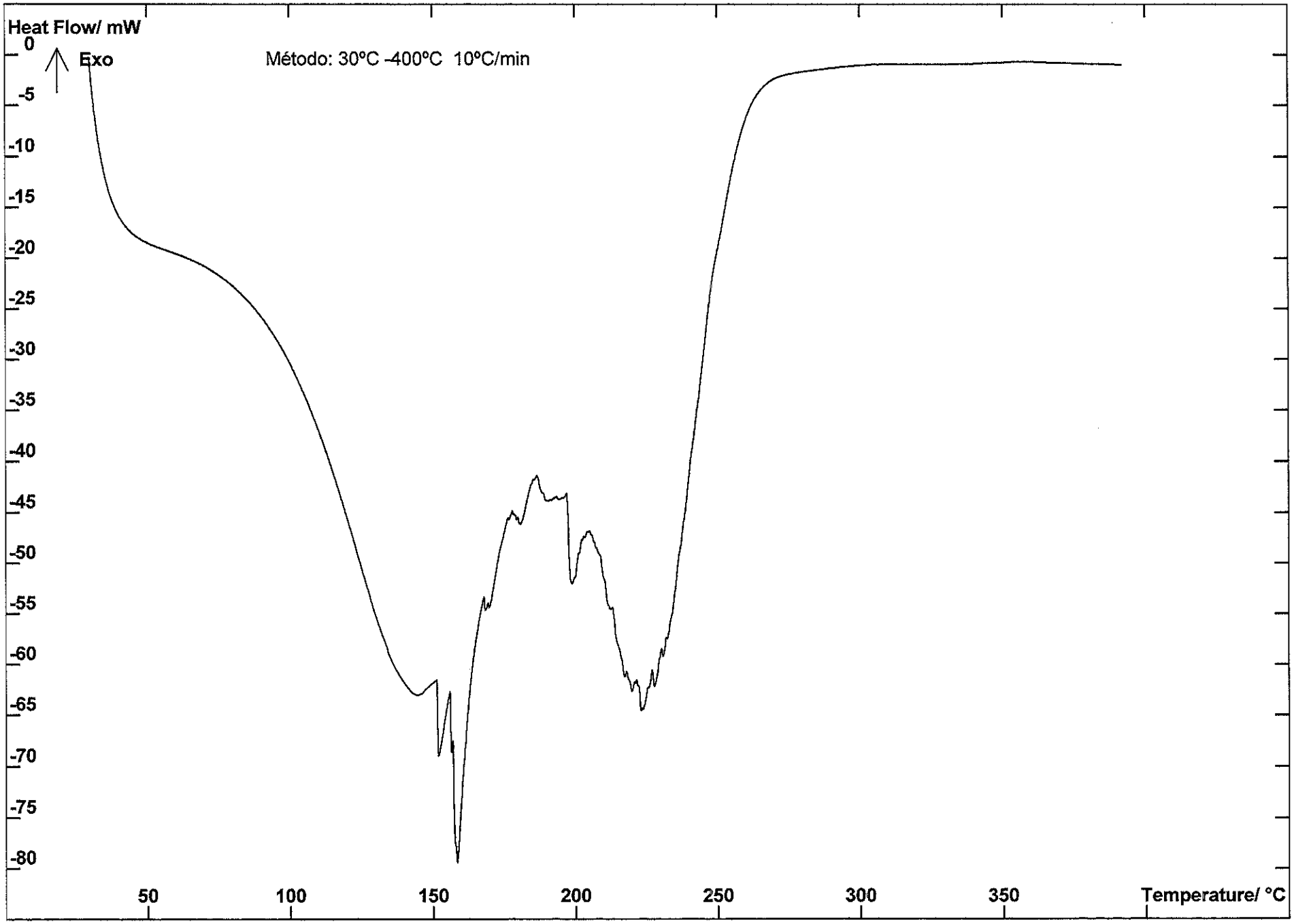

SETARAM INSTRUMENTATION - REGULATION	Fig. :	Experiment :	CA10(T>Amb)	Atm. :	N2	Crucible :	Al 100 µl
DSC 131	06-20-14	Procedure :	14-D017 (Seq 2)			Mass (mg) :	34,636

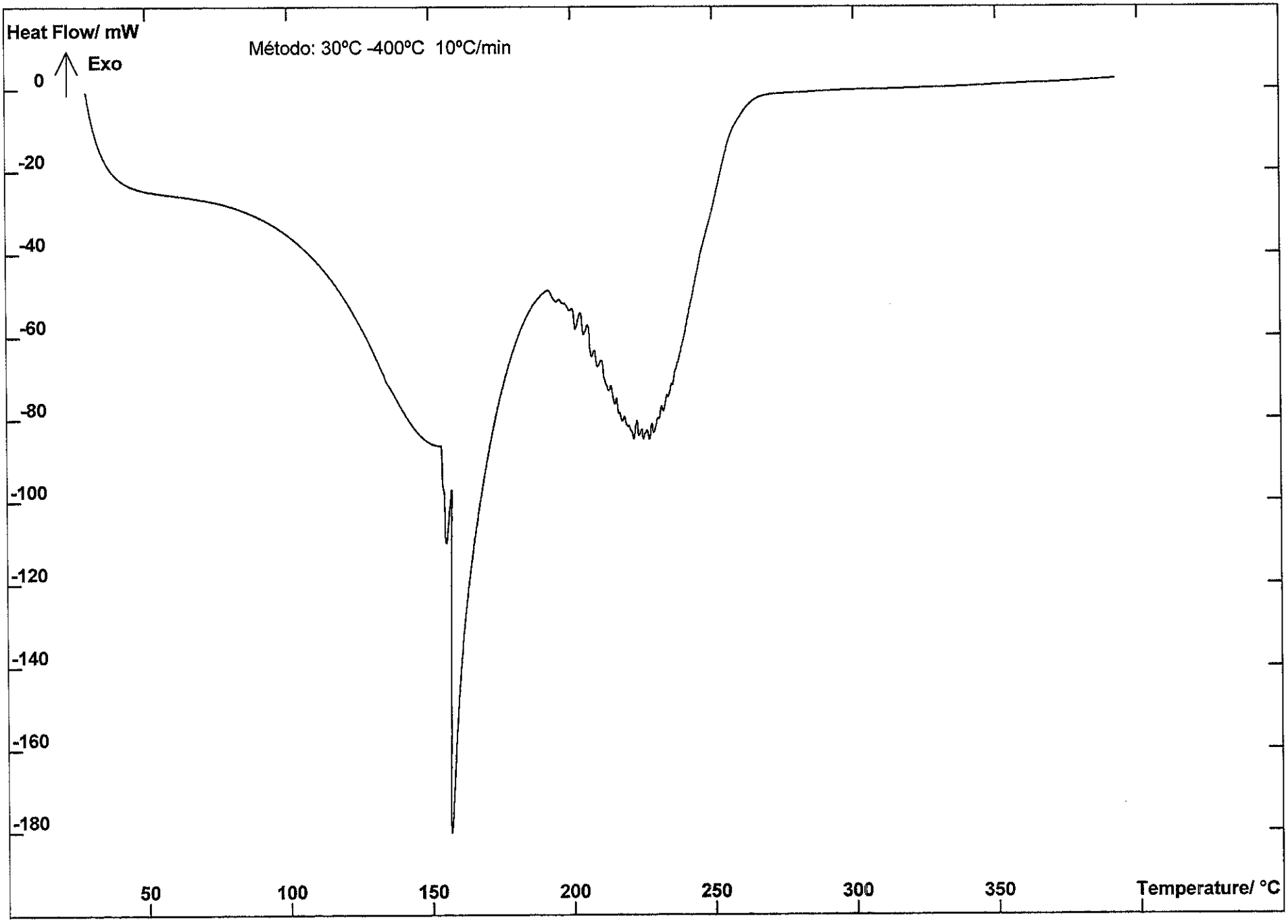

SETARAM INSTRUMENTATION - REGULATION	Fig. :	Experiment :	K10 water(T>Amb)	Atm. :	N2	Crucible :	Al 100 µl
DSC 131	06-20-14	Procedure :	14-D017 (Seq 2)			Mass (mg) :	37,35

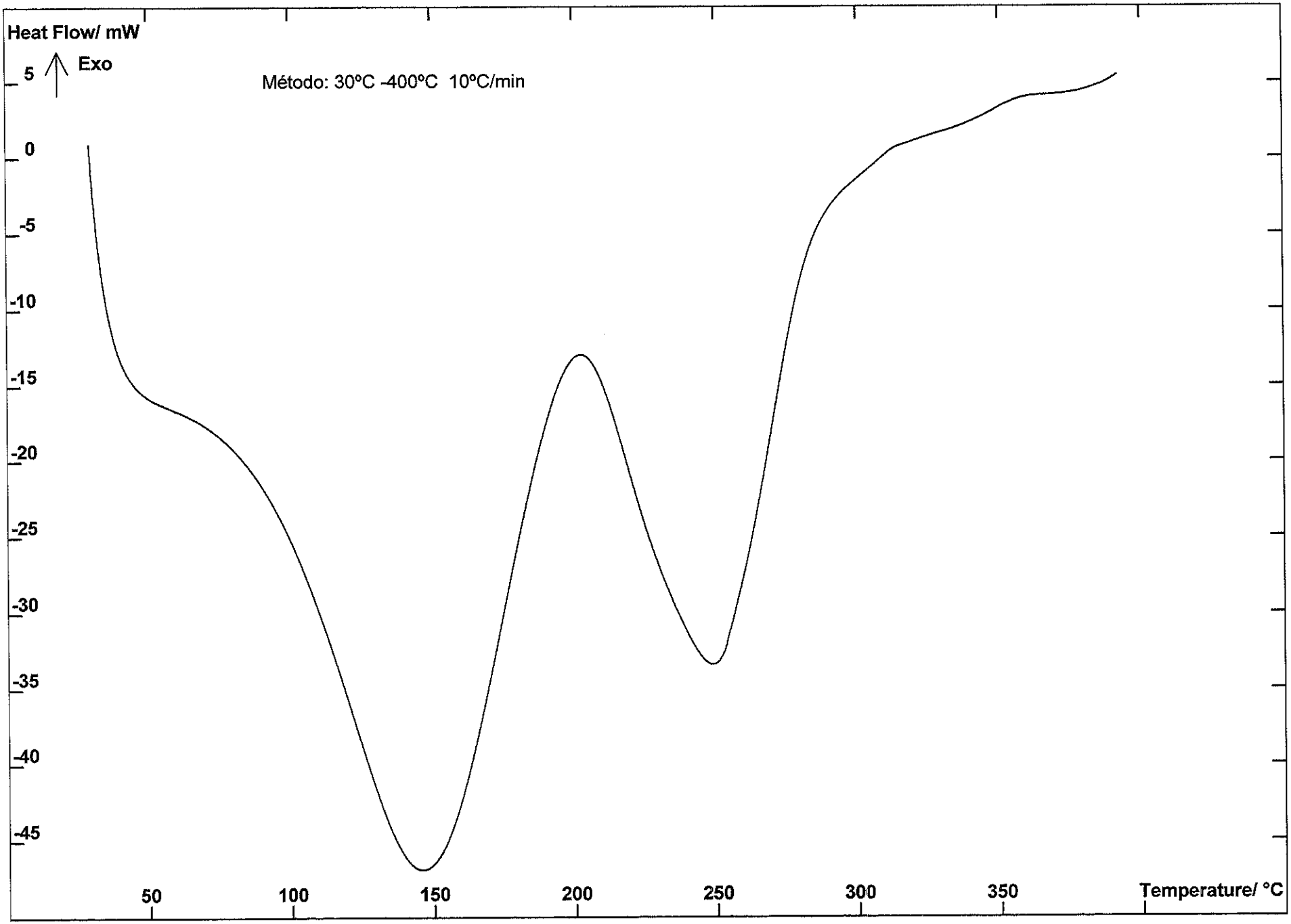

SETARAM INSTRUMENTATION - REGULATION	Fig. :	Experiment :	CGC MeOH(T>Amb)	Atm. :	N2	Crucible :	Al 100 µl
DSC 131	06-18-14	Procedure :	14-D017 (Seq 2)			Mass (mg) :	24,952

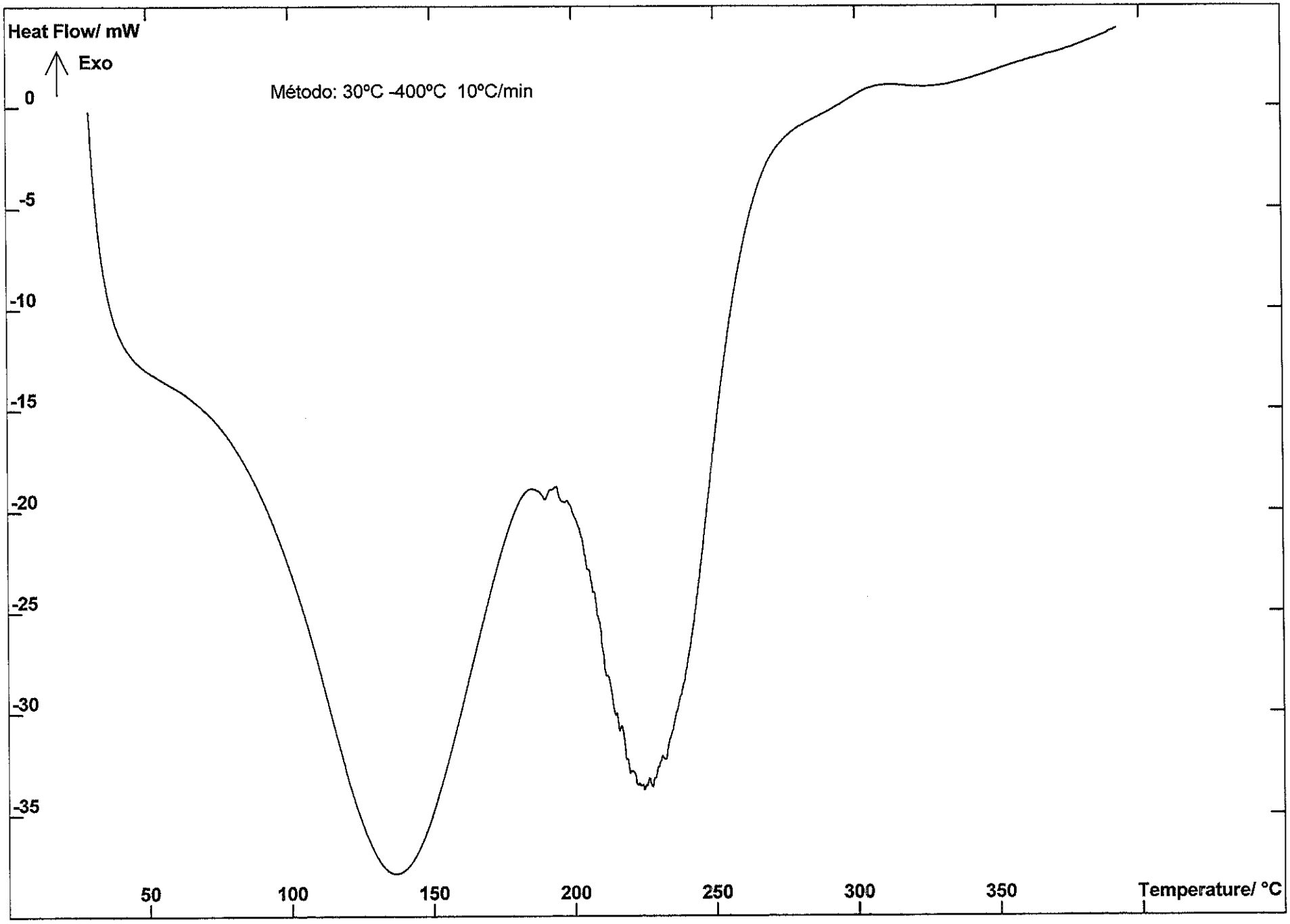

SETARAM INSTRUMENTATION - REGULATION	Fig. :	Experiment :	CGC water(T>Amb)	Atm. :	N2	Crucible :	Al 100 µl
DSC 131	06-18-14	Procedure :	14-D017 (Seq 2)			Mass (mg) :	19,144

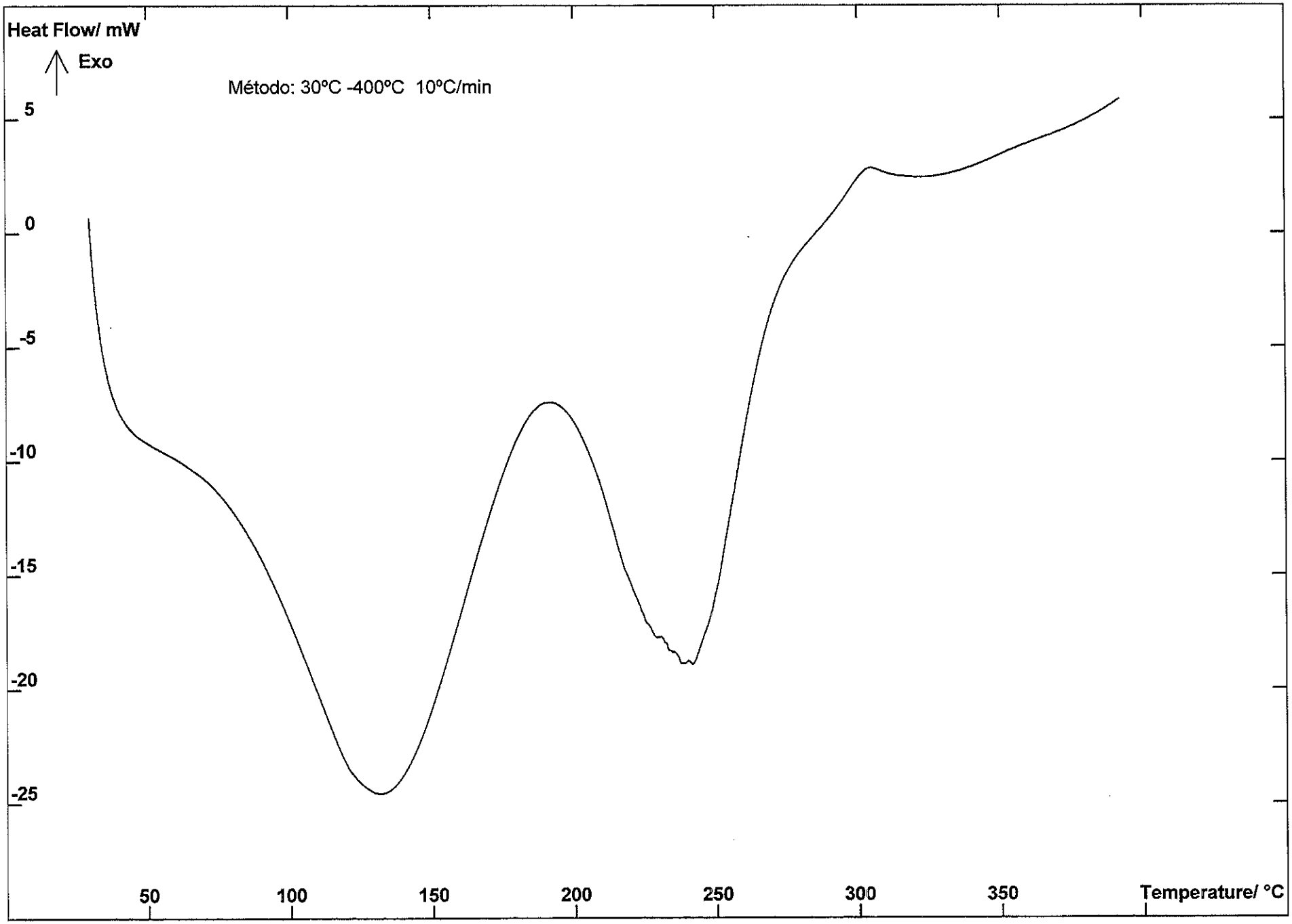

SETARAM INSTRUMENTATION - REGULATION	Fig. :	Experiment :	K10 glycerol(T>Amb)	Atm. :	N2	Crucible :	Al 100 µl
DSC 131	06-17-14	Procedure :	14-D017 (Seq 2)			Mass (mg) :	50,307

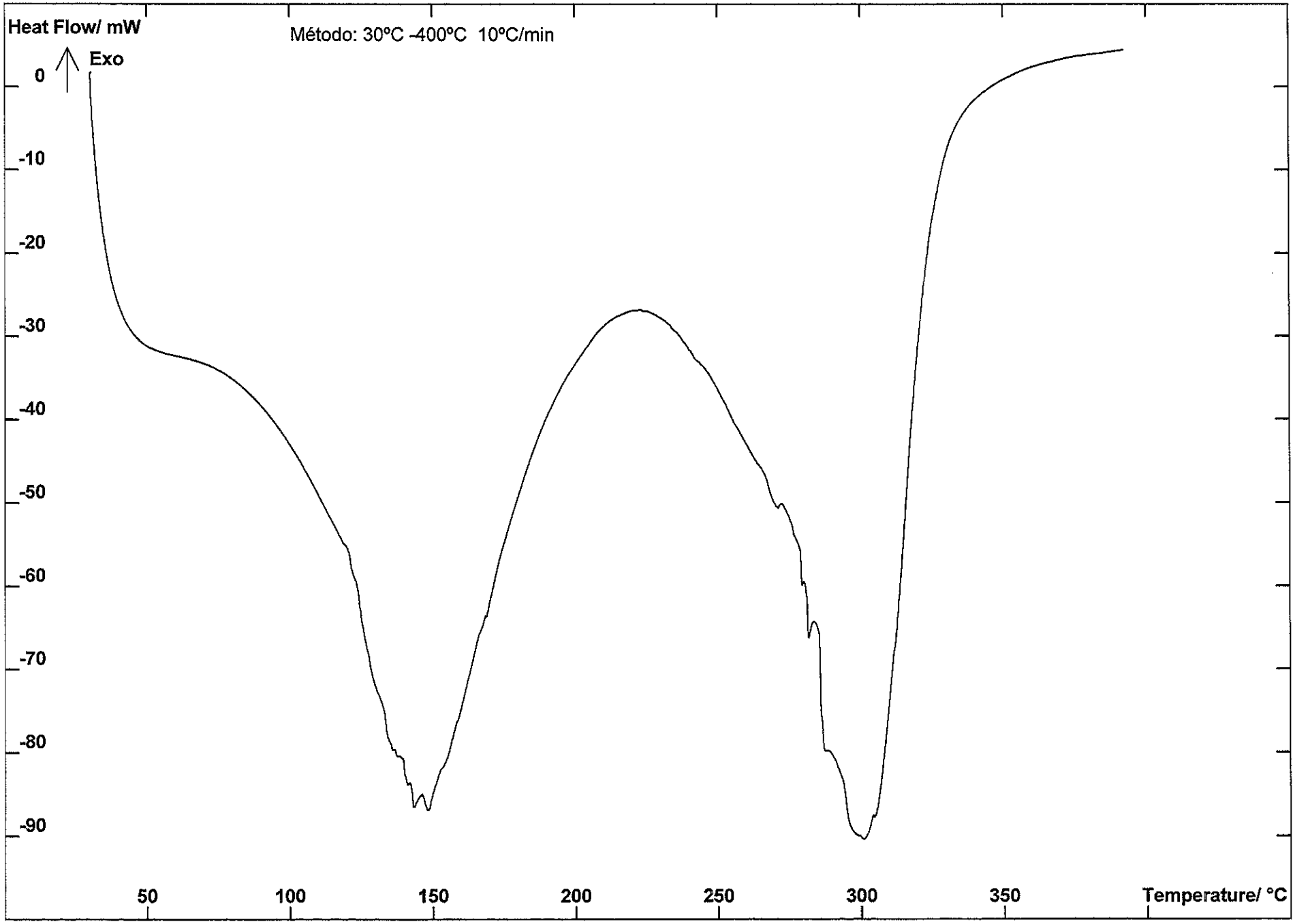

SETARAM INSTRUMENTATION - REGULATION	Fig. :	Experiment :	K10 Meth(T>Amb)	Atm. :	N2	Crucible :	Al 100 µl
DSC 131	06-17-14	Procedure :	14-D017 (Seq 2)			Mass (mg) :	22,701

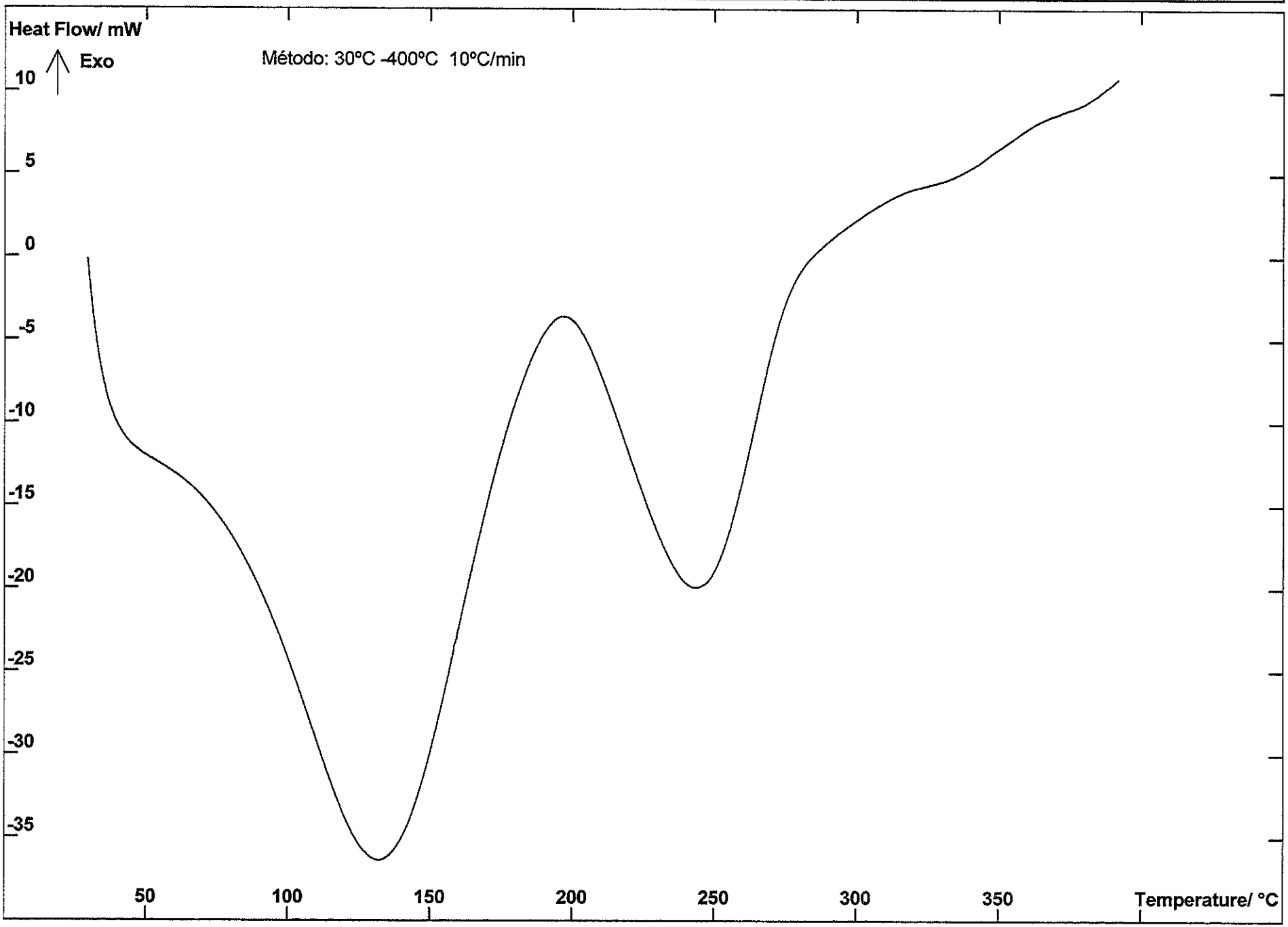

SETARAM INSTRUMENTATION - REGULATION	Fig. :	Experiment :	PEG glycerol(T>Amb)	Atm. :	N2	Crucible :	Al 100 µl
DSC 131	06-17-14	Procedure :	14-D017 (Seq 2)			Mass (mg) :	40,276

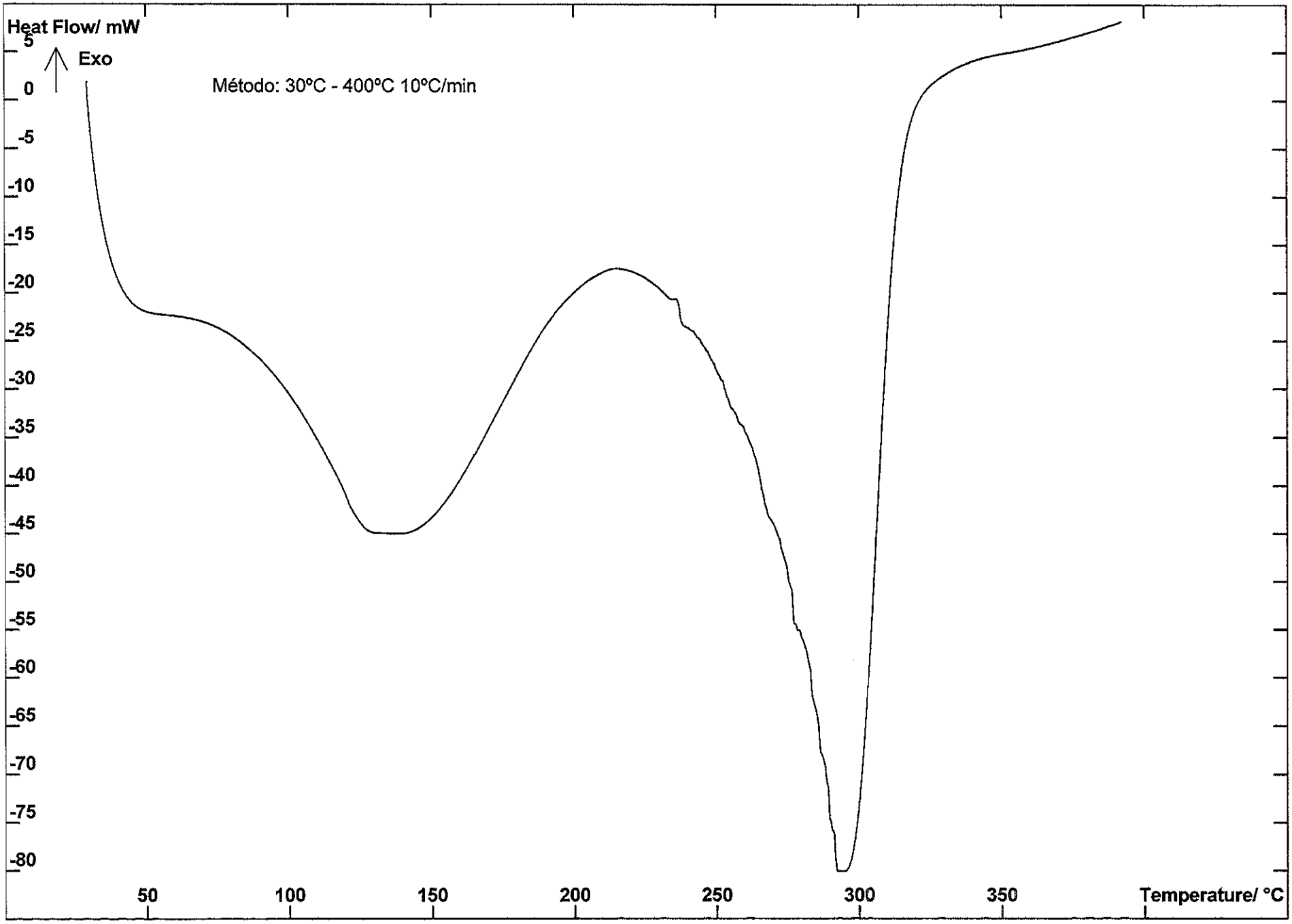

SETARAM INSTRUMENTATION - REGULATION	Fig. :	Experiment :	K10 water(crio)	Atm. :	N2	Crucible :	Al 100 µl
DSC 131	06-19-14	Procedure :	14-D026(crio) (Seq 4)			Mass (mg) :	37,35

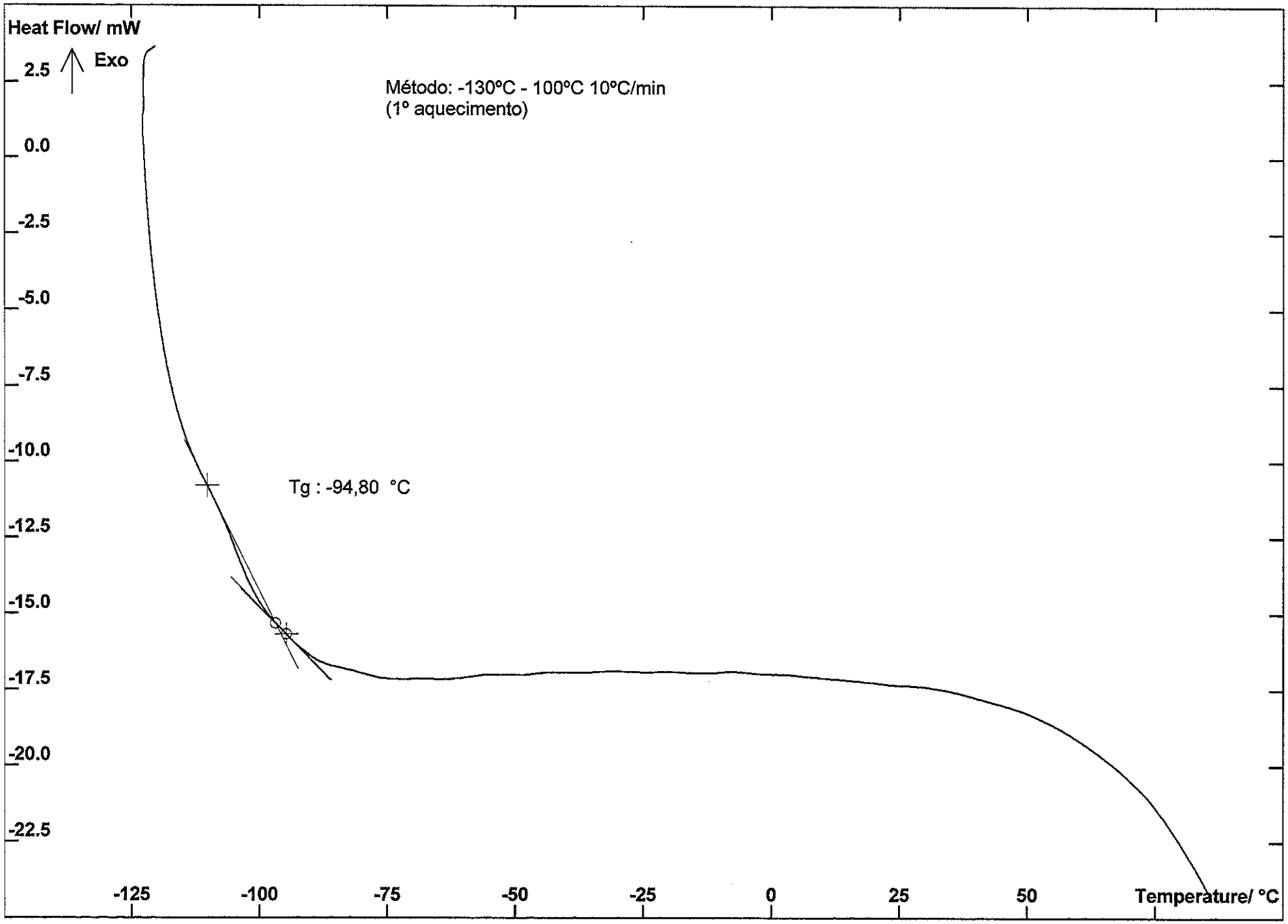

Appendix V: Total sugar analysis (Dubois Method) in coagulation bath

Table 7.2: Glucose concentration data for standards

Concentration (mg/L)	$C_{Corrected}$ (mg/L)	Absorbance
150	149.28	1.309
125	125.39	1.345
100	100.02	0.922
80	80.61	0.757
60	59.71	0.586
40	40.31	0.410
30	31.35	0.352
25	25.00	0.283
20	20.00	0.240
15	15.00	0.180
10	10.00	0.146
0	0.00	0.035

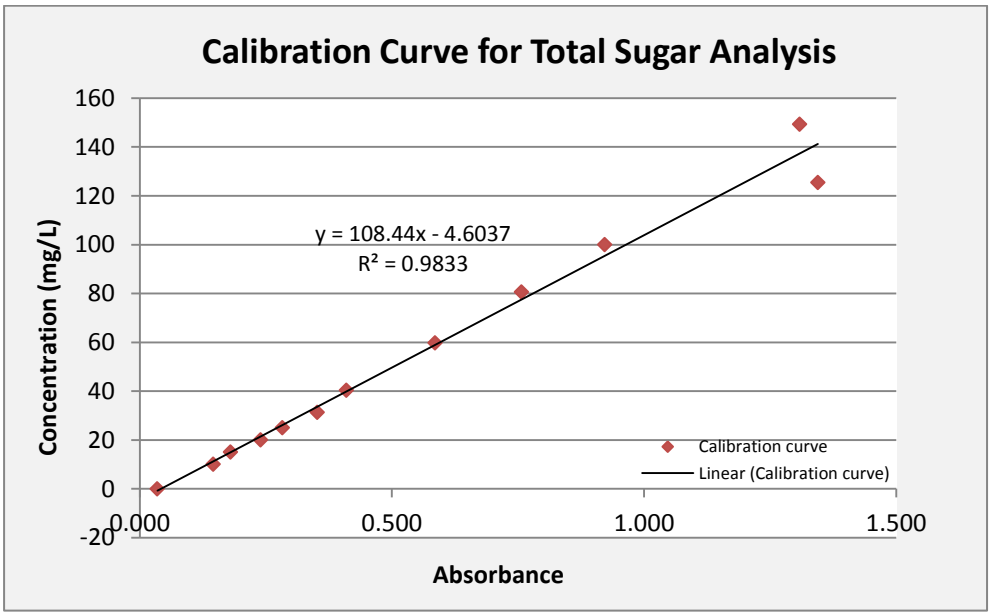

Fig. 7.5: Calibration curve represents the glucose concentration as a function of absorbance

Appendix VI: Puncture Test

Data of force and distance travelled by the probe is obtained from the software of the TA-xT texture is presented in Fig. 7.6 and Fig.7.7. The tension or stress is determined by dividing the force data by the probe surface area the probe on the sample. The problem is observed because the device only began to register a value when it felt a minimum force of 0.05 N, at the time when the films already underwent elongation.

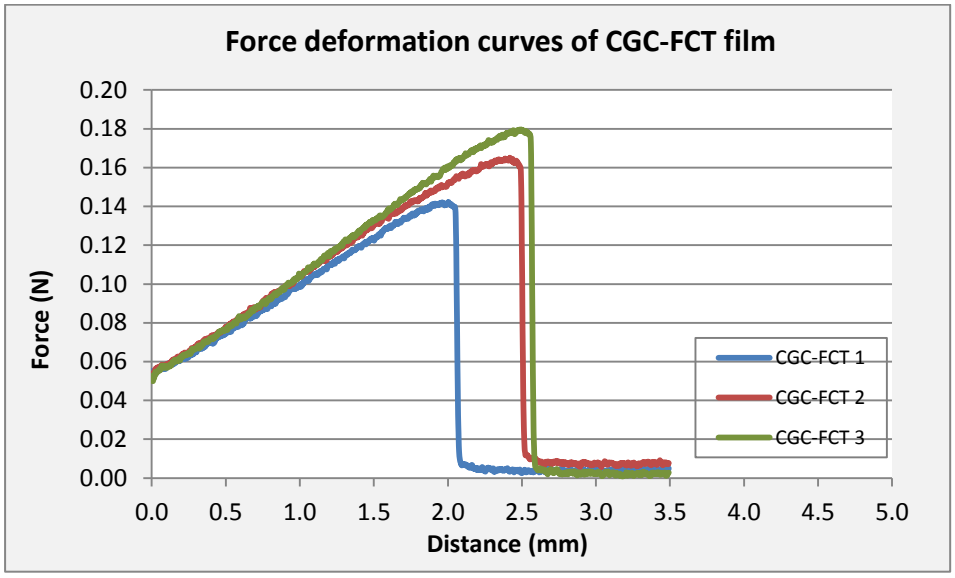

Fig. 7.6: Force deformation curves of CGC-FCT film represents the applied force as a function of elongation

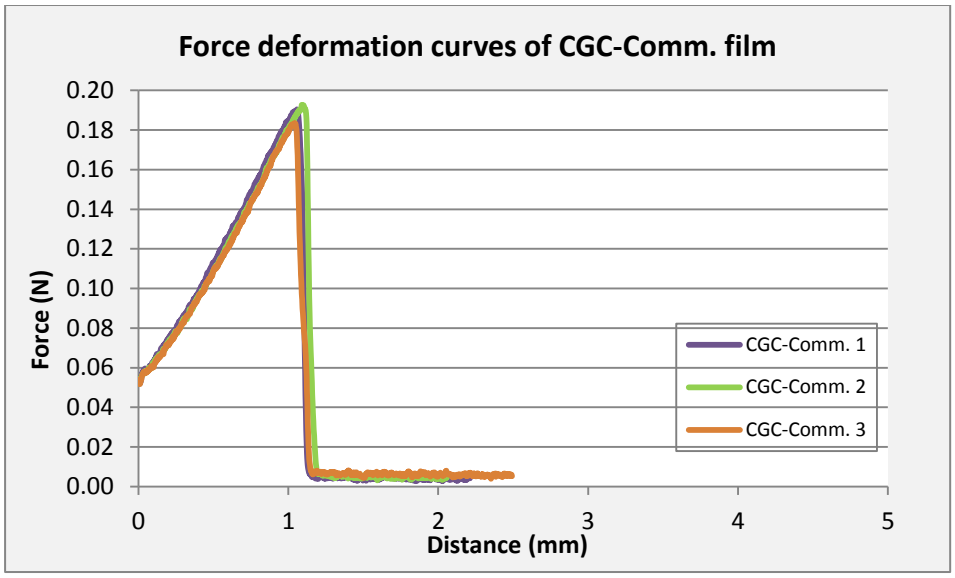

Fig. 7.7: Force deformation curves of CGC-Commercial film represents the applied force as a function of elongation